TECHNISCHE UNIVERSITÄT MÜNCHEN

Fakultät für Medizin

Lehrstuhl für molekulare Allergologie und Umweltforschung

Investigation into the role of the transcription factor RelB for the immunological tolerance induction

Maria Potthast

Vollständiger Abdruck der von der Fakultät für Medizin der Technischen Universität München zur Erlangung des akademischen Grades eines Doktors der Naturwissenschaften (Dr. rer. nat.) genehmigten Dissertation.

Vorsitzende(r): Prof. Dr. Percy A. Knolle

Prüfer der Dissertation:

1. Prof. Carsten Schmidt-Weber
2. Prof. Dirk Haller

Die Dissertation wurde am 04.11.2020 bei der Technischen Universität München eingereicht und durch die Fakultät für Medizin am 16.03.2021 angenommen.

This thesis is dedicated to my beloved family

1 Table of contents

2 List of acronyms and abbreviations

Acronym	Explanation
AAI	Allergic airway inflammation
ABTS	2,2′-Azino-bis(3-ethylbenzothiazoline-6-sulfonic acid) diammonium salt
ACK	Ammonium-chloride-potassium buffer
AF	Alexa Fluor®
Alum	Aluminium hydroxide
APC	Allophycocyanin
Appr.	Approximately
APRIL	A proliferation-inducing ligand
BAC	Bacterial artificial chromosome
BAFF	B-cell activating factor
BAL	Bronchoalveolar lavage
BATF3	Basic leucine zipper ATF-like transcription factor
BCL3	B-cell lymphoma 3-encoded protein
BM	Bone marrow
bp	Base pairs
BSA	Bovine serum albumin
BV	BD Horizon Brilliant™ Violet
Cbfβ	Core-binding factor subunit β
CCR	C-C chemokine receptor
CD	Cluster of differentiation
cDC (1/2)	Classical dendritic cells (type 1/2)
CDP	Common dendritic precursor cell
CFA	Complete Freund's adjuvant
CNS	Central nervous system
Csf2	Colony-stimulating factor 2
cTEC	Cortical thymic epithelial cell
CX3CR1	CX3C chemokine receptor 1
d	Day
DC	Dendritic cell
DMEM	Dulbecco's Modified Eagle's Medium
DMSO	Dimethylsulfoxide
DN	CD4-CD8- double negative
DNA	Deoxyribonucleic acid
DP	CD4+CD8+ double positive
DPBS	Dulbecco's phosphate buffered saline
EDTA	Ethylenediaminetetraacetic acid
eF	eFluor™
Esam	Endothelial cell-selective adhesion molecule
FACS	Fluorescence-assisted cell sorting
FCS	Fetal calf serum
FcεRI	High-affinity Fc receptors for IgE
FITC	Fluorescein
Flt3 (L)	Fms like tyrosine kinase 3 (ligand)
FoxP3	Forkhead box P3
Fwd.	Forward
GALT	Gut-associated lymphoid tissues
Gata3	GATA binding protein 3
GC	Germinal center
GF	Germ-free

Acronym	Explanation
GITR	Glucocorticoid-induced TNFR-related protein
GM-CSF	Granulocyte-macrophage colony-stimulating factor
HEPES	N-2-hydroxyethylpiperazine-N-2-ethane sulfonic acid
HPC	Hematopoietic progenitor cells
HRP	Horseradish peroxidase
i.g.	Intragastric
i.p.	Intraperitoneal
i.v.	Intravenous
ICOS	Inducible co-stimulator
IKK	IκB kinase
IL / IL-R	Interleukin / Interleukin receptor
ILF	Isolated lymphoid follicle
IMIDs	Immune-mediated inflammatory diseases
Int	Intermediate
IRF	Interferon regulatory factor
iTregs	Induced regulatory T cells
IκB	Inhibitor of NFκB
Klf4	Kruppel-like factor 4
KLRG1	Killer cell lectin-like receptor G1
KO	Knockout
LP (L)	Lamina propria (lymphocytes)
LPS	Lipopolysaccharide
LTβ	Lymphotoxin β
LZ	Leucine zipper domain
M cells	Microfold cells
MACS	Magnet-assisted cell sorting
MDP	Macrophage-dendritic cell precursors
MEM	Modified Eagle's Medium
MHCII	Major histocompatibility complex class II
mLNs	Mesenteric lymph nodes
MOG	Myelin oligodendrocyte glycoprotein
mTEC	Medullary thymic epithelial cell
MZ	Marginal zone
n.a.	Not applicable
NES	Nuclear export sequence
NF-κB	Nuclear factor κB
NIK	NF-κB-inducing kinase
NIR	Near infrared
Notch2	Neurogenic locus notch homolog protein 2
NP-40	Nonidet™ P 40 substitute
Nrp1	Neuropilin 1
nTreg	Naturally occurring Tregs
OE	Overexpression
OVA	Ovalbumin
OX40	Tumor necrosis factor superfamily member 4
PAMP	Pathogen-associated molecular patterns
PB	Pacific Blue (3-carboxy-6,8-difluoro-7-hydroxycoumarin)
PCR	Polymerase chain reaction
PD-1	Programmed cell death protein 1
pDC	Plasmacytoid dendritic cells
PE	Phycoerythrin
PerCP	Peridinin-chlorophyll-protein complex

Acronym	Explanation
PMA	Phorbol-12-myristate-13-acetate
PPs	Peyer's patches
PRR	Pattern recognition receptor
RA	Retinoic acid
Rel	V-rel avian reticuloendotheliosis viral oncogene homolog
Rev.	Reverse
RHD	Rel homology domain
RORγt	Retinoid-related orphan receptor γt
RPMI	Roswell Park Memorial Institute
RT	Room temperature
Runx	Runt-related transcription factor
SCFA	Short-chain fatty acid
SFBs	Segmented filamentous bacteria
SI	Small intestine
Sirpα	Signal regulatory protein α
SP	CD4+ / CD8+ single positive
SPF	Specific pathogen-free
sST2	Soluble IL-33 receptor ST2
TAE	Tris-acetate-EDTA buffer
T-bet	T-box transcription factor TBX21
TCR	T cell receptor
TD	T-cell dependent
Tfh	T follicular helper cell
TGFβ (R1)	Transforming growth factor β (receptor 1)
Th (1 / 2 / 17)	T helper cell (type 1 / 2 / 17)
TI	T-cell independent
TLR	Toll-like receptor
TMB	3,3′,5,5′-Tetramethylbenzidine
TNF	Tumor necrosis factor
TNFRSF	TNF receptor superfamily
TNFαR	TNFα receptor
TRAF	TNF receptor associated factor
TSA	Tissue-specific antigen
Ub	Ubiquitin
UV	Ultraviolet (light)
VAT	Visceral adipose tissue
Vis	Visible (light)
Wk	Week
WT	Wildtype

3 Summary

The gut harbors a vast number of bacteria and is continuously targeted by a plethora of antigens. Therefore, the establishment and maintenance of tolerance towards orally ingested antigens as well as symbiotic bacteria yet permitting specific responses towards invading pathogens is central for the proper function of the mucosal immune system. Regulatory T cells (Tregs) constitute the pivotal mediators of immunological tolerance. A subset of Tregs predominantly found in the gut develops in a microbiota-dependent manner and co-expresses the nuclear hormone receptor RORγt. Whereas the role of RORγt+ Tregs for the suppression of colitis and food allergy in the gut has been previously shown, their function for the induction of oral tolerance and inhibition of airway allergy has remained elusive. The results presented in this thesis have revealed that in contrast to their indispensable role for the maintenance of immune homeostasis in the gut, RORγt+ Tregs are dispensable for the suppression of allergic airway inflammation after induction of oral tolerance.

Dendritic cells (DCs) are professional antigen-presenting cells and are critically required for the development and maintenance of Tregs. Previous studies suggest that the nuclear factor κB (NF-κB) family member RelB is an essential regulator of the DC development and function. However, most of the available data derives from systemically RelB-deficient mice exhibiting a complex autoimmune phenotype and defective lymphoid organ development, thereby interfering with multiple aspects of DC biology. Due to these experimental shortcomings, the DC-intrinsic RelB function remained elusive. By using a DC-specific *Relb*-deletion mouse model ($RelB^{\Delta DC}$), an inherent requirement of RelB in DCs for the regulation of the Treg compartment and suppression of spontaneous type 2 immune activation was established in this thesis:

On the one hand, RelB-deficient DCs did not support the induction of oral tolerance and RORγt+ Tregs. The abrogated mucosal tolerance in absence of RelB in DCs was associated with the loss of type 2 classical DCs (cDC2s, CD11b+CD103+) in the small intestine, which are essential for the induction of mucosal tolerance.

On the other hand, total FoxP3+ Treg population was systemically expanded under steady-state conditions due to accumulation of tissue Tregs. In addition to their superior anti-inflammatory properties, tissue Tregs exhibit Th2-associated features, such as the expression of the transcription factor Gata3 and the IL-33 receptor ST2. Tissue Tregs can accumulate in response to IL-33 released from damaged cells. However, the data gained in this thesis has revealed that tissue Tregs accumulation in $RelB^{\Delta DC}$ mice takes place independently of IL-33. Instead, the extended population of tolerogenic cDC1s co-expressing the endocytic receptor DEC-205 might contribute to the elevated tissue Treg frequency. Further, the data presented here suggests a dispensable role of RelB in thymic DCs for proper negative selection of thymocytes, albeit an elevated thymic Treg output could not be excluded. In contrast to the DC-specific requirement, RelB was dispensable Treg-intrinsically for the establishment of normal Treg subpopulations.

Strikingly, the expanded Treg population conferred resistance towards actively induced experimental autoimmune encephalomyelitis (EAE) in RelB$^{\Delta DC}$ mice, whereas RelB was dispensable in DCs for efficient activation of the adaptive immune response. A transient Treg depletion restored the EAE development in mice lacking RelB in DCs.

In summary, this thesis contributes to the understanding of the role of NF-κB signaling in the regulation of the Treg compartment. The data presented here points out that RelB in DCs is a promising target for the treatment of autoimmune diseases. However, potential side effects associated with an abrogated mucosal tolerance induction and an expanded Treg compartment – such as allergy development and immunosuppression, respectively, must be kept in mind.

4 Zusammenfassung

Der Darm mit seiner dichten bakteriellen Besiedlung ist kontinuierlich einer Vielzahl von Antigenen ausgesetzt. Aus diesem Grund ist die Induktion und Aufrechterhaltung der mukosalen Toleranz gegenüber Antigenen aus Nahrungsmitteln und symbiotischen Bakterienspezies, die jedoch zielgerichtete Immunreaktionen gegen invasive Pathogene erlaubt, von zentraler Bedeutung für das Funktionieren des mukosalen Immunsystems. Regulatorische T-Zellen (Tregs) sind die wichtigsten Vermittler der immunologischen Toleranz. Eine Subpopulation von Tregs, die hauptsächlich im Darm zu finden sind, entwickelt sich in Abhängigkeit von Bakterien und ko-exprimiert den nukleären Hormonrezeptor RORγt. Während die Rolle der RORγt+ Tregs für die Suppression von Kolitis und Nahrungsmittelallergien im Darm bereits bekannt war, blieb ihre Funktion bei der oralen Toleranzinduktion und bei Allergien der Atemwege unklar. Die Ergebnisse dieser Arbeit verdeutlichen, dass die Suppression von Atemwegsallergien nach Induktion der oralen Toleranz unabhängig von RORγt+ Tregs stattfindet.

Dendritische Zellen (DCs) sind professionelle Antigen-präsentierende Zellen und sind unabdingbar für die Entwicklung und Aufrechterhaltung von Tregs. Daten aus einer Vielzahl von Studien deuteten darauf hin, dass RelB - ein Transkriptionsfaktor aus der Familie der nukleären Faktor-κB (NF-κB) Proteine - eine entscheidende Rolle bei der Entwicklung und Funktion der DCs spielt. Da die meisten dieser Daten unter Verwendung von Mäusen mit einem systemischen *Relb*-Knockout (RelB-KO) erhoben wurden, ist die Aussagekraft dieser Studien limitiert. Dabei interferieren die defekte lymphatische Organogenese sowie der komplexe Autoimmunphänotyp der RelB-KO Mäuse mit der Entwicklung und Funktion der DCs. Aufgrund dieser experimentellen Einschränkungen blieben viele Aspekte der DC-intrinsischen Funktion von RelB bisher unklar. Unter Einsatz von Mäusen mit einer DC-spezifischen *Relb*-Deletion ($RelB^{\Delta DC}$) belegt diese Doktorarbeit, dass RelB in DCs wichtige Funktionen bei der Regulation des Treg-Kompartiments und der Suppression spontaner Aktivierung der allergieassoziierten Typ-2-Immunantworten (Th2) übernimmt:

Einerseits konnten *Relb*-deletierte DCs keine effiziente Induktion der oralen Toleranz und der RORγt+ Tregs vermitteln; die gestörte mukosale Toleranz in Abwesenheit von RelB in DCs war verknüpft mit einer verringerten Population der für die mukosale Immuntoleranz essentiellen Typ-2-DCs (cDC2s, CD11b+CD103+) im Dünndarm.

Andererseits war die Gesamtpopulation der FoxP3+ Tregs durch die gestiegene Anzahl von Gewebe-Tregs (*tissue Tregs*) unter homöostatischen Bedingungen vergrößert. Neben starken anti-inflammatorischen Eigenschaften weisen Gewebe-Tregs Th2-assoziierte Eigenschaften wie die Expression des Transkriptionsfaktors Gata3 und des IL-33-Rezeptos ST2 auf. Gewebe-Tregs können nach Freisetzung von IL-33 aus verletzten Zellen expandieren. Jedoch wurde hier dargelegt, dass $RelB^{\Delta DC}$ Mäuse eine IL-33-unabhängige Treg-Akkumulation aufweisen. Stattdessen trägt möglicherweise die vergrößerte Population der tolerogenen cDC1s, die den endozytotischen Rezeptor DEC-205 auf ihrer Oberfläche zeigen, zur Expansion der Gewebe-Tregs bei. Ferner verdeutlicht diese Arbeit, dass RelB in DCs bei der Negativselektion von selbstreaktiven Thymozyten eine

untergeordnete Rolle spielt, wobei eine verstärkte Produktion von Tregs im Thymus nicht ausgeschlossen werden konnte. Im Gegensatz zu DCs, konnte eine Treg-intrinsische Funktion von RelB für die Regulation der Tregs ausgeschlossen werden.

Die Kernaussage dieser Doktorarbeit ist, dass die expandierte Treg Population in Abwesenheit von RelB in DCs eine Resistenz gegenüber der experimentellen autoimmunen Enzephalomyelitis (EAE) vermittelt: $RelB^{\Delta DC}$ Mäuse waren geschützt vor EAE; nach einer transienten Treg-Depletion jedoch konnte eine stark ausgeprägte EAE in $RelB^{\Delta DC}$ Mäusen induziert werden. Hiermit belegen die hier gezeigten Daten, dass RelB in DCs für die Induktion der EAE selbst nicht notwendig ist.

Insgesamt trägt die vorgelegte Doktorarbeit zum verbesserten Verständnis der Funktion des NF-κB Signalwegs in der Regulation des Treg Kompartimentes bei. Die hier gezeigten Daten verdeutlichen, dass RelB ein vielversprechender Kandidat für die Behandlung von Autoimmunerkrankungen ist. Dabei sollten jedoch potenzielle Nebeneffekte im Auge behalten werden, die mit einer gestörten mukosalen Toleranzinduktion oder einem vergrößerten Treg-Kompartiment, wie zum Beispiel die Entwicklung von Allergien bzw. Immunsuppression.

5 Introduction

The incidence of immune-mediated inflammatory diseases (IMIDs) has increased over the past decades in the westernized countries [1, 2]. The growing prevalence of allergies in the industrialized countries parallels this trend [3]. IMIDs include autoimmune diseases such as multiple sclerosis, psoriasis or type 1 diabetes and other inflammatory conditions such as inflammatory bowel disease. IMIDs as well as allergies are chronic conditions, which can cause a severe decline of life quality and can be disabling or even life threatening. Consequently, these immune-mediated diseases represent a major challenge for the affected individuals, the society, and the health systems.

A distorted immune homeostasis – maintaining the balance between an efficient protection against invading pathogens and establishing tolerance towards symbiotic microorganisms, dietary antigens, and innocuous stimuli – unites the pathology of these disorders. Therefore, it is imperative to understand the molecular processes which are involved in the regulation of the immune system.

5.1 Immune system

Immune responses are divided into two main branches: the innate and the adaptive immunity. The innate immune system is responsible for fast, yet unspecific detection of pathogens or damage. Upon evasion of the anatomical and chemical barriers, which represent the first line of defense, the pathogens activate innate immune cells. This process is facilitated by the recognition of conserved molecular patterns which are unique to bacteria, fungi and viruses (pathogen-associated molecular patterns, PAMPs) by innate recognition receptors, termed pattern recognition receptors (PRRs) [4]. This unspecific recognition of pathogenic patterns allows for prompt initiation of inflammation comprising innate humoral and cellular components. Humoral responses include secretion of lysozyme, antimicrobial peptides, acute phase proteins, cytokines, natural antibodies, and the activation of the complement system activation. Cellular responses include killing of virus infected host cells and destruction of pathogens by ingestion.

However, the adaptive immune system is required for the efficient antigen-specific clearance of pathogens and the formation of immunological memory. Consequently, a critical function of the innate immune system is to activate the adaptive immunity. Thereby, dendritic cells (DCs) represent a bridge between the two branches of the immune system.

The activation of the adaptive immune system is indispensable for an efficient defense against pathogens. The main features of the adaptive immune system are specific pathogen elimination and the formation of immunologic memory. To this end, the adaptive immune cells are equipped with specific receptors - which, upon activation trigger highly specialized effector cell responses. The adaptive immune response consists of a cellular and a humoral component. Whereas T cells with their T cell receptors (TCR) represent the cellular branch, B cells, upon differentiation to plasma cells, secreting immunoglobulins (Igs) are responsible for the humoral immune response [4].

Whereas B cells develop in the bone marrow and, upon activation, differentiate into antibody-secreting plasma cells, T cells develop in the thymus and exert their functions at the inflammatory sites upon activation as polarized T helper cells (Th) cells. In addition to that, follicular helper T (Tfh) cells govern the germinal center (GC) reaction, generating high-affinity Igs. In contrast to that, regulatory T cells (Tregs) critically govern proinflammatory immune responses and maintain homeostasis.

5.2 T-cell development

The thymus consisting of a cortical and a medullary region is responsible for the development of T cells bearing the αβTCR. Here, the thymic stromal cells provide signals supporting the T cell development from hematopoietic progenitor cells (HPC) via the cluster of differentiation 4 and 8 negative (CD4-CD8-) double negative (DN) and CD4+CD8+ double positive (DP) stages to the CD4+ or CD8+ single positive (SP) thymocytes [4]. To ensure a rich repertoire of functional but non-self-reactive TCRs, TCR gene segments undergo rearrangement in developing thymocytes. As a result, an exceedingly high proportion of TCRs with no functionality or high avidity to self-antigens are created by this stochastic process. Therefore, the thymocytes are rigorously selected by positive and negative selection. In the first step, DP thymocytes are subjected to positive selection in the thymic cortex. Here, cortical epithelial cells (cTECs) express and present major histocompatibility complex class II (MHCII) bound self-antigens and, upon low-affinity binding to a TCR, provide survival signals to the corresponding thymocyte [5]. In contrast to that, thymocytes with low affinity to the presented self-antigens are eliminated in a process called “death by neglect”. All thymocytes surviving the positive selection upregulate TCR and differentiate into SP thymocytes.

Remarkably, positive selection based on self-recognition creates a bias towards self-antigens. Consequently, self-reactive thymocytes need to be removed in the second selection step termed negative selection. This process not only ensures elimination of self-reactive thymocytes but also supports the generation of Tregs, thereby critically contributing to the establishment of central immunological tolerance. Negative selection takes place in the thymic medulla and is assisted by medullary thymic epithelial cells (mTECs) and DCs [6]. Medullary thymic stromal cells are responsible for the production of tissue-specific antigens (TSAs), Thereafter, mTECs either display the TSAs themselves or transfer them to thymic DC, which present the TSAs and support negative selection and induction of Tregs [7]. SP thymocytes bearing TCR with low affinity to the MHCII-bound TSAs become conventional T cells. In contrast to that, thymocytes with a high affinity TCR either undergo apoptosis or upregulate FoxP3 to become Tregs [8]. The mechanisms responsible for the Treg generation instead of clonal deletion are incompletely understood. However, there is evidence suggesting that the TCR signal strength required for negative selection is slightly stronger than that sufficient for Treg conversion [8]. Furthermore, certain TSAs support Treg induction instead of clonal deletion [9].

5.3 Helper T cells and adaptive immune responses

During an infection, naïve T cells polarize into either Th1, Th2 or Th17 cells upon encounter with the cognate antigen loaded onto an antigen-presenting cell. This specialization is inevitable and makes sure that each type of pathogen is cleared in the most efficient way with the least collateral damage. Therefore, each of the three T helper cell subtypes is responsible for the clearance of a specific set of pathogens. The polarization of T cells is orchestrated by a unique cytokine and chemokine environment, which is created by the cells of the first line of defense.

Th1 cells are involved in type 1 immune responses, which are crucial for the clearance of intracellular pathogens, such as viruses and bacteria. One of the most critical cytokines triggering Th1 polarization is IL-12 produced by activated DCs [10]. Th1 cells rely on the T-box transcription factor (T-bet) as the master regulator and secrete large quantities of interferon γ (IFNγ), thereby activating macrophages as effector cells [4]. Strikingly, activation of self-reactive Th1 cells may evoke autoimmune diseases (reviewed in [11]).

In contrast to intracellular pathogens, extracellular pathogens mediate type 2 immune responses involving the action of Th2 cells, IgE and innate effector cells such as eosinophils, basophils, and mast cells [4]. Aberrant type 2 immune responses against innocuous agents such as pollen or dietary proteins result in allergies. Th2 polarization is orchestrated by an interplay of alarmins, cytokines and chemokines secreted at the site of inflammation by epithelial and innate immune cells [12]. For example, damaged epithelial cells release the alarmin IL-33, which stimulates innate and adaptive immune cells expressing the IL-33 receptor ST2 including Th2 cells, Tregs and group 2 innate lymphoid cells (ILC2s) [13]. The activated innate immune cells in turn release further Th2-polarizing cytokines like IL-5 and IL-13 to trigger Th2 response [14]. Th2 cells depend on GATA Binding Protein 3 (Gata3) for their polarization and secrete several cytokines including interleukin 4 (IL-4), IL-13 and IL-5 [14, 15]. IL-4, in turn stimulates the production of IgE by B cells, thereby perpetuating the activation of innate lymphoid cells, including mast cells and basophils [16, 17]. These two innate cell types carry high numbers of high-affinity Fc receptors for IgE (FcεRI). Upon binding to IgE immune complexes, FcεRI molecules cross-link resulting in degranulation and release of the granule content [4]. The granula of basophils and mast cells include a plethora of factors including enzymes, cytokines, lipid mediators and histamine, thereby perpetuating inflammation (and depending on the context: helminth expulsion or anaphylaxis) [17, 18]. In addition to that, Th2 immune responses also contribute to tissue repair to restore normal tissue function after damage provoked by extracellular pathogens [19].

Most recently, Th17 cells were identified as the third major subtype of T helper cells [20, 21]. Th17 cells require retinoid-related orphan receptor γt (RORγt) as the master regulator and are particularly abundant in the gut mucosa as their generation requires bacterial cues derived from certain gut-resident bacterial species such as segmented filamentous bacteria (SFBs) and certain Clostridia species [22-24]. Th17 cells are important for the clearance of mucosal pathogens including viruses, bacteria and fungi [25-27]. However, aberrant Th17 cell activation is implicated in autoimmune diseases and chronic inflammatory conditions [22].

Tfh cells represent a separate subset of T cells and are essential for the formation and maintenance of GC, maturation of B cells into plasma cells, class switching, affinity maturation and memory B cell formation (reviewed in [28]). To this end, Tfh cells secrete high levels of IL-21 and also provide co-stimulatory signals like CD40 ligand (CD40L) [29]. Tfh are characterized by the expression of chemokine receptor CXCR5 and co-stimulatory molecules including inducible co-stimulatory molecule (ICOS) and programmed death 1 (PD-1) [30]. The master regulator of the Tfh cell development is the transcription factor B cell lymphoma (BCL6) [31, 32]. However, the origin of Tfh cells remains a subject of debate - whereas some findings suggest that Tfh cells can differentiate from Th17 cells, others postulate a naïve T cell-derived origin of Tfh cells [33, 34]. In Peyer's patches, Tfh cells can derive from FoxP3+ Tregs [35].

5.4 Tregs and immunological tolerance

In contrast to T helper cells, Tregs suppress proinflammatory responses. Therefore, they are crucial to contain overt inflammation and to maintain immunological tolerance. Tregs exert their action via multiple mechanisms and can suppress the function of a plethora of immune cells. Of those, the suppression of proinflammatory Th cells is one of the most important Treg function and takes place either directly via cell-cell contact or anti-inflammatory cytokines such as IL-10 and TGF-β or indirectly via regulation of the DC function (Reviewed in [36]).

Forkhead-box-protein P3 (FoxP3) has been identified as the master transcription factor of Tregs [37, 38]. Consequently, the absence of functional FoxP3 (due to mutations in the FoxP3 gene) clinically manifests in a severe multifocal autoimmune inflammatory disease in mice and humans [39, 40]. Based on their origin, Tregs are divided in two main subtypes: the thymus-derived, so-called naturally occurring (nTregs) and peripherally induced (iTregs).

In addition to the signals provided by thymic stromal cells which were discussed in the section "T cell development", nTreg development critically depends on the cytokine IL-2, mainly produced by T helper cells [41, 42]. To facilitate IL-2 mediated signaling, Tregs bear high affinity IL-2 receptor (IL-2R) consisting of the α (CD25), β and γ subunits [41]. Similar to FoxP3-deletion, the abrogation of IL-2R-signaling results in lethal autoimmunity [43].

In terms of the intrathymic Treg development, two alternative routes have been proposed. The classical route of Treg development suggests that the CD25 is upregulated prior to FoxP3 induction. Thereby, the IL-2R-mediated signaling facilitates the upregulation of FoxP3 to give rise to FoxP3+CD25+ mature Tregs (independently of TCR signaling) [44-46]. In the alternative route of Treg generation, FoxP3 is upregulated first and induces apoptosis unless rescued by IL-2 [47]. Since the amount of IL-2 is rather limited, the major fraction of newly developed Tregs undergo apoptosis, with the FoxP3+CD25- immature Tregs being the most apoptosis-prone subset [47]. The mature CD25+FoxP3+ Tregs leave the thymus and seed to secondary lymphoid organs or non-lymphoid tissues. Since the TCR repertoire of the thymic-derived Tregs is highly biased towards recognition of self-antigens, nTregs are responsible for the establishment of central immune tolerance suppressing autoimmune

diseases. Furthermore, thymus-derived Tregs express the transcription factor Helios, which is critically required for their function [48, 49].

In addition to self-antigens, the immune system is continuously challenged by millions of exogenous innocuous antigens such as commensal species, food proteins and pollen. Therefore, additional regulatory processes are required to maintain the peripheral tolerance towards these agents. Upon peripheral tolerance induction, a separate subset of Tregs, termed iTregs is generated outside the thymus, especially in the gut.

iTregs have unique properties making them a distinct Treg subset. In contrast to thymic Tregs, iTregs do not express Helios [48, 50]. iTregs are mainly induced in the gut by proteins derived from food and symbiotic microbiota. Consequently, iTregs rather than nTregs are essential for the suppression of exaggerated immune responses towards dietary and microbial antigens, thus preventing food allergies and inflammatory gut disease, respectively [50-53]. In addition to that, iTregs are essential for the maintenance of a healthy and diverse gut microbiome [51].

Microbiota, in turn, critically shape multiple aspects of the host immune system. Strikingly, a subset of iTregs develops in the gut in the presence of microbiota. This iTreg subset is characterized by the co-expression of the transcription factor RORγt and possesses a highly suppressive phenotype.

The microbiota-dependent RORγt+ Tregs are *bona-fide* Tregs with highly suppressive properties. The critical requirement of microbiota for the development of RORγt+ Tregs has been demonstrated in germ-free (GF) and antibiotics-treated mice showing severely diminished RORγt+ Treg population [50, 52-55]. Interestingly, not all symbiotic species support RORγt+ Tregs development to the same extent with certain *Firmicutes* and *Bacteroidetes* species exhibiting the highest tolerogenic potential [53]. Consequently, gut dysbiosis with a reduced abundance of RORγt+ Treg-inductive species has been linked to chronic inflammatory diseases like IBD and food allergy in human patients [56, 57]. In line with that, studies using several mouse models of colitis have highlighted the superior suppressive capacity of RORγt+ Tregs, which is independent of the type of the T cell polarization [52-54].

In addition to restraining colitis, RORγt+ Tregs are critical for the inhibition of allergic inflammation [52, 57, 58]. Consequently, GF and bacteria-eradicated mice exert hallmarks of allergic inflammation such as elevated levels of serum IgE, increased basophil and Th2 cells numbers [50, 52, 58]. Thereby, the action of RORγt+ Tregs seems to be restricted to the antigens provided via the gastrointestinal tract: whereas food allergy is restrained by RORγt+ Tregs, the latter are dispensable for the suppression of allergic airway inflammation [57, 59]. In line with that, feeding of GF with antigen-free diet resolves the Th2 bias observed in these mice [50].

In contrast to microbiota, the contribution of food antigens for the induction of RORγt+ Tregs is under debate. A number of publications suggests that dietary antigens play a minor role for the development of RORγt+ Tregs [50, 52, 53, 60]. In contrast to that, transgenic T cells recognizing ovalbumin (OT-II), attain a RORγt+ Treg phenotype upon transfer into immunocompetent hosts orally supplemented with the cognate protein [52, 55, 61].

Beyond the two previously discussed Treg subsets (thymically-derived nTregs and peripherally induced iTreg), a third major subpopulation of Tregs, termed tissue Tregs has recently came into focus. This Treg subset is predominantly found in peripheral non-lymphoid tissues like gut, VAT, muscle or skin and shows an activated, highly suppressive phenotype [62-67]. Tissue Tregs show a gene expression profile associated with an upregulated Tumor Necrosis Factor (TNF) receptor superfamily (TNFRSF) and nuclear factor κB (NF-κB) pathway [67, 68]. Further, tissue Tregs are characterized by the expression of ST2, Gata3, ICOS, killer cell lectin- like receptor G1 (KLRG1), CD103, CD44 and a low expression of CD62L, RORγt, CD25 and CCR7 [67, 68]. Interestingly, tissue Tregs from different organs show some degree of divergent gene expression, suggesting adaptation to the unique settings prevailing in different non-lymphoid tissues [67].

Tissue Tregs accumulate in inflamed tissues via clonal expansion and exert superior anti-inflammatory action facilitating tissue repair upon damage [62-67, 69]. Consequently, the gut being constantly subjected to epithelial cell damage and inhabited by a plethora of potentially harmful bacteria, harbors a large population of tissue Tregs [63, 69]. Thereby, tissue Tregs are able to receive signals from damaged epithelial cells. Among other factors, the alarmin IL-33 acting via IL-33R (ST2) is the most important factor for tissue Treg recruitment, activation, expansion and retention [62, 65, 70-73]. In addition to ST2+ tissue Tregs, IL-33 activates other ST2+ cells such as DCs [74]. IL-33-imprinted DCs, in turn elevate their IL-2 production, which contributes to the Treg expansion at inflamed sites [74, 75]. Similarly to RORγt+ Tregs, the recruitment and expansion of ST2+ Tregs in the non-lymphoid organs requires TCR activation and therefore critically depends on antigen presentation in the context of MHCII [64, 76]. Interestingly, tissue Tregs include Helios+ as well as Helios- cells and presumably constitute a mixed population in terms of their origin. Although the developmental origin of tissue Tregs remains elusive, distinct committed FoxP3+ tissue Treg precursors could be identified in the spleen and LNs [67, 77].

5.5 Dendritic cells

Dendritic cells have been discovered by Ralph Steinman as an adherent cell type with a stellate morphology [78]. The main role of DCs is immunosurveillance and activation of T cells, therefore representing the bridge between the innate and adaptive immunity. To this end, DCs recognize, take up, process and present antigens to activate and polarize T cells. DCs are equipped with several mechanisms for antigen uptake. One of them is the constitutive uptake of large amounts of extracellular fluid with dissolved molecules by a process called micropinocytosis [79]. In addition to that, DCs bear a broad range of PAMP-recognizing PRRs such as Toll-like receptors (TLRs), triggering endocytosis and phagocytosis of particulate antigens [4]. However, in contrast to other phagocytic cells - which destroy pathogens - the main feature of DCs is the processing and presentation of the captured antigens, thereby enabling effective activation and polarization of T cells.

Upon activation, DCs convert from a phenotype enabling efficient immunosurveillance to a professional antigen-presenting phenotype - to this end, DCs upregulate the expression of major histocompatibility complexes (MHC), co-stimulatory molecules and cytokines [80]. Furthermore, upon activation, the expression of the lymph-node homing chemokine

receptor CCR7 is upregulated, enabling the trafficking of DCs to the T-cell-zones of the secondary lymphoid organs (such as lymph nodes and spleen). Here, T cell activation takes place, thereby eliciting adaptive immune responses. In addition to the TCR stimulation by MHC-bound peptides, T cell activation requires two additional signals, which can be provided by activated DCs or other cell types. The second signal constitutes the complexing of co-stimulatory molecules such as CD80 or CD86 and their receptor CD28 expressed on T cells [81]. The third signal is delivered to T cells by cytokines, as mentioned in the section 5.3

There are two main DC subtypes: plasmacytoid and classical DCs. The DC development is stimulated by the cytokine colony stimulating factor 2 (Csf2, former known as GM-CSF) and the growth factor fms-related tyrosine kinase 3 ligand (Flt3L) [82]. DCs originate from the macrophage-dendritic cell precursors (MDPs) [83]. MDPs differentiate into common dendritic precursor cells (CDPs) and monocytes [84]. CDPs, in turn, give rise to pre-DCs, the direct precursors of cDCs or pDCs [85]. Pre-DCs give rise to two distinct cDC subpopulations: cDC1s and cDC2s, both sharing high expression levels of CD11c and MHCII. Each of the two cDC subsets requires a distinct set of transcription factors for the development and displays a distinct phenotype.

While the CD8α+ cDC1s require transcription factors like interferon regulatory factor (IRF)8 and basic leucine zipper ATF-like transcription factor BATF3; the CD8α- CD11b+ cDC2s are dependent upon IRF4 and neurogenic locus notch homolog protein 2 (Notch2) (reviewed in [86]). The cDC1s reside in the T cell zones of the spleen, exert a superior Treg-inducing capacity, and facilitate MHCII-mediated cross-presentation of exogenous antigens to CD8+ T cells [87-91]. In contrast to that, the red pulp-resident cDC2s efficiently stimulate CD4+ T cell responses [91]. Importantly, cDC2s represent a heterogenous population of DCs including the Klf4-dependent Esam^{low} subset and the Klf4-independent Esam^{high} subset, which requires Notch2, RelB and IRF4 [92, 93].

5.6 Intestinal DCs

DCs reside not only in lymphoid organs, but are also found in non-lymphoid tissues, especially at barrier sites. The gut mucosa is a particularly important barrier site continuously exposed to an exceptionally high density of bacterial and dietary antigens. Therefore, the gut and its gut-associated lymphoid tissues (GALT) including mesenteric lymph nodes (mLNs) and Peyer's patches (PPs) are central to the establishment of oral tolerance and maintenance of symbiotic bacterial population. At the same time, the GALT immune system ensures an efficient clearance of pathogens. To facilitate these processes, the lamina propria (LP) of the gut harbors a significant number of DCs.

Traditionally, DCs from the gut LP have been characterized by the high expression of CD11c and MHCII similarly to lymphoid DCs. However, recent publications have outlined that intestinal macrophages exert a similar CD11c+MHCII+ phenotype [94]. Due to this fact, the gut-LP DC population estimated to make up as many as 10 - 15 % of all lymphocytes has been overestimated for many years [95]. However, more recent research has outlined that around 70 % of the CD11c+MHCII+ cells in the small intestinal (SI) LP and up to 80 % in the colon are CD64+F4/80+CX3CR1^{high} macrophages [96-98]. Consequently, the

ontogeny and phenotype of GALT-associated mononuclear phagocytes (MNPs) remains somewhat unclear.

Four highly specialized *bona fide* DC subsets can be distinguished in the gut LP upon the expression of CD103 and CD11b [94, 96, 99-102]. Among those, CD103+ DCs possess superior migratory properties in comparison to the CD103- DCs and express the C-C chemokine receptor type 7 (CCR7), providing access to LNs [94, 101-103]. Generally, CD103+ DCs are considered as tolerogenic DCs with a high capacity to support generation of iTregs [95, 104]. Like splenic cDCs, the CD103+ DCs develop from BM-resident pre-DCs in Flt3- and GM-CSF-dependent manner and obtain gut tropic properties (by upregulating α4β7) upon the action of retinoic acid (RA) [103, 105, 106]. Among CD103+ DCs, CD11b- DCs share their phenotype and TF-requirements with cDC1s and the CD11b+ DCs correspond to cDC2s.

Unlike the tolerogenic CD103+ DCs, CD103- DCs mainly induce Th1 and Th17 immune responses, thereby enabling efficient antimicrobial immune responses [94, 96, 98, 104]. Like CD103+ DCs, CD103- DCs develop in a Flt3-ligand dependent manner from CDPs [107]. Interestingly, the CD11b-CD103- DC population seems to represent a unique subset resident within the isolated lymphoid follicle (ILF) rather than within the LP of the gut and is mainly responsible for the induction Th17 responses [94, 104, 108].

In contrast to pre-cDC-derived DCs, the gut resident macrophages differentiate from monocytes and produce high levels of anti-inflammatory cytokines, thereby rendering the gut mucosa tolerogenic, yet enabling sufficient anti-inflammatory responses upon activation [97].

5.7 Mucosal tolerance establishment in the gut

Oral tolerance is critical for the establishment of a state of non-responsiveness towards antigens from food. Intestinal tolerance was first demonstrated by Chase in 1946, who showed that oral administration of an antigen prevented both, intestinal and systemic inflammatory immune reaction after subsequent systemic challenge with that antigen [109]. Thus, oral tolerance is an active process requiring installation of regulated immune responses to the intestinal content and precluding immune reactions upon repeated systemic exposure to the antigen, even in the presence of an adjuvant. These regulated immune responses include T cell deletion, anergy and induction of regulatory T cells.

Central to the establishment of oral tolerance are CD103+ DCs and CX3CR1+ macrophages which orchestrate the generation and expansion of antigen-specific iTregs in the GALT [55, 95, 110]. Furthermore, gut microbiota critically contributes to the oral tolerance induction [111]. Dietary antigens arriving in the lumen of the SI are physically separated from the immune cells residing in the small intestinal lamina propria (SI-LP) by an epithelial layer, therefore, a specialized antigen-uptake is required to deliver luminal peptides to the immune cells across this barrier (Scheme A). To this end, several mechanisms of antigen uptake have evolved. Among those, the most important routes include transport of luminal content by microfold cells (M cells) of the PPs, and antigen sampling by specialized CX3CR1+ macrophages [112-114]. The latter extend

transepithelial protrusions into the gut lumen and take up food peptides as well as whole living bacteria [114, 115].

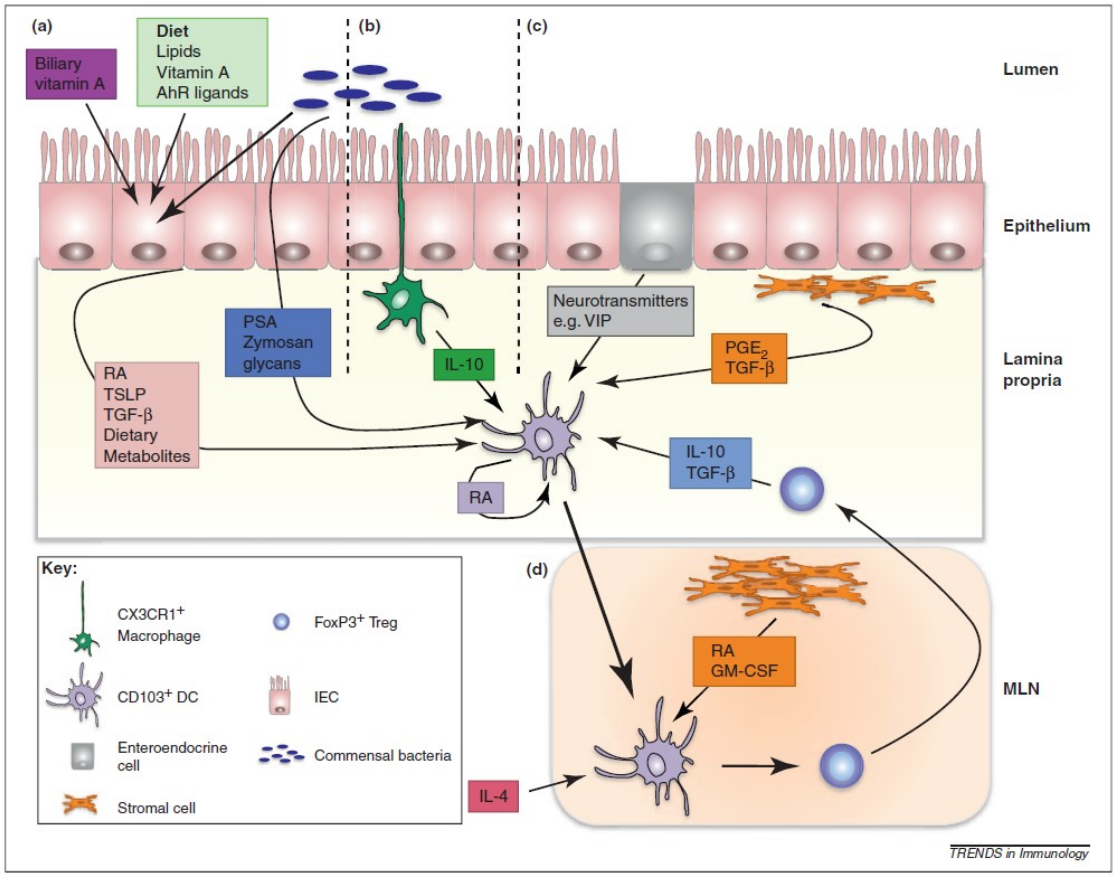

Scheme A. Induction of oral tolerance. Macrophages (green cell) take up luminal content and, stimulated by microbiota produce high quantities of IL-10. Upon uptake, antigens are transferred onto CD103+ DCs (violet cell). CD103+ DCs, in turn migrate into mLNs, where they present the processed peptides to T cells and convert them into Tregs with gut-homing properties. Upon homing to the lamina propria, Tregs expand upon the action of IL-10 and confer tolerance towards intestinal antigens. Adopted from Scott et al., 2011 [116].

The induction of food-protein-specific iTregs as the central event in the installation of oral tolerance takes place in mLNs [117]. As CX3CR1+ macrophages are non-migratory cells residing in the SI-LP, they rely on DCs for efficient transport and presentation of the antigens to T cells [101]. CD103+ DCs represent the main population of DCs in the intestinal LP and mLNs [95, 110, 114]. Consequently, the macrophages transfer the luminal peptides via gap junctions to CD103+ DCs, which, in turn are not able to take up luminal content themselves [114]. Upon receiving peptides from macrophages, the CD103+ DCs migrate to mLNs in a CCR7-dependent manner [118]. There, they present the processed MHCII-bound antigens to T cells thereby facilitating Treg induction [118]. This spatial separation is central to avoid aberrant immune activation.

The mLNs provide an exceptionally tolerogenic environment supporting efficient Treg induction [119]. The stromal cells of mLNs have a unique capacity to receive microbial cues and translate those into tolerogenic stimuli by producing high levels of TGFβ and RA-synthesizing enzymes [119, 120]. These factors, in turn, imprint DCs with high

Treg-inducing properties elevating the production of IL-10, TGFβ and RA by CD103+ DCs [119-121]. Thereby, RA and TGFβ in a cooperative manner to support the Treg induction and imprint cognate T cells with gut-homing properties by mediating the upregulation of CCR9 and α4β7 integrin [95, 104, 110, 122-126].

Gut homing of antigen-specific iTregs is essential for the oral tolerance formation [117]. Here, the tolerogenic microenvironment of the SI-LP exposed to a plethora of microbial and food proteins not only allows the iTreg population to exert its tolerogenic function but also critically supports its expansion [55, 117, 127]. Similar to other processes involved in the oral tolerance induction, microbiota play the central role in the latter process by stimulating IL-10 production in CX3CR1+ macrophages [55]. In turn, IL-10 triggers the expansion of iTregs and induces production of IL-10 by regulatory T cells further potentiating the tolerogenic capacity of the LP [127]. In summary, the ultimate result of the oral tolerance induction is the generation and expansion of iTregs. Hence, the immune cells of the GALT and the commensal bacteria closely cooperate to create a tolerogenic environment for the generation of iTregs and suppression of proinflammatory responses.

In addition to the oral tolerance induction against dietary proteins, mucosal tolerance induction against commensal bacteria is of central importance. In contrast to the dietary peptides, microbial antigens do not prevent systemic responses but only establish a locally restricted state of unresponsiveness at sites with bacterial colonization (reviewed in [112]). In addition to the generation of iTregs and maintenance of tolerogenic environment in the gut discussed above, the host produces large amounts of bacteria-specific IgA molecules. IgA not only confers tolerance towards the commensal bacteria and prevents the invasion of pathogenic bacterial species, but most critically controls the composition and maintains the bacterial diversity. The composition of the gut microbiota is critical to its homeostatic properties and a shift in bacterial communities, termed “dysbiosis” has profound effects on the health [57]. Dysbiosis has been associated with food allergies, inflammatory bowel diseases (such as Morbus Crohn and Ulcerative Colitis) and autoimmune diseases [57, 128].

IgA is produced in large quantities at the mucosal tissues, especially in the small intestine and secreted into the intestinal lumen [129]. Here, IgA exerts its action by coating of bacteria. IgA can be induced either by a T-cell dependent (TD) or by a T-cell independent (TI) route, both of which are regulated by symbiotic bacterial species [129]. PP play the most important role for the induction of IgA [113, 130]. There, the M cell-directed uptake of luminal content from the SI together with DCs transporting luminal peptides and living bacteria sustain constitutively active germinal centers (GCs) [131, 132]. The germinal centers, in turn support efficient class switch from IgM to IgA by a TD process involving the aid of Tfh cells and creating high-affinity IgA [129]. Among those Tfh-mediated signals, CD40-CD40L interaction is particularly important to trigger class switch and support survival and affinity maturation of B cells. [133].

Interestingly, most commensals trigger the TI response creating low-affinity IgA molecules [34]. In contrast to the TD class switch, the TI class switch does dependent on GCs and therefore may occur within non-lymphoid tissues in the ILFs of the SI [133, 134]. The TI class switch is supported by DCs via secretion of cytokines and accessory molecules such

as RA, TGFβ, TNF family ligands B-cell activating factor (BAFF) and its homologue APRIL (a proliferation-inducing ligand) [135]. Additionally, LTβ is critical for the TI induction of IgA [133]. Eventually, class-switched B cells migrate into mLNs or PPs for further maturation, after which they finally home to the gut LP and secrete large quantities of IgA there [135].

5.8 Commensal gut bacteria maintain immune homeostasis

Albeit a large proportion of commensal bacteria is coated by IgA to prevent interaction and activation of immune responses, there is a considerable proportion of bacterial cues arriving in the host. The host cells receive microbial signals via activation of PRRs such as TLRs and the constant activation of TLRs by commensal bacteria is critical for the establishment of intestinal epithelial homeostasis and is protective upon intestinal injury [136].

On the one hand, the TLR stimulation regulates the innate immune cell functions. The innate cell activation, in turn, triggers the production of antimicrobial peptides and cytokines, thereby preventing pathogen invasion. On the other hand, microbiota-primed innate immune cells contribute to the development and maintenance of MNPs, critically required for the establishment of mucosal tolerance by stimulating the release of Csf2 [137].

Macrophages, making up the majority of MNPs within the intestinal LP, are critically dependent on the TLR stimuli delivered by the microbiome. Strikingly, bacteria-derived signals prevent immune activation by inhibiting the trafficking of bacteria-loaded CX3CR1+ MNPs into the mLNs [138]. Furthermore, commensal species suppress inflammation and facilitate iTreg generation by inducing IL-1β and IL-10 production by macrophages and DCs [55, 137, 139, 140]. Additionally, the production of RA by DCs, critically required for the iTreg generation and induction of gut-homing properties depends on TLR-mediated signals [141].

Importantly, bacteria-primed DCs produce cytokines essential for the induction of mucus-protective Th17 cells in TLR-dependent manner [22]. Th17 cells, in turn stimulate the production of antimicrobial proteins by intestinal epithelial cells [142, 143]. In summary, the microbiome regulates adaptive immune responses by orchestrating the innate immune cell function.

Not only innate immune cells but also the cells of the adaptive immune system are responsive to the TLR-mediated stimulation by bacteria. Most importantly, the generation and suppressive capacities of Tregs are critically dependent upon microbial cues sensed by TLRs [55, 57, 144]. This Treg-specific TLR requirement has been highlighted by *Foxp3*-cre-specific genetic ablation of the MyD88 adaptor molecule which resulted in reduced Treg abundance and elevated Th17 immune response [145]. As an effect, disruption of Treg-intrinsic TLR signaling results in dysbiosis and diminished IgA production [145].

IgA generation also critically dependents on TLR signaling. During the TD-class switch, which requires CD40 activation by CD40L provided by Tfh cells, TLR ligands can act as a substitute for CD40L [146]. For the TI class switch, TLR activation stimulates the production of co-stimulatory molecules BAFF and APRIL [147-149]. Moreover, commensal bacteria prompt RA production by DCs, which, in turn elicits the generation of IgA-secreting plasma

cells with gut-homing properties [135]. On the other hand, TLR stimulation of B cells downregulates the production of IgE [58].

In addition to the activation of the host TLRs by bacteria, microbial metabolites play an important role in the regulation of the immune system. Among those, short-chain fatty acids (SCFAs) possess potent anti-inflammatory properties. SCFAs are bacterial products originating from the fermentation of dietary fiber and exert a plethora of anti-inflammatory effects on the immune system, thereby promoting immune homeostasis in the gut. The most predominant SCFAs are acetate, butyrate and propionate. Mechanistically, SCFAs exert a dichotomous mode of action: in addition to the activation of G-protein-coupled receptor signaling, some SCFAs such as butyrate act as a histone deacetylase inhibitor [150-152].

Intestinal MNPs belong to the most important cellular targets of SCFAs. Here, SCFAs downregulate an array of proinflammatory molecules, thereby promoting iTreg induction [151-155]. For example, butyrate inhibits danger-signal-mediated release of proinflammatory cytokines from intestinal macrophages [156]. Furthermore, butyrate polarizes macrophages towards alternatively activated or anti-inflammatory phenotype, suppressing the responsiveness towards the gut mutualistic bacteria [157].

Interestingly, the downregulation of the transcription factor RelB in macrophages and DCs has been described as one of the most important effects of SCFA action contributing to the immune homeostasis [153, 155]. RelB is a member of the nuclear factor (NF)-κB family, which is pivotal mediators of pro-inflammatory immune responses.

5.9 NF-κB family and signaling

The NF-κB family consists of 5 members: RelA (p65), RelB, p100/p52, p105/p50 and c-Rel. All five members share the Rel homology domain (RHD), which supports nuclear localization, dimer formation and DNA binding (Reviewed in [158]). NF-κB members can be further subdivided into two groups: the first group consisting of RelA, RelB and c-Rel contain a transactivation domain (TAD), necessary for transcriptional activation [158]. In contrast to that, the second group comprising p100/p52 and p105/p50 act as inhibitors of κB (IκB) due to their ankyrin repeats responsible for the inhibition of nuclear localization and DNA binding [159, 160].

The IκB family is not restricted to the p100 and p105 and is grouped into the classical and atypical IκB subfamilies (Reviewed in [161]). Whereas IκBs α, β and ε, in addition to p100 and p105 belong to the typical subfamily - Bcl3, IκBζ, $IκB_{NS}$, IκBη and IκBL make up the atypical subfamily [161]. The atypical IκBs are mainly localized in the nucleus and regulate transcriptional activity of NF-κB TFs [161].

In contrast to that, the classical IκBs are responsible for the retention of NF-κB TFs in the cytoplasm, unless activated by the NF-κB signaling [161]. Upon activation, the (classical) IκBs become a subject to degradation thereby enabling the translocation of NF-κB dimers into the nucleus. Here, they regulate gene expression by binding to specific κB sites within promoter and enhancer regions of target genes.

NF-κB TFs can be activated via the canonical and the alternative (or non-canonical) NF-κB signaling [158]. Whereas the canonical pathway usually results in the translocation of RelA-p50 and c-Rel-p50 heterodimers into the nucleus, the alternative NF-κB signaling predominantly activates RelB-p52 heterodimers [158, 162].

A multitude of receptors including TCR, Igs, inflammatory cytokine receptors (TNFαR, IL-1R) and TLRs activate the canonical NF-κB pathway [163]. Without stimulation, IκBs α, β and ε prevent nuclear translocation of preformed RelA-p50-heterodimers into the nucleus [161]. Although p105 functions as IκB, it is constitutively processed to p50 [164]. The canonical NF-κB pathway recruits IκB kinase (IKK) complex consisting of IKK α, β and NEMO which phosphorylate IκBs, rendering them a subject to proteasomal degradation thereby enabling RelA-p50 to enter the nucleus [158].

In contrast to that, TNFRSF members initiate the alternative NF-κB pathway ultimately resulting in the processing of p100, which restrains RelB in the cytosol [160]. Thereby, the stabilization of NF-κB-inducing kinase (NIK) by degradation of TNF-receptor associated factor 3 (TRAF3) permits the activation of IKKα, which in turn phosphorylates p100 [165, 166]. Consequently, p100 is exposed to proteasomal processing to p52, whereby the C-terminal domain containing a nuclear export sequence (NES) is cleaved off enabling the RelB-p52 complexes to enter the nucleus [160, 162].

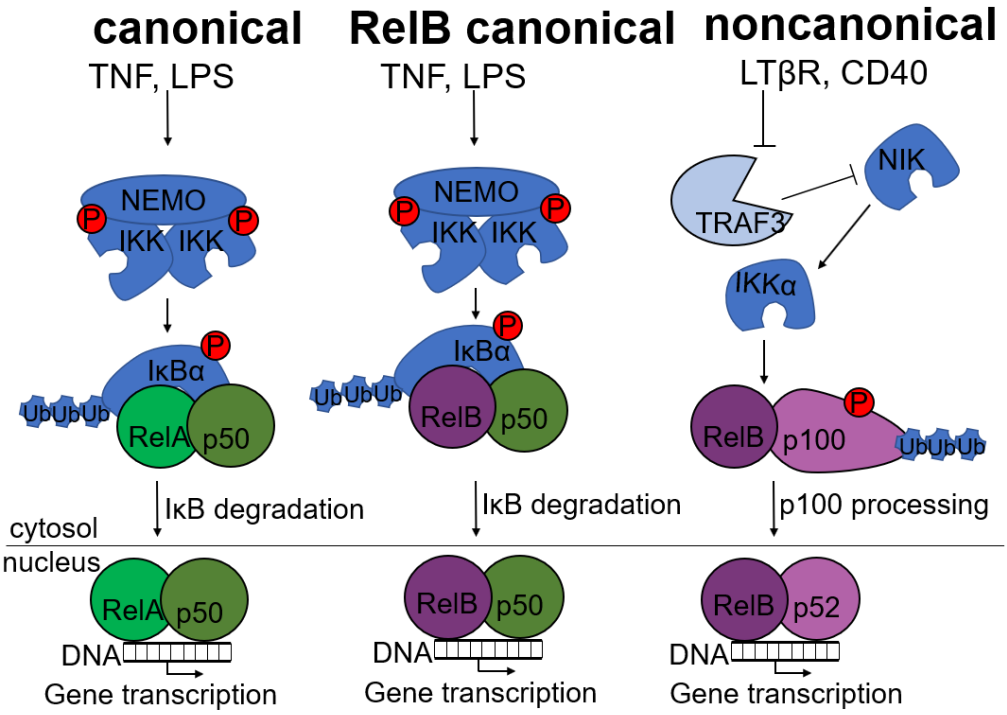

Scheme B. NF-κB signaling in DCs. In addition to the classical and alternative pathway known from other cell types, DCs deploy an additional pathway, whereby activation of the canonical NF-κB signaling results in the recruitment of atypical RelB-p50 heterodimers. Ub, ubiquitin; P, phosphorylation; LPS, Lipopolysaccharide; LTβR, Lymphotoxin β receptor. Adopted from Hayden et al., 2012 [167].

Surprisingly, dendritic cells deploy a distinct mechanism of the RelB recruitment upon stimulation with maturation stimuli like TLR ligands (Scheme B). Thereby, the canonical pathway activated by ligands such as TNF or lipopolysaccharide (LPS) recruits RelB-p50

heterodimers via NIK alongside with RelA-p50 heterodimers [168]. In addition to that, DCs exhibit nuclear RelB-p52 complexes at steady state [168].

5.10 The role of RelB in the immune system

In contrast to other members of the NF-κB family, RelB harbors a leucine zipper domain (LZ) and can bind a broader spectrum of NF-κB consensus sequences than other NF-κB family members [169]. RelB plays an important role in the development and maintenance of the immune system. Consequently, the genetic ablation of *Relb* in mice (RelB-KO) has a severe impact on the development of lymphoid organs such as the thymus, LNs and PPs [170-172]. Whereas the thymus and the spleen develop with a distorted microarchitecture, LNs and PPs are completely absent in RelB-KO mice [170-172]. Furthermore, mice lacking RelB exhibit a complex phenotype with multiorgan inflammation, splenomegaly, myeloid hyperplasia and extramedullary hematopoiesis [170, 173, 174]. The severe inflammation can be attributed to an inefficient negative selection with a reduced intrathymic Treg development due to the defective thymic microarchitecture [170, 173, 175, 176]. Interestingly, whereas autoimmune diseases are usually associated with overt Th1 and Th17 activation, RelB-KO mice exhibit hallmarks of strong Th2 type immune reactions [177, 178].

Notably, the severe phenotype of RelB-KO mice can be partially ascribed to the requirement of RelB in non-hematopoietic cells. For example, the containment of the myeloid cell proliferation, the development of thymic stromal cells, the exaggerated chemokine secretion by RelB-deficient fibroblasts and the GC formation with marginal zone (MZ) structures require RelB in non-hematopoietic cells [93, 170, 173, 176, 179-181]. In contrast to that, within hematopoietic cells, RelB expression is mainly confined to DCs [182, 183]. In line with that, RelB-sufficient DCs transferred into RelB-deficient mice suppress autoimmunity, overt Th2-mediated airway inflammation and reduce thymic inflammation, suggesting a critical requirement of RelB for the DC-mediated establishment of immune tolerance [169, 176, 178, 184]. Indeed, RelB-KO mice lack CD8α- cDC2s and the remaining DCs show defective maturation and antigen-presenting function [173, 185].

In contrast to that, bone marrow chimera (BMC) experiments deploying wildtype (WT) recipients reconstituted with RelB-KO BM, allowed for narrowing down the hematopoietic-intrinsic requirement to the development of the Notch2-dependent Esam^{high} cDC2 subset [93]. Despite this narrow developmental requirement of RelB, the DCs derived from the RelB-KO BMCs show defects in the uptake of antigens and T cell priming, depending on the route of delivery. Whereas the uptake of subcutaneously injected antigens by DCs and their migration to the LNs seems not to be affected, the uptake of intravenously and intranasally supplied antigens is impaired in BMCs reconstituted with RelB-deficient BM [186-189].

In contrast to that, *in vitro*, DCs from RelB-KO BMCs neither exhibited defects in cross-presentation of heat-killed OVA-expressing *Listeria monocytogenes* to OT-I cells nor in priming of OT-II cells by OVA-loaded (MHCII-deficient) splenocytes [93].

The most recent data using DC-specific *Relb* ablation by targeting *Relb*-floxed alleles by Cre recombinase under the control of the CD11c gene *Itgax* further narrowed down the

requirement of RelB to the Notch2-dependent Sirpα+ cDC2 subset co-expressing CD117 (C-Kit) [190]. Albeit CD117 is critically involved in the development of DCs, *Itgax*-cre mediated *Relb* gene excision does not affect DC precursors [190, 191]. Instead, the CD117+ DC subset seems to be critically required for the Th2 polarization and consequently, RelB$^{\Delta DC}$ mice fail to install efficient immune response upon induction of allergic airway inflammation upon active immunization with OVA in aluminium hydroxide (alum) [190]. However, the mechanism underlying this defect in Th2 priming by RelB-deficient DCs remains elusive. One possibility is the potent suppression of proinflammatory immune responses by the expanded Treg population which has been observed in RelB$^{\Delta DC}$ mice [192]. Concomitantly, the generation of antigen-specific iTregs upon subcutaneous antigen delivery is impaired in RelB$^{\Delta DC}$ mice [192]. In summary, the requirement of RelB in DCs for the initiation of pro-inflammatory immune responses and for the installation of tolerance remain elusive.

6 Aim of the study

The role of the Nuclear factor κB family (NF-κB) RelB in the lymphoid organogenesis and the establishment of an intact immune system has long been appreciated. Dendritic cells (DCs) are one of the major players of the immune system representing the link between the innate and the adaptive immune responses and regulating the regulatory T cell (Treg) compartment. Findings from mice with a systemic *Relb* deletion (RelB-KO) and corresponding bone marrow chimeras (BMCs) have shown a critical involvement of RelB in the DC biology. Given the fact that RelB exerts a multitude of effects on other hematopoietic and non-hematopoietic cell types, these findings might be somewhat unreliable.

To circumvent these caveats, a mouse model with DC-specific deletion of the *Relb* gene, termed RelB$^{\Delta DC}$, has become available. RelB$^{\Delta DC}$ mice show normal DC development, except from the missing splenic CD117+ cDC2 subpopulation. Interestingly, the mice lacking RelB in DCs do not develop any apparent immunoproliferative disease and fail to install proinflammatory immune responses as has been published for Th2 allergic airway inflammation. The inhibition of proinflammatory immune responses is possibly suppressed by the enlarged Treg compartment present in the RelB$^{\Delta DC}$ mice. Due to this fact, the correct interpretation of the data obtained from RelB$^{\Delta DC}$ mice, suggesting inhibited initiation of immune reactions was hampered so far. In addition to that, the role of RelB in DCs for the development of Tregs in the light of the newly discovered microbiota dependent RORγt+ as well as tissue Treg subsets remained unclear.

The aim of this thesis is to delineate the role of RelB in DCs for the regulation of the Treg compartment and its contribution in the inhibition of immune reactions. To this end, RelB$^{\Delta DC}$ mice will be utilized, and the mouse model of an autoimmune inflammation – experimental autoimmune encephalomyelitis (EAE) – will be used to assess the disease progression in presence of Tregs and in a Treg-depleted context.

To gain further understanding of the role of RelB in DCs for the regulation of the Treg population, Tregs in the RelB$^{\Delta DC}$ mice will be studied in detail. Thereby, the Treg compartment will be comprehensively characterized and the implementation of RelB in DCs during the generation of thymic-derived nTregs, as well as RORγt+ iTregs and tissue Tregs will be analyzed. The general aim of these experiments is to understand the mechanisms underlying the Treg accumulation in the RelB$^{\Delta DC}$ mice.

In addition to that, RelB expression and the effects of its absence on the DC phenotype from various organs will be assessed to gain further insight into the role of RelB in DCs.

The role of the microbiota-dependent RORγt+ Tregs for the suppression of colitis and intestinal allergy towards orally applied antigens has been addressed in previous studies. In contrast to that, the role of this Treg subset in the installation of oral tolerance and suppression of airway allergy remains elusive, this issue will be addressed by a model of allergic airway inflammation after induction of oral tolerance.

7 Materials

7.1 Instruments and consumables

Table 1. List of instruments used in this thesis. FACS, fluorescence-assisted cell sorting; MACS, magnet-assisted cell sorting; PCR, polymerase chain reaction; BD, Beckton Dickinson

Instrument	Manufacturer
Analytic scales	Mettler
Autoclave	H + P
Catheter	B. Braun
Centrifuges	Eppendorf
CO_2 Incubator	Heraeus
Continuous flow vaporizer TEC5	Megamed
Cytospin® centrifuge	Shandon
DNA/RNA UV-Cleaner Box	Grant Bio
Electronic balance	G&G
Electrophoresis cell	Peqlab
Erlenmeyer flask	Omnilab
Flow cytometer BD Accuri™ C6	BD
Flow cytometer BD FACSAria™ III	BD
Flow cytometer BD FACSCanto™ II	BD
Flow cytometer BD LSRFortessa™	BD
Fluorescence microscope	Leica
Forceps	FST
Freezer -20 °C	Liebherr
Freezer -80 °C	New Brunswick
Gel casting system	Peqlab
Gel documentation system	Intas
Hybridization oven	Biometra
Ice machine	Manitowoc
Infrared lamp	Philips
Inhalator Pari Boy® SX	Pari
MACS magnet and stand	Miltenyi
Magnetic stirrer	Ikamag
Microplate reader	Tecan, BioTek
Microscope	Zeiss, Leica
Microplate washer	Tecan
Microwave	Philips
Mouse restrainer	Labart
Multichannel pipet 20 µl, 200 µl	Eppendorf, Brand
Neubauer cell counting chamber	Hecht Glaswarenfabrik
Operation table	Medax GmbH
PCR cycler Mastercycler® nexus gradient	Eppendorf
PH-Meter	VWR
Pipets 20 µl, 100 µl, 200 µl, 1 ml	Eppendorf

Instrument	Manufacturer
Pipette controller Brand® accu-jet®	Merck
Plexiglas® chamber for nebulization	HMGU workshop
Powder funnel	Neolab
Power supply E0303	Peqlab
Precision scales PB 303 DeltaRange	Mettler
Refrigerator	Liebherr
Safety cabinet ScanLaf Mars 1500	Mars
Scissors	FST
Spectrophotometer NanoDrop™ 2000 UV/Vis	Thermo Scientific
ThermoMixer® 5437	Eppendorf
Ultrapure water system Milli-Q®	Merck
Vacuum collecting bottle	Roth
Vacuum pump	Gilson
Vortex Genie 2	Scientific industries

Table 2. List of consumables used in this thesis

Consumable	Company
0,5; 1,5 ml; 2 ml tubes	Th. Geyer
1 ml, 2 ml, 5 ml, 10 ml syringes	B. Braun
10 µl, 200 µl, 1000 µl pipet tips	Fisher Scientific, Sarstedt
15 ml, 50 ml Falcon® tubes	Sarstedt
200 µl tube stripes	Fisher Scientific
5 ml, 10 ml, 25 ml serological pipets	Sarstedt
6-, 12-, 24 well plates	Sarstedt
96 well NUNC™ MaxiSorp® F-shaped bottom	Sigma-Aldrich
96 well plate U-shaped bottom	Greiner
Blood capillary tubes	Neolab
Cell strainer	Omnilab, Greiner
FACS tubes large	BD
FACS tubes small	Greiner
MACS LS columns	Miltenyi Biotec
Needles for injections	Roth
Pasteur pipettes	Fisher Scientific
Petri dishes	Sarstedt
Serum tubes with gel Microvette®	Sarstedt
Serum tubes with Li-Heparin	Sarstedt

7.2 Reagents

Table 3. List of general reagents used in this thesis. (D)MEM, (Dulbeccos's modified) Eagle's minimum essential medium; DPBS, Dulbecco's phosphate buffered saline.

Reagent	Company
100 bp DNA Ladder	Invitrogen
10x / 1x DPBS, pH 7.4	Gibco

Reagent	Company
3,3′,5,5′-Tetramethylbenzidine (TMB)	Sigma-Aldrich
Agarose	Sigma-Aldrich
Albumin Fraction V	AppliChem
Baytril ® Enrofloxacin	Bayer
BD GolgiStop™	BD
BD-instruments operating solutions	BD
Bovine serum albumin (BSA) fraction V	Sigma-Aldrich
Brefeldin A	Sigma
$CaCl_2$	Sigma-Aldrich
Citric acid monohydrate	Sigma-Aldrich
Diff-Quick kit	Medion Diagnostics
Dimethyl sulfoxide (DMSO)	Sigma-Aldrich
DMEM	PAA
DNA Stain clear G	Serva
EDTA ultrapure solution	Gibco
EDTA-2Na-2H_2O	Sigma-Aldrich
Ethanol absolute / denatured	Merck
Fetal calf serum (FCS)	PAA Laboratories
Folic acid	Sigma-Aldrich
Gentamicin	Invitrogen
H_2O_2 (30%)	AppliChem
H_2SO_4	Merck
HCl 37%	AppliChem
HEPES buffer solution, 1 M	Gibco
Ionomycin	Cayman chemical
KCl	VWR
$KHCO_3$	Sigma-Aldrich
L-Arginine	Sigma-Aldrich
L-Asparagine	Sigma-Aldrich
L-Glutamine	Life Technologies
L-Glutamine	Gibco
MEM non-essential amino acid sln.	Invitrogen
MEM vitamin sln.	Invitrogen
Mouse naïve CD4+ T cell Isolation Kit	Miltenyi Biotec
Na_2CO_3	Sigma-Aldrich
NaCl	Sigma-Aldrich
$NaHCO_3$	Merck
NaN_3	Morphisto
NaOH	Sigma-Aldrich
NH_4Cl	Sigma
Nonidet™ P 40 substitute (NP-40)	Sigma-Aldrich
O_2	Linde
Ovalbumin (OVA) grade V	Sigma
Penicillin-Streptomycin	Gibco, Invitrogen

Reagent	Company
Percoll®	GE Healthcare
Phorbol 12-myristate 13-acetate (PMA)	Biomol
RNeasy® Mini kit	Qiagen
Roswell Park Memorial Institute (RPMI) 1640	Gibco
Streptavidin	Sigma-Aldrich
Trizma® base	Sigma-Aldrich
Trypan blue	Sigma-Aldrich
Tween® 20	Sigma-Aldrich
β-Mercaptoethanol (β-ME)	Sigma

Table 4. List of *in vivo* reagents used in this thesis

Reagent	Company
Ampicillin sodium salt	Cayman chemical
Complete Freud's Adjuvant (CFA)	Sigma-Aldrich
Imject™ Alum Adjuvant	Fisher Scientific
Isoflurane	Baxter
Ketamine	WDT
Metronidazole (pure)	Actavis
Mycobacterium tuberculosis H37Ra	BD Difco
Myelin oligodendrocyte glycoprotein fragment 35-55 (MOG 35-55)	Auspep
OVA V	Sigma-Aldrich
OVA VI	Sigma-Aldrich
Ovalbumin fraction V	Sigma-Aldrich
PBS	Invitrogen
Pertussis toxin	Sigma-Aldrich
Saccharose	Sigma-Aldrich
Sevoflurane	Baxter
Soluble (sST2)	D. Rußkamp, HMGU
Streptomycin sulfate	Sigma-Aldrich
Vancomycin hydrochloride	Cayman
Xylazine	aniMedica

Table 5. Staining reagents for flow cytometry

Substance	Fluorophore	Company
Fixable viability dye	Zombie Aqua™	BioLegend
Fixable viability dye	Zombie NIR™	BioLegend
Streptavidin	BV711	BioLegend
Streptavidin	FITC	BioLegend
Streptavidin	PE	BD
Viability dye	DAPI	Sigma-Aldrich
Viability dye	PI	R&D Systems

Table 6. PCR primers. All primers were produced by Metabion.

Primer name	Sequence
Itgax-Cre fwd.	ATCTGGCAGCTGTCTCCA
Itgax-Cre rev.	GCGAACATCTTCAGGTTC
Foxp3-Cre fwd.	CAGTTTCAGTCCCCATCCTC
Foxp3-Cre int. fwd.	CAAATGTTGCTTGTCTGG TG
Foxp3-Cre int. rev.	GTCAGTCGAGTG CACAGT TT
Foxp3-Cre rev.	CGG GTCAGAAAGAATGGTGT
Relb-flox fwd.	GGGTATGGCTTATATCCCAGCAG
Relb-flox rev.	CTGGTGCTTGCTTTAATTTGGTT
Rorc-flox fwd.	TTCCTTCCTTCTTCTTGAGCAGTC
Rorc-flox rev.	CAGAAGAAAAGTATATGTGGCTTGTTG

Table 7. Enzymes

Enzyme	Catalogue no.	Company
Collagenase IA	C9891	Sigma-Aldrich
Collagenase D	11088882001	Roche
DNase I	D4263	Sigma-Aldrich
EconoTaq® DNA Polymerase	30031	Lucigen
Proteinase K	P2308	Sigma-Aldrich

7.3 Antibodies

Table 8. *In vivo* antibody used in this thesis

Reactivity	Clone	Lot	Company
a-CD25	PC-61.5.3	5569-1-3/0116	BioXCell

Table 9. ELISA antibodies and kits

ELISA Assay	Antibody function	Antibody description	Company; catalogue number
Total IgE	Primary antibody	Sheep anti-mouse IgE	The binding site #PC284
	Secondary antibody	Biotinylated rat anti-mouse-IgE	Clone R35-118 BD #553419
	Standard	Purified mouse IgE	Clone C38-2 BD #557079
OVA-IgG1	Primary antibody	n.a.	n.a.
	Secondary antibody	Biotinylated rat anti-mouse IgG1	Clone A85-1 BD #553441
	Standard	Purified mouse anti-chicken egg albumin	Clone OVA 14 Sigma#A6075
Ig panel	Primary antibody Secondary antibody Standard	SBA clonotyping system-HRP Southern Biotech Cat. No. 5300-05	

Table 10. FACS extracellular antibodies

Reactivity	Fluorophore	Clone	Company
Annexin V	FITC	#ANNEXINV01	Caltag
CD103	APC	2E7	eBioscience
CD103	BV510	2E7	BD
CD11b	eF450	M1/70	eBioscience
CD11b	PE-Cy7	M1/70	BD
CD11c	APC-Cy7	N418	BioLegend
CD11c	APC	N418	eBioscience
CD11c	FITC	HL3	Pharmingen
CD11c	PE-Cy7	N418	BioLegend
CD134	PE-Cy7	OX-86	eBioscience
CD152	PE-eF610	UC10-4B9	BioLegend
CD154	PE-Cy7	MR1	eBioscience
CD16/32	Unlabeled	2.4G2	BD
CD172a	PerCP-eF710	P84	eBioscience
CD185	Biotin	SPRCL5	eBioscience
CD205	PE	NLDC-145	BioLegend
CD25	AF700	PC61	BioLegend
CD25	PE	PC61.5	eBioscience
CD252	APC	RM134L	BioLegend
CD252	PE	RM134L	BioLegend
CD27	Pe-Cy7	LG.3A10	BioLegend
CD27	PE-Dazzle 594	LG.3A10	BioLegend
CD273	BV421	TY25	BD
CD274	BV711	MIH5	BD
CD278	BV421	C398.4A	BioLegend
CD278	PE-Cy7	C398-4A	BioLegend

Reactivity	Fluorophore	Clone	Company
CD279	BV785	29F.1A12	BioLegend
CD3	APC	145-2C11	eBioscience
CD357	APC	DTA-1	eBioscience
CD3e	AF700	17A2	BioLegend
CD3e	FITC	145-2C11	BD
CD4	AF700	RM4-5	eBioscience
CD4	BV711	RM4-5	BioLegend
CD4	PB	GK1.5	BioLegend
CD4	PerCP-Cy5.5	RM4-5	BD
CD4	PerCP-eF710	RM4-5	eBioscience
CD44	PE	IM7	eBioscience
CD45	AF700	30-F11	BioLegend
CD45	APC-eF780	30-F11	eBioscience
CD45.1	Biotin	A20	BD
CD45.2	BV421	104	BioLegend
CD45R	AF488	RA3-6B2	BioLegend
CD62L	FITC	MEL-14	eBioscience
CD64	PE-Cy7 ™	X54-5/7.1	BioLegend
CD8	AF700	53-6.7	eBioscience
CD8	eF450	53-6.7	eBioscience
CD80	APC	16-10A1	eBioscience
CD8a	APC	53-6.7	eBioscience
CD8a	APC-AF780	5H10	Invitrogen
CD8a	eF450	53-6.7	eBioscience
KLRG1	BV421	2F1/KLRG1	BioLegend
Ly-6C	AF700	AL-21	BD
Ly-6G	BV570	1A8	BioLegend
MHC II	APC-eF780	M5/114.15.2	eBioscience
MHCII	FITC	2G9	BD
Siglec-F	PE-CF594	E50-2440	BD
ST2	Biotin	DJ8	MD Bioproducts
ST2	APC	RMST-2	Affymetrix
ST2	Biotin	RMST2-2	eBioscience
TCR Vα3.2	APC	RR3-16	BioLegend
TCR Vβ11	PE	RR3-15	BioLegend
TCR Vβ2	FITC	B20.6	BD
TCR Vβ3	FITC	KJ25	BD
TCR Vβ4	FITC	KT4	BD
TCR Vβ5.1, 5.2	FITC	MR9-4	BD
TCR Vβ6	FITC	RR4-7	BD
TCR Vβ7	FITC	TR310	BD
TCR Vβ8.1, 8.2	FITC	MR5-2	BD
TCR Vβ8.3	FITC	1B3.3	BD
TCR β	Biotin	H57-597	BD
TCRVβ10^{b}	FITC	B21.5	BD
TCRVβ11	FITC	RR3-15	BD

Reactivity	Fluorophore	Clone	Company
TCRVβ12	FITC	MR11-1	BD
TCRVβ13	FITC	MR12-3	BD
TCRVβ14	FITC	14-2	BD
TCRVβ17[a]	FITC	KJ23	BD
TCRVβ9	FITC	MR10-2	BD

Table 11. FACS intracellular antibodies

Reactivity	Fluorophore	Clone	Company
FoxP3	FITC	FJK-16s	eBioscience
Foxp3	PerCP-Cy5.5	FJK-16s	eBioscience
FoxP3	eF450	FJK-16s	eBioscience
Gata3	eF660	TWAJ	eBioscience
Gata3	PE-Cy7	L50-823	BD
Helios	Pacific Blue	22F6	BioLegend
Helios	PerCP-Cy5.5	22F6	BioLegend
IFN-γ	PE	XMG1.2	BD
IFN-γ	PE-Cy7	XMG1.2	eBioscience
IL-17A	PerCP-Cy5.5	TC11-18H10	BD
IL-17A	PE	TC11-18H10	BD
Ki-67	Pe-Cy7	B56	BD
RORγt	PE	AFKJS-9	eBioscience

7.4 Mouse lines

Table 12. Mouse lines used in this thesis. KO, knockout; OE, overexpression; TCR, T cell receptor.

Type	Line, reference	Description	Source
Complete KOs	Bcl3-KO (*Bcl3* ^{tm1Ver}) [193]	Genetic targeting of the *Bcl3* gene resulting in the lack of functional BCL3 protein	E. Glasmacher, Helmholtz Center Munich
	IL-33-KO (IL-33 $^{Gt/Gt}$) [73]	IL-33-LacZ gene trap knockout	J.-P. Girard, Université de Toulouse
	p50-KO (*Nfkb1* ^{tm1Bal}) [194]	Genetic targeting of the *Nfkb1* gene encoding p50 protein	E. Glasmacher, Helmholtz Center Munich
	RelB-KO [170]	Genetic targeting of exon 4 resulting in constitutive ablation of RelB protein	Falk Weih, FLI Leibniz Institute for Age Research, Jena
Cre lines	Foxp3-cre (Tg(FoxP3-EGFP/cre) [195]	Foxp3 promotor-driven BAC transgenic Cre mice	The Jackson laboratory
	CD11c-cre (Tg(*Itgax*-cre)$^{1\text{-}1Reiz}$) [196]	Insertion of a BAC transgene containing Cre-recombinase under the control of CD11c gene *Itgax* promotor	The Jackson laboratory

Type	Line, reference	Description	Source
Floxed lines	RORγt-flox (*Rorc* ^{tm3Litt}) [197]	Insertion of *loxP* sites in exons 3-6 of the *Rorc* gene	The Jackson laboratory
	BALB/c; Relb-flox (BALB/c *Relb*$^{fl/fl}$)	*LoxP* flanked exon 4 of the *Relb* gene on BALB/c genetic background	U. Zimber-Strobl, Helmholtz Center Munich
	Relb-flox (Relbfl/fl) [181]	*LoxP* flanked exon 4 of the *Relb* gene on C57BL/6 genetic background	M. Riemann, FLI Leibniz Institute for Age Research, Jena
Conditional KO/OE lines	BCL3^{TOE} (*Rosa26*^{flox}*STOP*^{flox} B*cl3-eGFP*; *Cd4*-cre) [198, 199]	Insertion of a *Bcl3* transgene into the *Rosa26* locus downstream of *loxP* flanked STOP cassette, intercrossed with *Cd4*-cre-mice resulting in T cell specific BCL3 overexpression (TOE)	E. Glasmacher, Helmholtz Center Munich
	RelB$^{\Delta DC}$ (*Relb*$^{fl/fl}$- *Itgax*-cre)	CD11c (*Itgax*)-cre mediated conditional ablation of *Relb*-floxed alleles	Generated in the lab
	RelB$^{\Delta Treg}$ (*Relb*$^{fl/fl}$- *Foxp3*-cre)	*Foxp3*-cre mediated conditional ablation of *Relb*-floxed alleles	Generated in the lab
	RORγt$^{\Delta Treg}$ (*Rorc* ^{tm3Litt}; *Foxp3*-cre)	*Foxp3*-cre mediated ablation of *Rorc*-floxed alleles	Generated in the lab
TCR transgenic/reporter mice	2D2; FoxP3-GFP (Tg(Tcra2D2, Tcrb2D2)^{1Kuch}-*Foxp3*^{tm1Kuch}) [200, 201]	*Foxp3*-GFP knock-in reporter mice intercrossed with mice carrying TCR specific for MOG 35-55 epitope	T. Korn, Technical University Munich
	Foxp3-mRFP (*Foxp3*^{tm1Flv}) [202]	FoxP3-mRFP knock-in reporter mice	G. Eberl, Institut Pasteur, Paris
	Katushka-RelB (Relb-Cre-P2A-Katushka) [181]	BAC transgenic mice containing Cre-P2A-Katushka (TurboFP635) gene inserted into the first exon of *Relb* locus	M. Riemann, FLI Leibniz Institute for Age Research, Jena
	OT-II; CD45.1+; Rag1-/- (Tg(TcraTcrb)425Cbn; B6129S7-*Rag1* ^{tm1Mom}; B6.SJL-Ptprc^{a} Pepc^{b}) [203]	Mice producing no other but exclusively OVA 323-339 peptide-specific congenically marked CD45.1+ T cells	D. Baumjohann, Ludwig-Maximilians-Universität München and V. Buchholz, Technical University Munich
	RelB$^{\Delta DC}$ FoxP3-mRFP	Mice with *Itgax*-cre mediated ablation of *Relb* intercrossed with the Foxp3-mRFP reporter mice	Generated in the lab

7.5 Buffers and media

Table 13. List of buffers and media used in this thesis

Type	Buffers and solutions	Composition
Genotyping	1x TAE Buffer	40 mM Tris pH 7.6, 20 mM acetic acid, 1 mM EDTA
	50x TAE	2 M Tris, 50 mM EDTA 1 M acetic acid, pH 8.0
	Agarose Gel, 1.5%	1x TAE buffer, 1.5 % (m/v) agarose, 4 x 10^{-3} % DNA stain clear G
	Ear clip digestion buffer	10 mM Tris pH 8.0, 50 mM KCl, 0.5 % NP-40, 0.5 % Tween® 20, 0.2 mg/ml Proteinase K
ELISA	10x Tris	500 mM Tris base, pH 7.4 with HCl
	10x DPBS	Gibco
	ABTS stock	15 mg/ml ABTS in *Aqua dest.*
	ABTS substrate	0.05 M citrate buffer, 0.03 % H_2O_2, 0.3 mg/ml ABTS
	carbonate-bicarbonate coating	0.1 M $NaHCO_3$, 0.034 M Na_2CO_3, pH 9.5
	PBS-BSA blocking	1x PBS, 1 % BSA, 0.05 % NaN_3
	PBS-T washing buffer	1x PBS, 0.05 % Tween® 20
	Stop solution TMB	2 M H_2SO_4
	TMB stock solution	24 mg/ml TMB in 50/50 (v/v) Ethanol/DMSO
	TMB substrate buffer	0.2 M citric acid, pH 3.95 with 4 M KOH
	TMB substrate solution	0.2 M citrate buffer pH 4, 0.01 % H_2O_2, 24 µg/ml TMB
	Tris-BSA blocking	1x Tris, 1 % BSA
	Tris-T washing buffer	1x Tris, 0.05% Tween® 20
Cell preparation	30 - 80 % Percoll®	RPMI-1640, 30 - 80 % Percoll® in 1x PBS
	ACK	155 mM NH_4Cl, 10 mM $KHCO_3$, 1 mM EDTA-2Na-2H_2O, pH 7.2 - 7.4 with 1 N HCl
	Annexin V binding	10 mM HEPES, 0.14 M NaCl, 0.25 mM $CaCl_2$, pH 7.4
	FACS buffer	1x PBS, 5 mg/ml BSA, 10 mM NaN_3, 2 mM EDTA
	FoxP3 / Transcription Factor Staining Buffer Set	eBioscience
	MACS Buffer	1x DPBS, 0.5 % FCS, 2 mM EDTA
	Permeabilization buffer 10x	eBioscience
	PBS-BSA	1x PBS, 0.5 % BSA
Cell culture media	Clone medium	DMEM, 10% FCS, 50 U/ml penicillin/streptomycin, 1x MEM-non-essential amino acids solution, 1x MEM vitamin solution, 0.66 mM L-Arginine, 0.27 mM L-Asparagine, 13.6 µM folic acid, 0.2 mM β-ME, 0.1 mg/ml gentamicin
	RPMI complete	RPMI-1640, 1 % Glutamine, 1 % Pen-Strep, 10 % FCS, 50 µM ß-ME
	RPMI with FCS	RPMI-1640, 5 % FCS
	RPMI with HEPES	RPMI-1640, 25 mM HEPES

Type	Buffers and solutions	Composition
Digestion media	Adipose tissue	1x DPBS, 0.5 % BSA, 10 mM $CaCl_2$, 0.5 mg/ml Collagenase D
	CNS mononuclear cells	DMEM, 2.5 mg/ml Collagenase D and 1 mg/ml DNase
	DC isolation	RPMI-1640, 0.5 mg/ml Collagenase D and 50 µg/ml DNase I
	Gut-LPL digestion	RPMI-1640, 25mM HEPES, 0.5 mg/ml Collagenase D and 50 µg/ml DNase I
	Gut LPL pre-digestion	PBS, 30 mM EDTA, pH 8.0
	Lung mononuclear cells	RPMI-1640, 2 % FCS, 1 mg/ml Collagenase IA, 50 µg/ml DNase I

8 Methods

8.1 Mouse protocols

i) Breeding and interventions

All mouse strains, unless stated otherwise, were backcrossed on the C57BL/6 background for a minimum of 10 generations and used between the ages of 6 and 20 weeks. Mouse lines were either bred in the mouse facility (E-stripe) of the Helmholtz Center Munich or provided by cooperation partners according to Table 12. All interventions were performed in accordance with the European Convention for Animal Care and Use of Laboratory Animals and were approved by the local ethics committee and the competent authorities.

ii) *Intraperitoneal (i.p.)* injection

Mice were injected *i.p.* with sterile fluids using a 1 ml syringe and a 25 G needle. To this end, mice were restrained by the scuff with the abdomen side up and the head pointed down. The needle was injected in the lower right quadrant of the abdomen at an angle of appr. 20 degrees to a depth of around 4 - 5 mm to prevent intestinal injury. A maximum of 10 ml/kg weight was injected per mouse.

iii) *Intravenous (i.v.)* injection

I.v. injections were used for transfer of bone marrow cells or naïve T cells into recipient mice. To this end, mice were warmed for 5-10 min using an infrared lamp put around 35 cm away from the mice. Thereafter, the mice were restrained in a restrainer device and a maximum volume of 1 % of the mouse weight was injected into the tail vein using a 30 G needle and a 1 ml syringe.

iv) Anesthesia

Mice were anesthetized by *i.p.* injection with 10 µl per 1 g body weight of injectable anesthetic solution containing 10 % ketamine and 2 % xylazine in PBS. For short term anesthesia, inhalation with 2 % isoflurane in O_2 was applied.

v) Euthanasia

Mice were killed by cervical dislocation except when intact CNS or airways for BAL were required. For the latter, an overdose of injectable anesthetic solution was applied.

vi) Blood collection

A maximum of 200 µl blood were collected by retroorbital bleeding using capillary tubes after anesthetizing mice with 2 % isoflurane in O_2.

vii) Generation of bone marrow chimeras

Recipient mice were lethally irradiated with two doses of 6 Gy γ-irradiation from a Co-60 source 4 hours apart. After that, the recipients were reconstituted with 8 x 10^6 purified bone marrow cells in a volume of 150 µl PBS *i.v.* The recipient mice were kept on 0.25 mg/ml

Enrofloxacin (Baytril®; Bayer Vital GmbH) in drinking water for 3 weeks after irradiation. The reconstitution of lymphoid organs in the bone marrow chimeras were analyzed after 10 - 12 weeks.

viii) Induction of oral tolerance and allergic airway inflammation

Tolerance induction towards ovalbumin (OVA) was induced by intragastric gavage of 20 mg OVA V in 200 µl PBS at days -13, -10 and -7 prior to the immunization with OVA in aluminum hydroxide (alum). Additionally, non-tolerized control groups were gavaged with PBS instead of OVA. Immunization of mice was performed by *i.p.* injections with 10 µg OVA complexed with 2 mg alum in a total volume of 200 µl PBS at days 0, 7 and 14. The challenges were done by nebulizing the immunized mice with 1 % OVA aerosol at days 28, 30 and 33. To this end, mice were put into an acrylic glass chamber and exposed to the OVA aerosol generated by a Pariboy® inhalator for 15 min. The analysis was done at day 34.

ix) In vivo neutralization of IL-33 with soluble ST2 (sST2)

Soluble ST2 was generated as previously described by Dennis Rußkamp, Helmholtz Center Munich [61]. Mice were injected *i.p.* with 100 mg sST2 three times per week for 3 weeks. Thereafter, splenic T cells were analyzed by flow cytometry (fluorescence-assisted cell sorting, FACS).

x) Eradication of mouse microbiota by antibiotics treatment

Pregnant mice at appr. day 7 of pregnancy were supplemented with a combination of antibiotics containing 1 mg/ml Ampicillin, 0.5 mg/ml Vancomycin, 0.5 mg/ml Metronidazole, 1 mg/ml Streptomycin and 2 % saccharose in drinking water. The drinking bottles were replaced weekly. After birth of the pups, the supplementation with antibiotics was continued until analysis. At 4 weeks of age, the pups were euthanized and the lymphocytes from the SI-LP were isolated according to the corresponding protocol. For the flow cytometric analysis, samples of three RelB-Katushka+ antibiotics-treated mice were pooled. As controls, two untreated RelB-Katushka+ mice and one RelB-Katushka negative control were used as separate sample, each.

xi) Experimental autoimmune encephalomyelitis (EAE) induction

EAE induction was performed in cooperation with prof. T. Korn, Technical University Munich. To this end, mice were immunized subcutaneously at the base of the tail at day 0 with 200 µl of an emulsion containing 200 µg of the immunodominant epitope of the myelin oligodendrocyte glycoprotein (MOG 35-55) and 500 µg Mycobacterium tuberculosis in complete Freund's adjuvant (CFA). Additionally, mice received 200 ng pertussis toxin intravenously at days 0 and 2 after the immunization. Alternatively, EAE was induced in cooperation with Nico Andreas, Leibniz Institute on Aging using a kit from Hooke laboratories according to the manufacturer's instructions. Clinical signs of disease were monitored according to the following scheme: 1 — tail paralysis; 2 — hind limb impairment; 3 — hind limb paralysis; 4 — front limb paralysis; 5 — death. In case the hind limb movement was strongly impaired, mice were provided with a HydroGel® water pads and easily

accessible wet food. At the peak of disease, mononuclear cells were recovered from the CNS according to the protocol and analyzed by FACS.

xii) Treg depletion with anti-CD25 antibody PC61

Tregs were ablated by i.p. injection of 500 mg of anti-CD25 Ab (clone PC61; BioXCell) on days -5 and -3 prior to MOG 35-55 immunization. EAE induction and recording of the EAE severity score were done as described (see EAE induction section). Treg depletion efficiency was analyzed by FACS of blood lymphocytes. At the peak of EAE, mice were euthanized, and mononuclear cells recovered from the CNS were analyzed by FACS.

xiii) De-novo induction of MOG-specific Tregs from naïve T cells after EAE induction

For analysis of de-novo MOG-specific Treg induction during EAE, 2.5 x 10^6 sort-purified naïve MOG-specific 2D2 T cells (according to the protocol in 8.8.1i)) were injected *i.v.* 24 h prior to EAE induction into RelB$^{\Delta DC}$ or WT mice. EAE was induced in the recipient mice according to the protocol 8.1 . At day 7 after EAE induction, cells from inguinal lymph nodes were analyzed by flow cytometry. Thereby, MOG-specific Tregs were identified as TCR Vα3.2+ Vβ11+ Foxp3(GFP)+ T cells.

xiv) OT-II transfer and oral tolerance induction

WT and RelB$^{\Delta DC}$ mice were *i.v.* injected with 0.5 x 10^6 naïve CD45.1+ OT-II cells. The recipient mice were provided with 1.5 % OVA fraction V (Sigma-Aldrich-Aldrich) in drinking water *ad libidum* for 9 days. On 10^{th} day, mice were sacrificed and the induction of OVA-specific OT-II Tregs in various organs was analyzed by FACS.

8.2 Mouse genotyping

8.2.1 Genotyping FACS

i) FoxP3-mRFP mice

FoxP3-mRFP mice were genotyped by flow cytometric analysis of blood. To this end, 100 µl blood were subjected to erythrocyte lysis according to the section 8.4 and stained with DAPI, as well as anti-CD3-APC antibodies. The mRFP was excited by the yellow-green laser and was detected in the 610/20 (Pe-Texas Red) channel using BD LSRFortessa^{TM}.

ii) Katushka-RelB

Katushka-RelB mice were genotyped equivalently, but without CD3 staining. The Katushka fluorophore was excited by the yellow-green laser and was detected in the 670/30 (PE-Cy5) channel.

8.2.2 Genotyping polymerase chain reaction (PCR)

i) Ear clip digestion

Ear clips were collected in 1.5 ml tubes and digested over night at 56 °C with 100 µl ear clip lysis buffer containing 0.2 mg/ml Proteinase K. Prior to the ON-digestion, ear clips were heated to 95 °C in 50 µl lysis buffer without Proteinase K for 10 min to activate the digestion. After that, another 50 µl of lysis buffer containing the doubled concentration of Proteinase K (0.4 mg/ml) were added. After the ON-digestion, the tubes were mixed using a vortex mixer and the proteinase K was inactivated by heating the tubes to 95 °C for 15 min after which the remaining undigested material was centrifuged off for 10 min at 10000 g. For the genotyping PCR reactions, the indicated amount of the supernatant was used.

ii) PCR protocols

Genotyping PCR was performed using the digested ear clip supernatant, primers (10 µM) and EconoTaq® according to the pipetting scheme shown in Table 14. The genotyping PCRs were run according to the corresponding PCR programs shown in Table 15 and Table 16 in the PCR cycler. The PCR products were detected after gel electrophoretic separation in agarose gels.

Table 14. Genotyping PCR pipetting schemes for 1 sample

	Genotyping PCR			
Volumes in µl	***Relb*-flox**	***Itgax*-Cre**	***Rorc*-flox**	***Foxp3*-Cre**
EconoTaq®	10	10	12.5	12.5
Water	8	5	6.5	2.5
Fwd. primer	0.5	2	2.5	2.5
Rev. primer	0.5	2	2.5	2.5
DNA template	1	1	1	3
Int. fwd. primer	-	-	-	1
Int. rev. primer	-	-	-	1
Total sample volume	20	20	25	25

Table 15. PCR programs for *Itgax*-cre, *Relb*-flox, *Foxp3*-cre genotyping

	Genotyping PCR					
	***Itgax*-Cre**		***Relb*-flox**		***Foxp3*-Cre**	
Step	**T (°C)**	**t (sec)**	**T (°C)**	**t (sec)**	**T (°C)**	**t (sec)**
denaturation	94	240	95	240	94	180
denaturation	94	45	94	30	94	30
annealing	58	30	58	30	62	30
elongation	72	45	72	90	72	30
close loop	72	300	72	600	72	120
store	6	hold	6	hold	10	hold
cycles	35 cycles		32 cycles		30 cycles	

Table 16. PCR program for *Rorc*-flox genotyping PCR

Step	T (°C)	t (sec)	Cycles
denaturation	94	120	
denaturation	94	20	10 cycles
annealing	65	15	-1,5°C
elongation	68	10	per cycle
denaturation	94	15	
annealing	50	15	28 cycles
elongation	72	10	
close loop	72	120	
store	10	hold	

iii) Agarose gel preparation

For 1.5 % agarose gel, 100 ml TAE buffer containing 1.5 g agarose were boiled in an Erlenmeyer flask in a microwave at 700 W for 3 min. After that, the solution was allowed to cool down to appr. 60 °C, 4 µl of the DNA stain clear G (Serva) were added and the agarose solution was poured into the DNA gel caster with combs and allowed to polymerize for 1 hour before use.

iv) DNA electrophoresis

After the completion of the genotyping PCR programs, the PCR products were loaded onto agarose gels submerged in 1x TAE buffer in an electrophoresis chamber. A 100 bp DNA ladder served as a size reference. DNA agarose gel electrophoresis was run at 100 mA for 45 min. Thereafter, the fluorescence of the DNA complexed with DNA stain clear G was visualized upon excitation with UV light. The signal was digitalized by a camera.

8.3 Cell isolation from mouse organs

All digestion steps were performed at 37 °C, unless otherwise stated. If not indicated differently, all centrifugation steps were done at 4 °C at 400 g, Percoll® gradient centrifugations were done at RT.

i) Isolation of T cells from lymphoid tissues:

For the analysis of T cells, single cell suspension of lymphoid organs (thymi, spleens, LNs) was obtained by meshing the organs through 70 µm cell strainers which were placed into wells of a 6-well plate containing 5 ml FACS buffer. The cell suspension of thymi and LNs was centrifuged and the cell pellet was resuspended in FACS buffer and stored on ice.

ii) Isolation of DCs from lymphoid tissues and digestion of non-lymphoid organs

For the recovery of DCs from lymphoid organs such as spleen, thymus and LN and for digestion of liver and PPs, the tissues were collected in 24-well-plates containing 1 ml DC isolation medium, fragmented and digested for 20 min at 37 °C with shaking at 100 rpm. After that, the digested tissues were pipetted up and down several times and transferred

into a 70 µm tissue strainer placed on top of a 50 ml Falcon tube. The organs were meshed with a plunger and the cell strainer was washed twice with 5 ml FACS Buffer. The cell suspension was centrifuged, and the pellet was resuspended in FACS buffer and stored on ice until further analysis.

iii) Isolation of lymphoid cells from visceral adipose tissue

Fat pads were cut in 2 ml PBS-BSA into fine pieces and digested at 37 °C at 200 rpm for 20 min with 3 ml adipose tissue digestion medium in 50 ml tubes. After the digestion, 10 ml PBS-BSA were added and the tissue was homogenized by pipetting. The samples were centrifuged at 500 g and 4°C for 10 min, the fat containing upper layer was removed and the pellet containing lymphocytes was analyzed by FACS.

iv) Isolation of CNS mononuclear cells

At the peak of EAE, mice were sacrificed and perfused with 10 ml cold PBS through the left cardiac ventricle using a 10 ml syringe and a 20 G needle after opening the right ventricle. Additionally, the spinal cords were flushed by PBS through a syringe. After excising the CNS tissue, it was cut into small pieces and digested for 45 min at 37 °C in CNS digestion medium. The digested CNS tissue was homogenized through a 70 µm cell strainer and centrifuged at 400 g for 10 min. For isolation of mononuclear cells, a discontinuous Percoll gradient was performed by resuspending the cell pellet in 30 % Percoll® and layering the latter onto a 70 % Percoll® layer. Centrifugation was run at 1800 g for 20 min without break, and the interphase containing mononuclear cells was collected for further analysis.

v) Isolation of gut LPLs

Small intestine was removed from the peritoneal cavity and flushed with PBS. Peyer's patches were cut off and stored on ice cold PBS until further steps. The gut was cut longitudinally and then transversally into 2-3 cm pieces and incubated in 50 ml tubes with gut LPL pre-digestion medium on ice. Thereafter, the tubes were shaken vigorously for 30 sec, and the gut pieces were washed several times with ice cold PBS until the PBS appeared clear and free of mucus. Thereafter, gut pieces were transferred into 6-well-plates, minced into fine pieces, and digested with gut LPL digestion medium at 37 °C for 15 min. After the digestion, the samples were pipetted up and down for appr. 50-100 times to disaggregate the tissue. The tissue was left to settle down for appr. 3 minutes and the supernatant was carefully transferred into a fresh 50 ml tube through a 100 µm cell strainer. 6 ml of fresh gut LPL digestion medium were added to the gut samples and the digestion/disaggregation procedure was repeated two more times. For the second digestion step, the samples were incubated for 20 min and for the third digestion step for 30 min. The supernatants of each digestion step were collected in the same tube and centrifuged for 10 min at 500 g. The cell pellet was resuspended in 40 % Percoll® and transferred into 15 ml tubes on top of an 80 % Percoll® layer. The discontinuous Percoll® gradient was run at room temperature, at 1500 g for 15 min without brake. The upper layer was removed and the interlayer containing LP lymphocytes was collected and washed with PBS for further analysis.

vi) Isolation of lymphocytes from lung tissue

The lung tissue was removed from the pleural cavity, placed into 6-well-plates, minced into fine pieces, and digested with 3 ml lung digestion medium for 30 min at 37 °C. The digested tissue was transferred onto a 70 µm cell strainer and meshed using a plunger. The cell suspension was centrifuged and a discontinuous Percoll® gradient was performed. To this end, the pellet was resuspended in 40 % Percoll® and transferred into new 15 ml tubes. 80 % Percoll® was poured underneath that layer through a Pasteur pipette. The centrifugation was run at 1500 g, at room temperature for 15 min without brake. After the upper layer was removed, the interlayer containing lymphocytes was collected, washed with FACS buffer and stored on ice for further analysis.

vii) Collection of bronchoalveolar lavage fluid (BAL) fluid

The BAL collection, sample preparation in the Cytospin® centrifuge and analysis by differential cell counting was performed with the help of Dr. F. Alessandrini (Helmholtz Center Munich).

BAL fluid was recovered by instillation of PBS through a catheter inserted into the trachea of euthanized mice. To this end, five times 0.8 ml PBS were injected and aspirated through the catheter by a 1 ml syringe while gently massaging the thorax of the mouse. The recovered BAL fluid was collected in a 15 ml tube on ice and stored until further analysis.

viii) Peritoneal exudate cells (PEC)

Peritoneal exudate cells were recovered by flushing the peritoneal cavity of mice with PBS. To this end, the skin covering the abdomen was removed and 10 ml ice cold PBS were injected into the peritoneal cavity using a 10 ml syringe and a 25 G needle. The needle was removed, and the abdomen was gently massaged to elevate the PEC cell recovery. After that, the PEC fluid was retrieved by the same syringe and needle, transferred into 15 ml tubes and kept on ice until further analysis.

ix) Bone marrow preparation

For bone marrow isolation, femurs and tibia were flushed with sterile ice-cold PBS using a 23 G needle and a 10 ml syringe filled with PBS. Afterwards, the collected BM was passed through a 70 µm cell filter and washed 3 times with sterile PBS before cell counting.

x) Preparation of cells and serum from blood

For serum, blood was collected into Microvette® serum tubes and centrifuged at 7000 g for 5 min and stored at -80 °C. When cells were required, blood was collected in Li-Heparin tubes and centrifuged at 400 g for 5 min. The pellet was subjected to erythrocyte lysis prior to further analysis.

8.4 Erythrocyte lysis

Samples with a high contamination with erythrocytes were subjected to erythrocyte lysis. To this end, single cell suspension was centrifuged for in 50 ml tubes, the cell pellet was resuspended in 1 ml ACK buffer and incubated for 2 min at room temperature. After that,

10 ml FACS buffer were added to stop the lysis and the cells were washed by centrifugation and resuspension in FACS buffer. Prior to further analysis, the cell suspension was filtered through 40 µm strainer.

8.5 BAL cytospins

The Cytospin® sample holder consisting of the microscope slide, filter card, Cytofunnel® sample chamber and a steel slide Cytoclip™ was assembled. The sample holders were placed into the Cytospin® centrifuge. 150 µl of the cell suspension were pipetted into the funnel. The centrifugation was done at 400 g for 10 min. Afterwards, the slides were taken out and let dry overnight. On the next day, the cells were fixed and stained with Diff-Quick kit according to the manufacturer's protocol and the cells were differentially counted under the microscope.

8.6 Cell counting

Cells were counted by either of the methods:

i) Manual counting using Neubauer hemocytometer under a microscope. Typically, cell suspensions were diluted to a concentration of around 10^6 cells/ml and 10 µl of the cell suspension was loaded into each side of the chamber. 0.2 % trypan blue was used as viability dye.

ii) By BD Accuri™ C6 flow cytometer (BD) using 50 µl PI-stained cell suspension in small FACS tubes.

iii) Using a Cytometer Guava® easyCyte™ 5HT (Merck Millipore) to count samples in 96-well format with 7-AAD (BD Biosciences) as viability dye.

8.7 Flow cytometry

Cells were analyzed by BD LSRFortessa™, BD FACSCanto™ II or by BD FACSAria™ III flow cytometer. The data was further analyzed by FlowJo software (Tree Star).

i) Extracellular cell staining for FACS

For extracellular FACS staining, appr. 1 x 10^7 cells were used. The cell suspensions were prepared according to the protocols in the section 8.3 and transferred into 96 well U-bottom shaped plates. The cells were washed with PBS and resuspended in PBS containing fixable live-dead reagent (Table 5). After incubation for 10 min at 4 °C, the cells were washed once by adding 200 µl FACS Buffer and centrifuging for 5 min at 400 g at 4°C. The cell pellet was resuspended in 50 µl of antibody mix for 20 min at 4 °C. The cells were washed twice and either analyzed immediately by transferring into FACS tubes or fixed by resuspension in 200 µl Fixation/Permeabilization solution (FoxP3 / Transcription Factor Staining Buffer Set, eBioscience) over night at 4 °C or for 1 h at RT in the dark. In cases when cells were labelled with biotinylated antibodies, an additional staining step with streptavidin-conjugates was done before fixation. To this end, the washed cells were resuspended in at least 50 µl of

the appropriate streptavidin solution and incubated for 10 min at 4 °C in the dark before washing and fixation.

ii) Annexin V staining

For Annexin V staining, extracellularly stained cells were washed with Annexin V binding buffer (ABB) once and stained with Annexin V antibodies diluted in ABB for 15 min in the dark. Thereafter, the cells were washed with ABB twice and fixed if intracellular staining was required or analyzed by FACS unfixed.

iii) Intracellular staining for FACS

The cells which were fixed with Fixation/Permeabilization solution (FoxP3 / Transcription Factor Staining Buffer Set, eBioscience) were spun down at 500 g for 5 min and washed with permeabilization buffer (FoxP3 / Transcription Factor Staining Buffer Set, eBioscience) twice. After that, the cells were resuspended in 50 µl permeabilization buffer containing intracellular antibodies.

iv) T cell restimulation for cytokine analysis

Analysis of cytokine producing T cells was performed by flow cytometry of *ex vivo* restimulated cells. To this end, isolated cells were restimulated in culture medium containing phorbol 12-myristate 13-acetate (PMA, 20 ng/ml, Sigma), ionomycin (1 µg/ml, Sigma), and GolgiStop™ (1 µl/ml, BD Biosciences) at 37 °C, 5 % CO_2 for 4 h. Thereafter, restimulated cells were washed and treated as described in the corresponding sections (extracellular and intracellular cytokines staining).

8.8 Cell sorting

8.8.1 FACS sorting

All single cell suspensions were kept in RPMI complete and FACS sorted into polystyrene tubes containing 5 ml PBS-BSA. The purity of sorted cells was confirmed by FACS re-analysis.

i) Isolation of naïve T cells from 2D2; FoxP3-GFP mice

Naïve T cell sorting for the analysis of MOG-specific *de-novo* Treg induction was performed in cooperation with Prof. T. Korn, Technical University Munich. To this end, CD3+CD4+FoxP3-GFP- cells were sorted from 2D2; FoxP3-GFP reporter mice using BD FACSAria™ III cell sorter.

ii) Isolation of Tregs from FoxP3-mRFP reporter mice

Treg sorting of the $RelB^{\Delta DC}$ and control mice on the FoxP3-mRFP background for RNA-Seq was performed in cooperation with the Flow Cytometry Unit of the Technical University Munich. Tregs were sorted as live/dead-AQUA-CD45+CD3+CD4+ CD8-FoxP3-mRFP+ cells.

iii) Naïve cell sorting from OT-II; CD45.1+; Rag1-/- mice

For OT-II transfer experiments, FACS sorting of naïve T cells was performed with the help of Nico Andreas, Leibniz Institute on Aging. To this end, naïve T cells were sorted as DAPI-CD45+CD4+MHCII-CD19-CD62L+.

8.8.2 Magnet-assisted cell sorting (MACS)

Alternatively to the FACS sorting, naïve T cells from the CD45.1+; OT-II; Rag-1-/- mice for transfer experiments were isolated using mouse naïve CD4+ T cell Isolation Kit according to the manufacturer' instructions.

For isolation of naïve T cells from 10^8 total cells obtained from spleens and lymph nodes of OT-II mice, the following protocol was used: 400 µl single cell suspension were mixed with 100 µl Biotin-Antibody Cocktail and incubated for 5 min in the refrigerator. 200 µl MACS buffer and 200 µl anti-biotin Micro Beads as well as 100 µl CD44 Microbeads were added, mixed and incubated for 10 minutes in the refrigerator. The cells were washed by adding 2 ml MACS buffer, centrifuging, and aspirating the supernatant. Meanwhile, an LS column was placed in a MACS magnet and rinsed with MACS buffer. The cell pellet was resuspended in 500 µl and loaded onto the column. The flow-through containing the naïve T cells was collected. The column was washed with 3 ml buffer to recover the remaining naïve T cells from the column. Thereafter, cells were washed three times with sterile PBS and injected i.v. into recipient mice (according to the protocol).

8.9 Immunoassays

For all ELISA immunoassays, 96 well flat-shaped bottom NUNC-MaxiSorp™ plates were used (NUNC # 439454). Unless stated otherwise, the blocking of the plates and the dilution of sample and reagents were done in blocking buffer (Tris-BSA). If not indicated differently, after each incubation step, plates were washed three times with 200 µl washing buffer (Tris-T). If not indicated differently, 50 µl of the reagent solutions were used. The TMB substrate solution was made immediately before use consisting of substrate buffer, 0.01 % H_2O_2 and 24 µg/ml TMB. The reaction was stopped by adding 25 µl 2M H_2SO_4 solution. The absorption was measured at 450 nm.

i) IgE ELISA

For IgE ELISA, plates were coated with 10 µg/ml primary antibody (Sheep Anti-Mouse-IgE) in coating buffer (carbonate buffer pH 9.5) overnight at 4 °C. For blocking, the plates were incubated with 300 µl blocking buffer for 1 h at RT. The samples, controls and standards were incubated for 2 h at RT or overnight at 4 °C. For detection, the plate was incubated with 1.25 µg/ml secondary antibody (biotin conjugated Rat Anti-Mouse-IgE) for 2 h at RT. Thereafter, streptavidin-peroxidase was applied at a concentration 1 µg/ml for 30 min at RT in the dark. Thereafter, the plates were washed eight instead of three times. The detection was done with the TMB substrate solution, which was stopped by adding H_2SO_4 after appr. 10 min.

ii) OVA-specific IgG1 ELISA

For OVA-specific IgG1 ELISA, coating was done with 100 µl 1 µg/ml OVA in coating buffer (carbonate buffer pH 9.5) overnight at 4°C or 2h at RT. Blocking was performed with 300 µl Blocking-Puffer either 2 h at RT or overnight at 4 °C, the plates were washed and 50 µl of the samples, blank and positive control as well as the standard were applied to the plate as duplicates. The incubation was done at RT for 2 h or overnight at 4°C. The samples, controls and standards were incubated for 2 h at RT or overnight at 4 °C. The detection was done with 1.25 µg/ml secondary antibody (biotinylated anti-IgG1). Afterwards, streptavidin-peroxidase was applied at a concentration 1 µg/ml for 30 min at RT in the dark and the plate was washed 5 times. The TMB substrate reaction and detection after addition of H_2SO_4 were done as described above.

iii) Mouse Immunoglobulin Panel - ELISA

For Ig ELISA, a Clonotyping System-HRP 5300-05 Kit) from Southern Biotech #5300-01 was used. For this assay type, PBS-T instead of Tris-T was used as washing buffer.

96 well flat bottom plates were coated with 5 µg/ml capture antibody diluted in PBS pH 7.4. 50 µl of the solution was used per well and the plates were incubated overnight at 4 °C. After that, the plates were washed. Thereafter, the plates were blocked by adding 300 µl of PBS-BSA blocking buffer per well and incubating 1 h at RT. The plates were washed and the samples, blank, positive controls and standards were applied as duplicates to the plate with 50 µl/well. The plate was incubated for 2 h at RT or overnight at 4 °C. Thereafter, the plate was washed and 50 µl 1:500-diluted HRP-conjugated antibody (in PBS-BSA) were applied on the plate. The plate was washed 5 times instead of three times and the substrate solution was added. Substrate solution was made freshly immediately before detection by diluting ABTS stock solution (15 mg/ml) 1:50 in substrate buffer (0.05 M citrate buffer) and adding 0.03 % H_2O_2. The detection was done in the ELISA Reader at 405 nm after appr. 10 - 15 min.

iv) Multiplex assay

The cytokine levels were measured with a multiplex assay (Meso Scale Diagnostics) according to the manufacturer's instructions in cooperation with Ferdinand Gürth, ZAUM, Technical University Munich. For further details, see the related paper (Ref. [61]).

8.10 RNA-Seq analysis of FACS sorted Tregs

All centrifugation steps were done at 8000 g.

i) RNA extraction

Sorted FoxP3/RFP+ Tregs were washed with PBS by centrifugation at 400 g for 5 min at 4 °C. 350 µl of RLT buffer (containing ethanol) were added to the cell pellet and the pellet was disrupted by pipetting up and passing the lysate through a blunt 20 G needle fitted to a syringe. After that, 350 µl of 70 % ethanol were added and the sample was immediately mixed by pipetting up and down. The sample is transferred to an RNeasy spin column

placed into a 2 ml collection tube. The columns were spun for 15 sec and the flow-through was discarded. The columns were washed by adding 350 µl RW1 buffer to the columns and repeating the centrifugation as before. Thereafter, DNA remaining in the columns was digested with 80 µl DNase incubation mix for 15 min at RT and the column was washed with 350 µl RW1 buffer.

RNA is purified by adding 500 µl RPE buffer (with ethanol) to the column and spinning the tubes as above. The latter step was repeated with a prolonged centrifugation (for 2 min) to ensure that buffer residues are left in the column. Thereafter, the columns were placed into fresh tubes and the centrifugation was repeated for 1 min. The RNA was eluted from the columns by adding 30-50 µl RNase-free water on the column membrane and the columns were spun for 1 min. The flow-through was transferred onto the same membrane and the centrifugation was repeated. The RNA quality was analyzed using NanoDrop™ spectrophotometer. Thereby the 260/280 and 260/230 ratios should be ≥ 2. The RNA was stored at -80 °C until further analysis.

ii) RNA-Seq analysis

After the RNA extraction, further preparation steps and the RNA-sequencing analysis were done at the Deep Sequencing Core Facility of the Center for Molecular and Cellular Bioengineering, Technical University Dresden and are described in the associated publication (Ref. [61]).

8.11 Statistical tests and software

FACS data was recorded using BD FACSDiva ™ software and analyzed using FlowJo software (Tree Star). If not indicated differently, the data was analyzed by two-tailed Student's t test using GraphPad Prism software. Statistical significance was defined as *$p \leq 0.05$, **$p \leq 0.01$, ***$p \leq 0.001$, and ****$p \leq 0.0001$.

9 Results

9.1 Mice with a systemic *Relb* deletion show Helios+ Treg expansion and an impaired RORγt+ Treg induction

RelB is a transcription factor from the nuclear factor κB (NF-κB) family and critically contributes to the establishment of central tolerance [170, 173]. Mice with a systemic deletion of the *Relb* gene (RelB-KO) mice exhibit spontaneous autoimmune multiorgan inflammation, which has been previously attributed to defective negative selection in the thymus [170, 173]. Although autoimmune inflammation is usually dominated by a type 1 T helper (Th1) and Th17 immune response, RelB-KO mice exhibit hallmarks of a Th2 immune activation, usually activated by large extracellular pathogens or during an allergic immune response [177, 178]. Since the analyzed mice are reared under specific pathogen-free (SPF) conditions, Th2-associated immune responses against invading pathogens are very unlikely. Therefore, allergic immune reaction might contribute to the overt Th2 immune response in RelB-KO mice. Establishment of oral tolerance is pivotal for the suppression of sensitization towards food antigens, and mucosal tolerance induction is a similar process acting locally in the gut to prevent immune activation by symbiotic bacteria (reviewed in [112]). Both processes ultimately result in the induction of FoxP3+ regulatory T cells (Tregs) in the gut. A subpopulation of microbiota-dependent induced Tregs (iTregs) co-expressing nuclear hormone receptor retinoid-related orphan receptor γt (RORγt) has been recently characterized. RORγt+ Tregs are mainly induced in the gut and critically contribute to the suppression of food allergy [52, 53, 57]. RORγt+ Tregs are absent in Th2-prone germ-free mice and also effectively suppress colitis irrespective of the type of T cell polarization [52]. Remarkably, circulating RORγt+ Treg frequency is reduced in food allergic infants and this reduction is paralleled by gut dysbiosis [57]. In a mouse model of food allergy, disrupted microbiota failed to induce RORγt+ Tregs in the gut of Th2-prone mice and protect them from allergy [57].

Given the importance of the mucosal RORγt+ Treg subpopulation, the Treg subsets in the small intestinal lamina propria (SI-LP) of RelB-KO and wildtype (WT) mice was analyzed by flow cytometry (fluorescence-assisted cell sorting analysis, FACS). Whereas RORγt is mostly expressed by iTregs, Helios expression in Tregs from the gut is majorly confined to the thymus-derived (nTregs) in the gut [52]. Using these two transcription factors, nTregs and iTregs were distinguished in the following sections.

In support of previous data, RelB-KO mice showed an elevated splenic total Treg frequency and a significantly reduced frequency of FoxP3+ cells within CD4+CD8- single-positive thymocytes (Figure 1A and Refs. [176, 183]). Whereas in the spleens of WT mice, FoxP3+ Tregs made up around 10 % of all CD4+ T cells, 20 % of CD4+ T cells constituted Tregs in the RelB-KO mice.

Strikingly, a strong total Treg accumulation was observed in the SI-LP of RelB-KO mice – the frequency of FoxP3+ Tregs within CD4+ T cells was increased by a factor of three (from 20 % to 60%) in absence of RelB. Among FoxP3+ Tregs, RelB-deficiency shifted the Treg populations towards the Helios+ nTregs away from RORγt+ iTregs: the proportion of

Helios+ nTregs was elevated in the SI-LP from around 60 % in WT to appr. 80 % in RelB-KO mice, and the frequency of RORγt+ iTregs significantly dropped from around 30 % to less than 5 % in absence of RelB (Figures 1B, C).

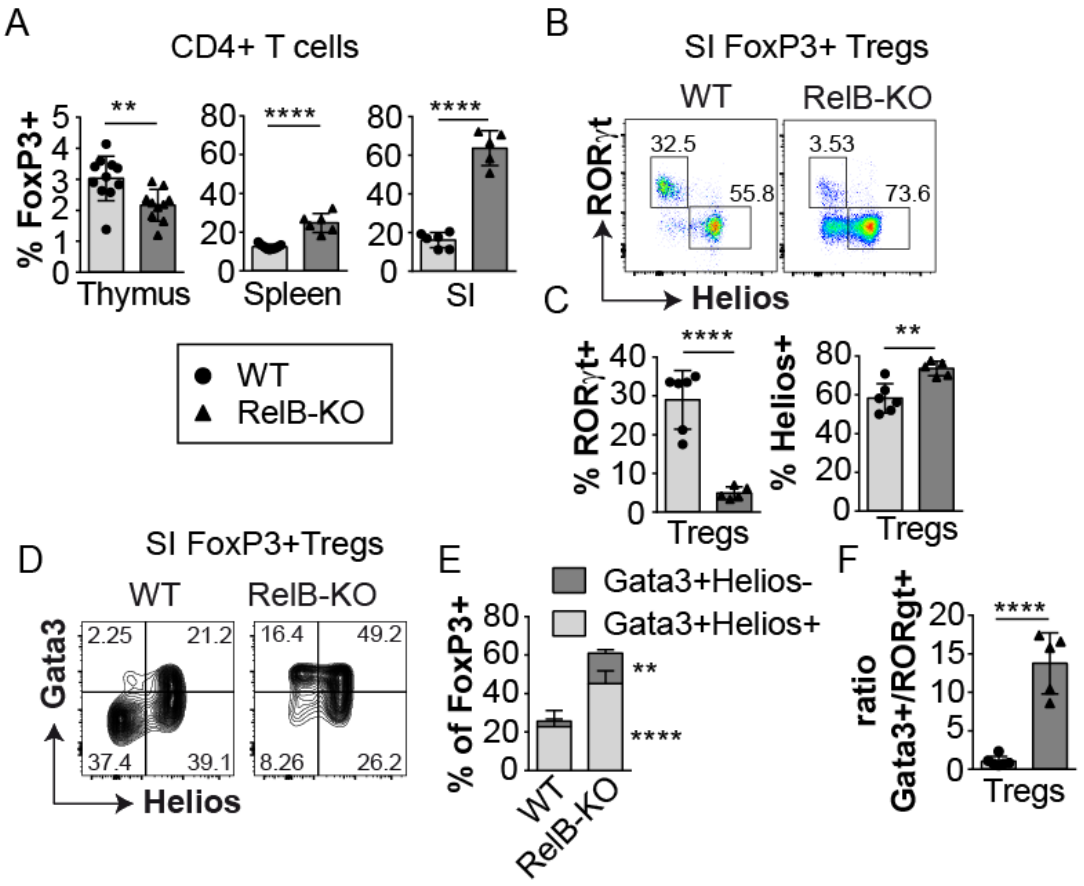

Figure 1. Systemic RelB deficiency shifts the Treg populations away from RORγt+ Tregs towards Helios+Gata3+ Tregs. Tregs in the indicated organs were analyzed by FACS. (A) Percentage of FoxP3+ Tregs out of CD4+ T cells from spleens, thymi and SI of RelB-KO mice or WT mice. (B, D) FACS plots of FoxP3+ Tregs from the SI showing the expression of (B) RORγt versus (vs.) Helios or (D) Gata3 vs. Helios in WT and RelB-KO mice. (C) Quantification plots showing the percentages of RORγt + (left) and Helios+ within FoxP3+ Tregs. (E) Stacked bar diagram illustrating the frequency of Gata3+Helios- and Gata3+Helios+ out of FoxP3+ Tregs. (F) Ratio of Gata3+/ RORγt + Tregs in WT or RelB-KO mice. All bars represent mean ± SD. Data of at least five mice per group is shown. A part of data points for spleen and thymus in A were obtained by Nico Andreas. **p ≤ 0.01; ***p ≤ 0.001; ****p ≤ 0.0001. (A, C, F) Unpaired Student's t-test. (E) Ordinary two-way ANOVA with Sidak's multiple comparison test.

Another important marker for effector Tregs at barrier sites such as the gut is Gata3. Gata3 is upregulated upon interleukin 2 (IL-2) and T-cell receptor TCR stimulation and is important for the accumulation of Tregs at inflammatory or at barrier sites [69]. Additionally, Gata3 is vital for the maintenance of the Treg identity under inflammatory conditions [63].

In the gut of WT mice, Gata3 is usually co-expressed with Helios, whereas within the Helios-negative (Helios-) subset, Gata3 expression is rather low [63]. In line with that, 90 % of Gata3+ Tregs co-expressed Helios, with only a minor proportion of Helios- Tregs

co-expressing Gata3 in the SI-LP of WT mice, as depicted in Figure 1D. *Relb* deletion, however, resulted in a severe upregulation of Gata3 expression within Helios- as well as within Helios+ subsets (Figures 1D, E). The overall frequency of Gata3+ Tregs in the SI-LP of RelB-KO mice was three times higher compared to WT mice (from 20 % in WT to 60 % in RelB KO). Consequently, the ratio of Gata3+ to RORγt+ Tregs was massively elevated from less than 2 in WTs to over 10 in RelB-deficient mice (Figure 1 F). These findings indicate that RelB is systemically required to establish a normal balance between RORγt+ iTregs and Helios+ nTregs and to regulate the expression of transcription factors essential for Treg function such as Gata3. However, the severe inflammatory settings in the RelB-deficient mice might at least partially contribute to this misbalance.

9.2 RelB-deficient mice show a Th2 bias in the SI-LP

It has been shown before that RelB-KO mice exhibit a type 2 inflammation in different organs characterized by elevated type 2 cytokine and chemokine levels and increased total IgE levels [177, 178]. However, the phenotype of FoxP3- effector T cells (Teffs) in the SI-LP remained elusive. To further characterize the inflammatory settings within the SI-LP of RelB-KO mice, Th17 and Th2 cells were analyzed by FACS. To this end, Th17 cells were identified by the expression of RORγt and Th2 cells were characterized by Gata3 expression within FoxP3- CD4+ T cells.

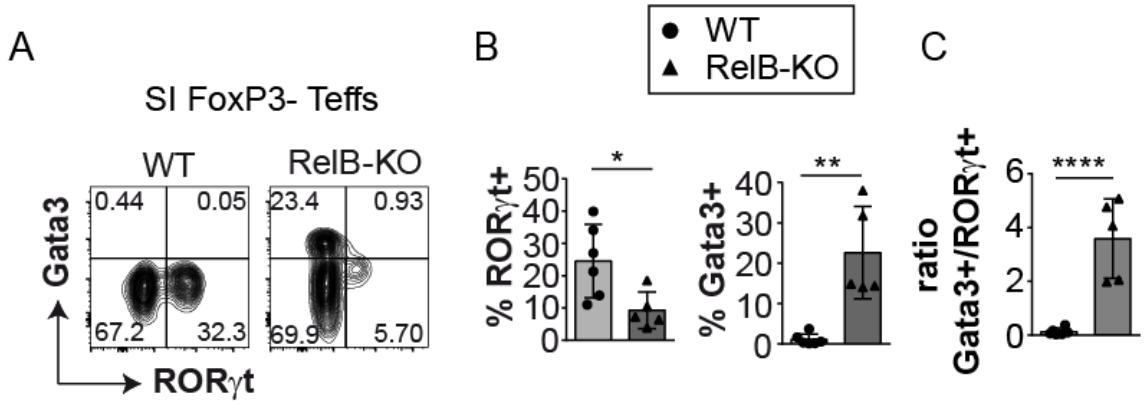

Figure 2. RelB-KO mice show elevated Th2 and reduced Th17 cell frequencies in the SI. The expression of RORγt and Gata3 within FoxP3- Teffs cells was analyzed by flow cytometry in the SI of RelB-KO or WT mice. (A) Representative FACS plots showing the expression of RORγt and Gata3 in FoxP3- Teffs from SI of WT or RelB-KO mice. (B) The percentages of RORγt+ Th17 (left) or Gata3+ Th2 (right) cells out of FoxP3- Teffs. C) Ratio Gata3+/ RORγt + Teffs in WT or RelB-KO mice. Bars represent mean ± SD. Data of at least five mouse per group is shown. *p ≤ 0.05; **p ≤ 0.01; ****p ≤ 0.0001. Unpaired Student's t-test.

In parallel to other organs, SI-LP of RelB-KO mice showed a strongly elevated frequency of Gata3+ Th2 cells from less than 5 % in WT mice to a mean frequency of around 20 %, as observed from five RelB-KO mice (Figures 2A and B). Hereby, the frequency of Gata3+ Th2 cells between the individual RelB-deficient mice had a high variation.

In contrast to that, the percentage of Th17 cells was strongly diminished from around 25 % in WTs to appr. 10 % in absence of RelB. Consequently, the ratio of Th2 to Th17 cells in

the SI-LP was significantly elevated in RelB-deficient compared to RelB-sufficient mice (Figure 2C). In summary, these results suggest that RelB plays a pivotal role for the induction of Th17 cells and for the containment of overt systemic Th2 responses.

9.3 NF-κB signaling members p50 and BCL3 are critically involved in the regulation of the Treg compartment

Since systemic *Relb* ablation had a major impact on the Tregs, the role of other proteins involved in the NF-κB signaling cascade and potentially regulating the activity of RelB in the establishment of normal Treg populations was analyzed.

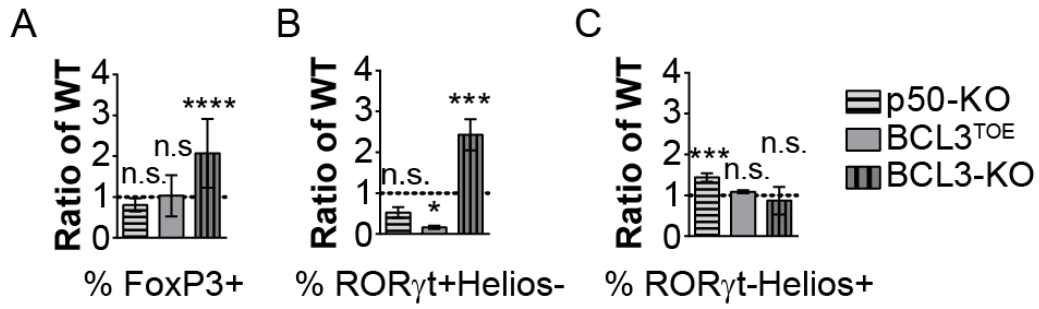

Figure 3. The role of NF-κB signaling in the Treg development. Treg from mLNs from p50-KO, BCL3^{TOE} and BCL3-KO mice were analyzed by flow cytometry. (A-C) Ratios of 'mutant'/WT are shown for each genetically modified mouse strain. (A) Frequency of FoxP3+ Tregs out of CD4+ T cells, (B) percentage of RORγt+Helios- and (C) percentage RORγt-Helios+ out of FoxP3+ Tregs are shown. Bars represent mean ± SD. Two independent experiments were performed with one group of WT mice serving as control for all three mutant mouse strains per experiment. For each experiment, the mean frequency of the respective cell populations was calculated, and a ratio mutant/WT was estimated using the means. Bars show mean ± SD of two data points with a total eight WT, five p50-KO and four BCL3^{TOE} mice. *p ≤ 0.05; ***p ≤ 0.001; ****p ≤ 0.0001. Unpaired one-way ANOVA of the original untransformed data comparing each of the three mutant mouse strains to the WT mice with Holm-Sidak Test.

To this end, mesenteric lymph nodes (mLNs) from *Nfkb1*-deficient (referred to as p50-KO), *Bcl3*-deficient (denoted as BCL3-KO) mice as well as mice with a T-cell-specific overexpression of *Bcl3* (Bcl3^{TOE}) were analyzed by flow cytometry. Specifically, the expression of RORγt and Helios on FoxP3+ Tregs in mLNs was tested.

Interestingly, the balance between RORγt+ iTregs and Helios+ nTregs was disturbed by all three genetic alterations, although the total Treg frequencies were not significantly affected in p50-KO and BCL3^{TOE} mice (Figure 3). In the p50-KO mice, the frequency of Helios+ Tregs was significantly increased 1.5-fold in comparison to WT mice. Further, p50-KO mice exhibited a tendency towards a reduced proportion of RORγt+ Tregs, however this difference was not statistically significant.

The overexpression of *Bcl3* in T cells disrupted the development of RORγt+ Tregs, and in reverse, BCL3-deficiency resulted in a more than twofold elevated frequency of RORγt+ Tregs. In contrast to that, neither of the two *Bcl3*-mutant mice affected the Helios+ Treg subset. This data shows that NF-κB signaling proteins p50 and BCL3 are important in the establishment of the intricate balance between RORγt+ iTregs and Helios+ nTregs.

9.4 Treg development is independent of Treg-intrinsic RelB

Since classical and alternative NF-κB family members including RelA, c-Rel and p100 are required Treg-intrinsically for normal Treg development and function, we hypothesized that RelB may be also important Tregs-intrinsically [204-207] To test this hypothesis, *Relb*-flox mice were crossed with *Foxp3*-Cre mice to generate a Treg-specific ablation of *Relb*, thereafter referred to as RelB$^{\Delta Treg}$. Tregs within mLNs, spleen, thymus, and peritoneal exudate cells (PEC) of RelB$^{\Delta Treg}$ mice were analyzed by flow cytometry.

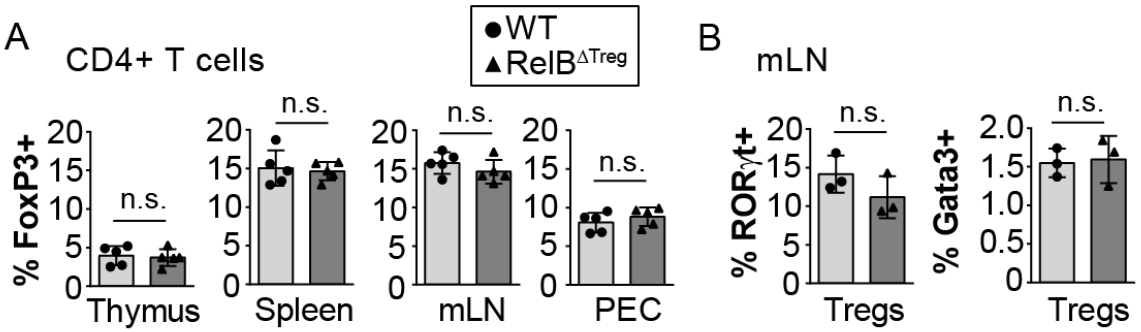

Figure 4. RelB in Tregs is dispensable for the Treg development. Tregs were analyzed by FACS in the indicated organs from RelB$^{\Delta Treg}$ or WT mice. (A) Percentages of FoxP3+ out of CD4+ T cells in the thymus, spleen, mLN and PEC from either RelB$^{\Delta Treg}$ or WT mice. (B) Expression of RORγt and Gata3 within FoxP3 Tregs in the mLNs. Bars represent mean ± SD. Data of 5 mice per group is shown. *p ≤ 0.05. Student's t-test.

Unexpectedly, RelB in Tregs was dispensable for the establishment of normal Treg population size, since the frequency of FoxP3+ Tregs was not affected in RelB$^{\Delta Treg}$ mice (Figure 4A). Furthermore, the frequency of RORγt+ and Gata3+ Tregs was not affected by a Treg-specific *Relb* deletion (Figure 4B). These findings support recent publications and suggest a dispensable role of RelB within Tregs for their development and establishment of a normal Treg balance [204, 205].

9.5 Tregs accumulate systemically in absence of RelB in dendritic cells

Dendritic cells (DCs) represent the bridge between the innate and the adaptive immunity and are essential for the Treg development. Previous investigations using systemically RelB-deficient mice and corresponding bone marrow chimeras (BMC) revealed a critical DC-intrinsic requirement of RelB for DC development and function. However, the interpretation of this data is difficult due to the broad implication of RelB in other cell types. To elucidate DC-intrinsic role of RelB, a DC-specific *Relb* knockout mouse model (hereafter referred to as RelB$^{\Delta DC}$ mice) was deployed. DC-specific targeting of *Relb* was achieved by crossing mice carrying an *Itgax*-cre allele, here referred to as CD11c-cre mice (*Itgax* gene encodes CD11c integrin commonly expressed by DCs) with *Relb*-floxed mice.

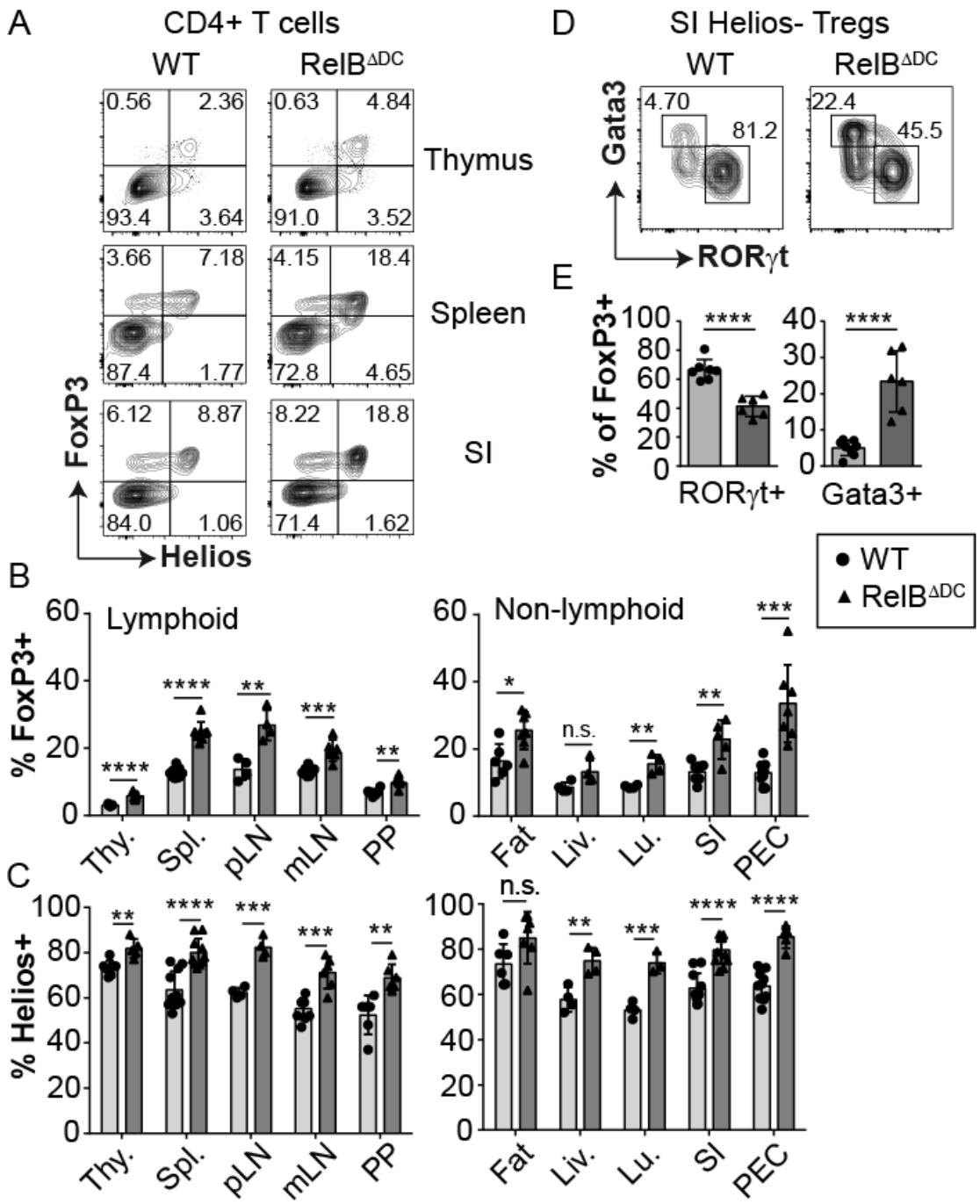

Figure 5. *Relb* ablation in DCs causes a systemic accumulation of FoxP3+ Tregs due to expanded Gata3+Helios+ Treg population with concomitant loss of RORγt+ Tregs. FoxP3+ Tregs from the indicated organs of RelB$^{\Delta DC}$ or WT mice were investigated by flow cytometry. Thy. – thymus, Spl. – spleen, Liv. – liver, Fat – visceral adipose tissue, Lu. – lung. (A) Representative FACS plots showing FoxP3 vs. Helios expression within CD4+ T cells from the thymus, spleen, and SI. (B) Frequency of FoxP3+ Tregs out of CD4+ T cells in lymphoid and non-lymphoid tissues. (C) Helios expression among Tregs shown as % Helios+ out of FoxP3+ Tregs in the indicated organs. (D) Representative FACS plots showing RORγt and Gata3 expression within Helios- Tregs from SI. Bars represent mean ± SD. Data of at least five mice is shown. *p ≤ 0.05; **p ≤ 0.01; ***p ≤ 0.001; ****p ≤ 0.0001. Unpaired Student's t-test with Holm-Sidak correction for multiple comparisons.

To investigate the effects of the DC-intrinsic ablation of *Relb* on the Treg compartment, Tregs from lymphoid and non-lymphoid organs of RelB$^{\Delta DC}$ or WT mice were assessed by flow cytometry. Thereby, nTregs were identified as Helios+ cells (Figure 5A).

In accordance with the previous findings, the frequency of FoxP3+ Tregs was increased twofold in the spleen and peripheral lymph nodes (pLNs) from around 7 % in the WTs to around 15 % in the RelB$^{\Delta DC}$ mice (Figure 5B and Ref. [192]). Notably, in all other organs tested, the Treg frequency was also significantly increased in the RelB$^{\Delta DC}$ mice in comparison to WT mice (except from the liver with a p value of 0.053). The analysis of Helios expression revealed a systemic expansion of Helios+ nTregs (Figure 5C). Each organ analyzed exhibited an elevated expression of Helios within FoxP3+ Tregs by at least 10 % (except from the visceral adipose tissue (here denoted as 'Fat').

Furthermore, the expression of RORγt in line with Gata3 expression within Helios- iTregs was analyzed in the SI-LP (Figure 5D). In contrast to the Gata3 expression which was strikingly elevated from around 5 % in the WT to more than 20 % in the RelB$^{\Delta DC}$ mice, RORγt+ iTregs were almost completely absent in the SI-LP of RelB$^{\Delta DC}$ mice (Figure 5D, E). Whereas in WT mice, around 60 % of all Helios- iTregs co-expressed RORγt, RelB$^{\Delta DC}$ mice harbored only 40 % of RORγt+ cells within Helios- Tregs.

These findings suggest that RelB in DCs is important to maintain normal Treg frequencies at steady state by containing exaggerated expansion of Gata3+ and Helios+ Tregs and supporting the induction of RORγt+ iTregs.

9.6 RelB$^{\Delta DC}$ mice show a spontaneous Th2 bias

RelB is systemically required to suppress overt spontaneous type 2 inflammation, however the contribution of RelB in DCs in this process remained elusive. To address this issue, Gata3+ Th2 cells in the SI-LP, spleen, Peyer's patches (PPs) and PEC from RelB$^{\Delta DC}$ mice were investigated. For PEC, ST2 was used in addition to Gata3 to clearly identify Th2 cells. Since systemic RelB has proven to be essential for the development of Th17 cells (Figure 2), RORγt+ Th17 cells in the SI-LP of mice with a DC-specific *Relb* deletion were investigated.

Interestingly, the frequency of RORγt+ Th17 cells was not altered in the SI-LP of RelB$^{\Delta DC}$ mice (Figure 6A). In contrast to that, the prevalence of Gata3+ Th2 cells was greatly enhanced in the SI-LP from an almost undetectable frequency in WTs to more than 5 % in RelB$^{\Delta DC}$ mice (Figure 6C). In line with the Th2 bias observed in the SI-LP, the spleen and PEC of RelB$^{\Delta DC}$ mice harbored significantly expanded Th2 cell populations compared to WT mice (from 5 % in WT to 10 % in RelB$^{\Delta DC}$ mice, and from 5 % in WT to 25 % in RelB$^{\Delta DC}$ mice, respectively) (Figures 6C-E). In contrast to that, PPs showed no significant increase in the frequency of Th2 cells.

To confirm the Th2 phenotype, the serum immunoglobulin E (IgE) levels were measured by an enzyme-linked immunosorbent assay (ELISA). In addition to that, the serum concentrations of IgG1, IgG2b, IgG3, IgA and IgM were investigated by ELISA to detect additional immunological defects associated with DCs-specific ablation of *Relb*. In accordance with the elevated frequency of Gata3+ Th2 cells, the serum IgE level was

elevated from an almost undetectable level in WT mice to more than 100 ng/ml in absence of RelB in DCs (Figure 6F). Among other immunoglobulins tested, only the level of serum IgG3 was affected, showing a significantly decreased concentration in RelB$^{\Delta DC}$ mice.

The elevated IgE levels prompted the investigation of T follicular helper (Tfh) cells, which play a pivotal role in the production of immunoglobulins by B cells. To this end, Tfh cells in the spleen, mLNs and PPs were assessed by flow cytometry and were identified by the expression of C-X-C chemokine receptor type 5 (CXCR5) as well as programmed cell death protein 1 (PD-1) within the FoxP3- CD4+ T cells (Figure 7A).

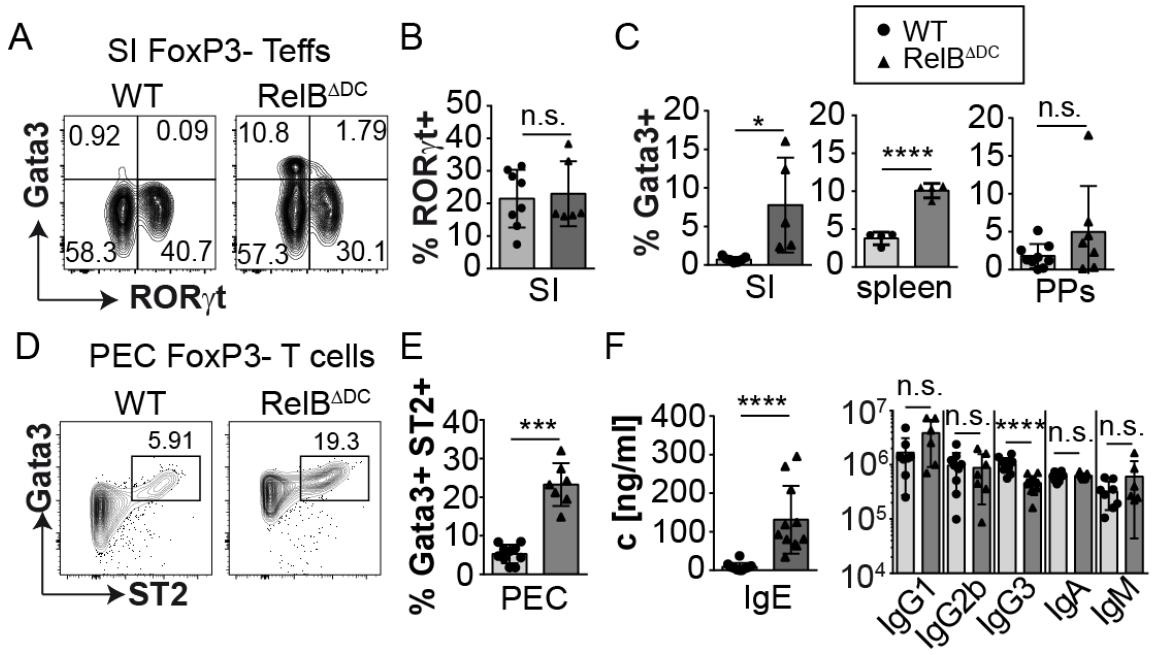

Figure 6. RelB$^{\Delta DC}$ mice show a Th2 bias under steady-state conditions. (A-E) FoxP3- Teffs from SI, spleen, PP and PEC of RelB$^{\Delta DC}$ mice or WT mice were investigated by flow cytometry. (A) Representative FACS plots showing Gata3 vs. RORγt on FoxP3- Teff cells (B) Percentage of RORγt+ Th17 cells in the SI. (C) The frequency of Gata3+ Th2 cells in the SI (left), spleen (mid) and PPs (right) out of FoxP3- Teffs. (D) Representative FACS plot showing the expression of Gata3 and ST2 in PEC Teffs. (E) Quantification plot showing the percentage of Gata3+ST2+ Th2 cells within FoxP3- Teffs in the PEC from RelB$^{\Delta DC}$ or WT mice. (F) Concentrations of the indicated Igs as measured by ELISA in the sera of RelB$^{\Delta DC}$ or WT mice. Data of at least four mice per group is shown. All bars represent mean ± SD. *p ≤ 0.05; ***p ≤ 0.001; ****p ≤ 0.0001. Unpaired Student's t-test.

Strikingly, RelB$^{\Delta DC}$ mice harbored an expanded Tfh population - mLNs showed twofold and PPs threefold higher total Tfh cell frequencies (Figure 7B). This difference became apparent when looking at the frequency of Tfh cells out of CD4 T cells, as well as out of total living cells. In contrast to that, splenic Tfh cells were not affected by DC-specific *Relb* ablation.

Interestingly, out of the three organs tested, PP from RelB$^{\Delta DC}$ mice exhibited the highest proportion of 6 % Tfh cells within total living cells. In contrast to that, WT mice showed comparable Tfh frequencies of around 2 % out of living cells, irrespective of the organ tested. Although only two data points for the WT mice is shown here, the data is very consistent and was confirmed in an independent experiment (not shown here).

Altogether, the data presented here suggests that RelB in DCs is crucial to negatively regulate Tfh cell generation and suppress spontaneous systemic Th2 polarization.

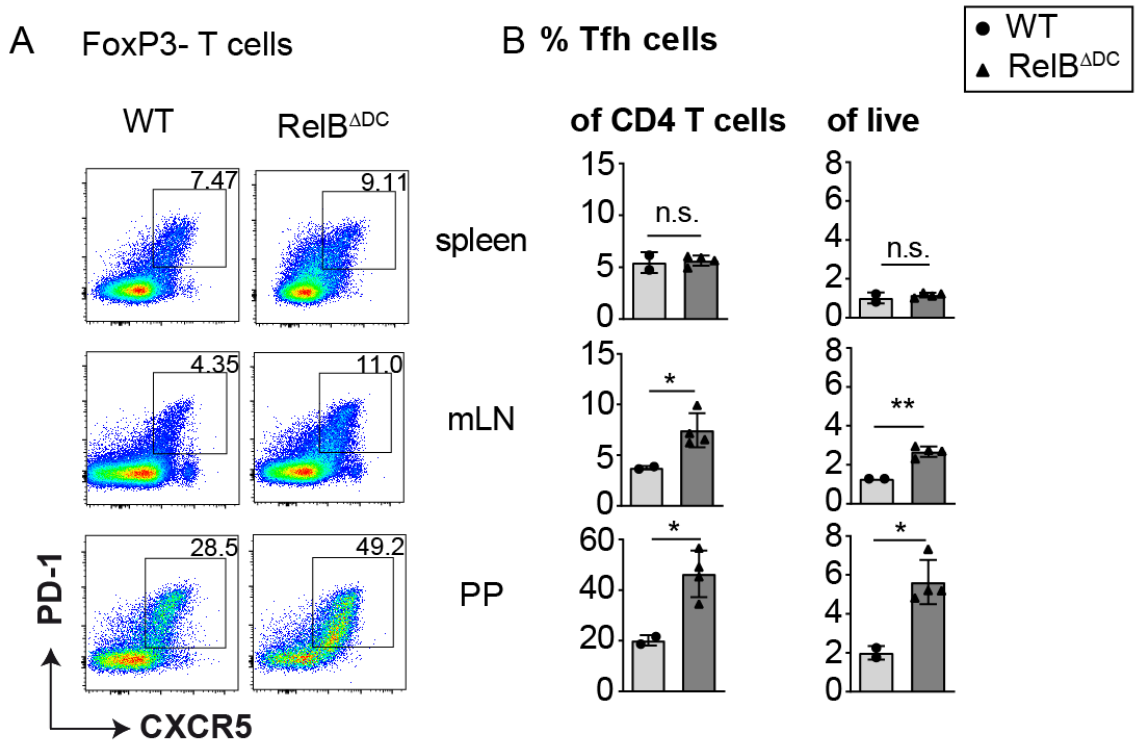

Figure 7. RelB$^{\Delta DC}$ mice show increased frequency of Tfh cells in mLNs and PPs. Flow cytometric analysis of the indicated organs identifying Tfh cells as CXCR5+ PD-1+ FoxP3- CD4+ T cells was performed. (A) Representative FACS plots showing gating strategy in the spleen (upper row), mLNs (middle low) and PP (bottom row) from WT (left) and RelB$^{\Delta DC}$ (right) mice. (B) Bar diagrams showing the percentage of Tfh cells out of total CD4+ T cells (left column) or out of total living cells (right column) of the indicated organs from RelB$^{\Delta DC}$ and WT mice. Bars represent mean ± SD. Data for two WT and four RelB$^{\Delta DC}$ is shown. *p ≤ 0.05; ** ≤ 0.01. Unpaired Student's t-test.

9.7 RelB-deficient DCs do to permit efficient oral tolerance induction

Since the induction of RORγt+ Tregs in the RelB$^{\Delta DC}$ mice was strongly impaired and the mice showed a Th2 bias, it was assumed that the induction of antigen-specific RORγt+ iTregs in the gut in response to an orally applied antigen is impaired.

To test this hypothesis, ovalbumin (OVA)-specific congenically marked (CD45.1+) OT-II cells were transferred into RelB$^{\Delta DC}$ or WT mice. The recipient mice were subjected to OVA *ad libitum* in drinking water for 9 days according to the experimental setup depicted in Figure 8A. Upon oral route of application, OVA passing the gastrointestinal tract triggers induction and proliferation of the antigen-specific OT-II Tregs conveying oral tolerance.

At day 10 after the start of OVA-supplementation, mice were euthanized and the expression of FoxP3, RORγt and Gata3 in the CD45.1+ OT-II cells was assessed by flow cytometry.

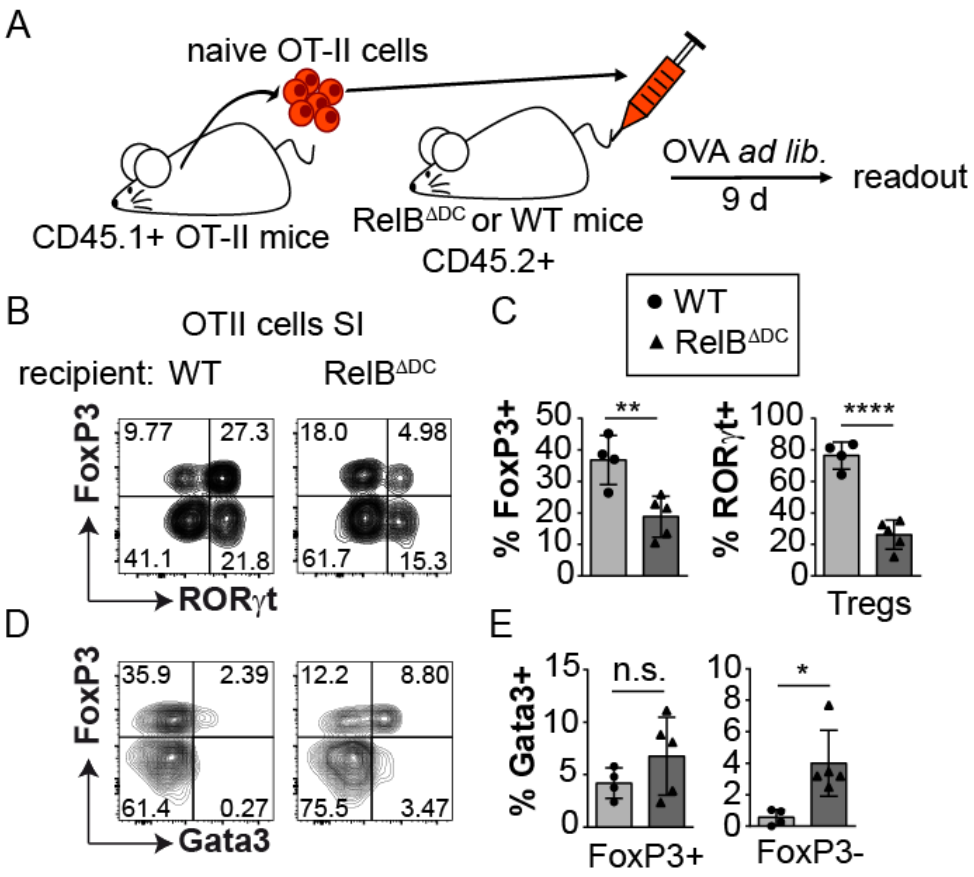

Figure 8. RelB-deficient DCs are less efficient in supporting the induction of antigen-specific RORγt+ Treg in favor of Th2 cells. WT or RelB$^{\Delta DC}$ mice were substituted with naïve congenically marked CD45.1+ OT-II cells and supplied with ovalbumin in drinking water for 9 d. FoxP3, RORγt and Gata3 expression was analyzed within CD45.1+ OT-II cells from SI by flow cytometry. (A) Experimental procedure. (B, D) Representative FACS plots of CD45.1+ OT-II CD4+ T cells showing (B) FoxP3 vs. RORγt expression or (D) FoxP3 vs. Gata3 expression (C) Percentage of FoxP3+ Tregs out of OT-II cells (left) and RORγt+ out of FoxP3+ Tregs (right). (E) Frequency of Gata3+ out of Tregs (left) and Percentage of Gata3+ out of Teff (right). Bars represent mean ± SD. Data points are pooled from two independent experiments with at least 4 mice per group shown here. *p ≤ 0.05; **p ≤ 0.01; ****p ≤ 0.0001. Unpaired Student's t-test.

OT-II cells recovered from the SI-LP of RelB$^{\Delta DC}$ mice showed a significantly reduced frequency of FoxP3+ Tregs (around 20 %) in comparison to WT mice (around 40 %) (Figure 8B). Whereas almost all FoxP3+ OT-II cells in the WT mice co-expressed RORγt (appr. 80 %), RelB-deficient DCs did not support an efficient RORγt upregulation, resulting in a frequency of RORγt+ Tregs as low as only 30 % (Figures 8B, C). Instead, FoxP3 negative (Teffs) and FoxP3 positive (Tregs) OT-II cells preferentially upregulated Gata3 in the context of RelB-deficient DC, although the difference within Gata3+ Tregs was not significant (Figures 8D, E). Whereas WT mice harbored less than 1 % of Gata3+ Teffs, RelB$^{\Delta DC}$ mice accumulated around 4 % of Gata3+ Th2 cells.

These findings suggest that RelB-deficient DCs are less efficient in supporting oral tolerance induction, which results in an accumulation of antigen-specific Th2 cells and a bias towards Gata3+ Tregs.

9.8 Tregs from RelB$^{\Delta DC}$ mice possess a tissue Treg signature

An elevated expression of Gata3 and Helios in Tregs is associated with a tissue Treg phenotype. Therefore, it was assumed that tissue Tregs accumulate in absence of RelB in DCs. First, the concomitant expression of Helios and Gata3 was verified.

In contrast to systemically RelB-deficient mice, the frequency of the Gata3+Helios-Treg subpopulation was not significantly elevated in absence of RelB in DCs: compare Figure 1 and Figure 9A (note that the FACS plot for WT mice is used twice, as WT, RelB-KO and RelB$^{\Delta DC}$ mice were analyzed side-by-side, therefore the same mice served here as control for both genetically modified mouse lines).

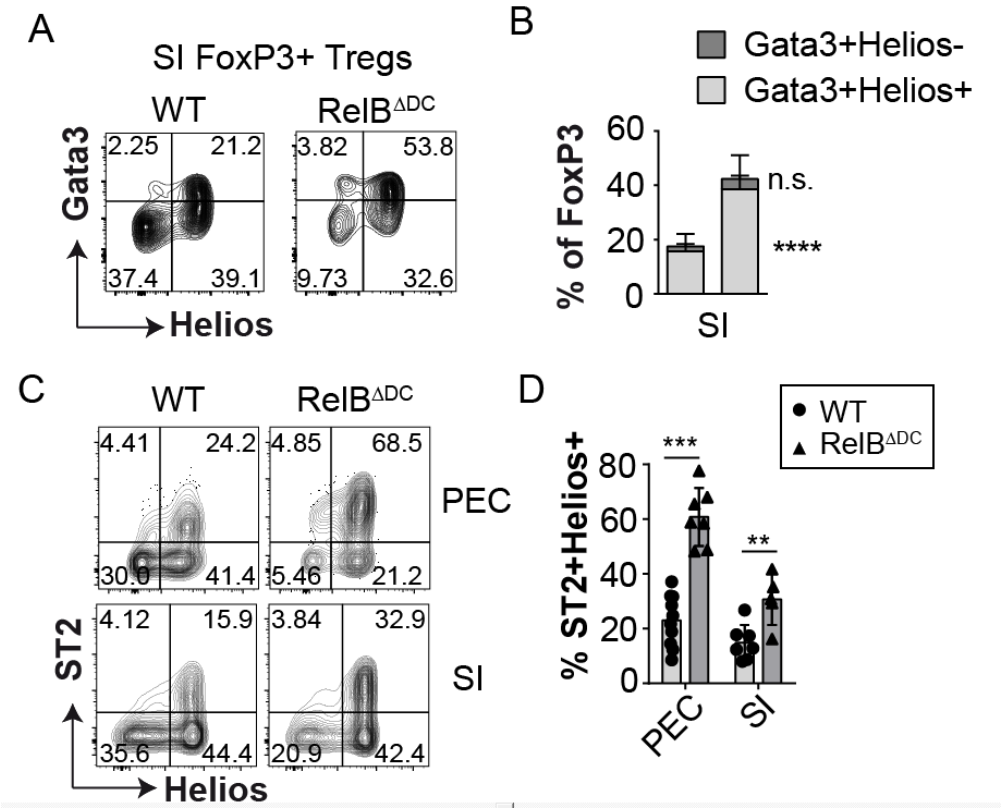

Figure 9. RelB$^{\Delta DC}$ mice accumulate Gata3+Helios+ST2+ Tregs. Gata3, ST2 and Helios expression were analyzed within FoxP3+ Treg cells from SI and PEC by flow cytometry. (A) Representative FACS plots and (B) quantification of Gata3 and Helios expression in Tregs from SI. (C) Representative FACS plots of ST2 vs. Helios expression in Tregs from PEC (top plots) or SI (bottom plots). (D) Frequency of ST2+Helios+ out of Tregs in PEC and SI. Bars show mean ± SD. Data of at least four mice is shown. **p ≤ 0.01; ***p ≤ 0.001; ****p ≤ 0.0001. Unpaired Student's t-test.

Comparable to RelB-KO mice, the Gata3+Helios+ Treg subset was accumulated in RelB$^{\Delta DC}$ mice (with appr. 40 %), whereas WT mice showed less than 20 % Gata3+Helios+ Tregs (Figures 9A, B). Thus, the exclusive accumulation of the Gata3+Helios+ Treg population points towards the expansion of a specific Treg subset, rather than an upregulated expression of Helios and Gata3 within the total Treg population in RelB$^{\Delta DC}$ mice.

It has been previously published that tissue Tregs express IL-33 receptor (ST2), are particularly enriched in non-lymphoid organs and show a highly activated phenotype [62, 66]. To further corroborate on the tissue phenotype of the expanded Treg population, the expression of IL-33 receptor (ST2) on Helios+ Tregs was assessed within PEC and in SI-LP of RelB$^{\Delta DC}$ and WT mice (Figures 9C, D). Side-by-side analysis of Helios and ST2 revealed that ST2 expression was almost completely confined to the Helios+ subset in WT as well as RelB$^{\Delta DC}$ mice, irrespective of the organ analyzed (Figure 9C).

Strikingly, RelB$^{\Delta DC}$ mice showed a strong systemic accumulation of ST2+Helios+ Tregs. Whereas around 20 % of Tregs within PEC and in the SI-LP of WT mice were ST2+Gata3+, RelB$^{\Delta DC}$ mice accumulated up to 40 % ST2+Helios+ Tregs in the SI-LP, and even up to 80 % within the PEC (Figure 9D). In addition to the PEC and SI data shown here, pLN, visceral adipose tissue (VAT), lung, spleen, thymus, PPs, mLNs and liver exhibited accumulation of ST2+Helios+ Tregs in absence of RelB in DCs (data not shown).

To gain a deeper insight into the Treg phenotype of RelB$^{\Delta DC}$ mice, the expression of various activation markers in Tregs from the spleen and PEC – with latter representing the site of the strongest ST2+ Treg accumulation - was assessed by flow cytometry. The frequencies of the tissue Treg markers is summarized in Figure 10A.

The data gained here revealed that the expression of the activation makers: tumor necrosis factor (TNF) superfamily member 4 (OX40), PD-1, inducible T cell co-stimulator (ICOS), glucocorticoid-induced TNFR-related protein (GITR) and killer cell lectin like receptor G1 (KLRG-1) - was increased in Tregs within the PEC and from the spleen in absence of RelB in DCs (Figure 10A). Although the difference of the OX40 expression in the spleen was not significant. Additionally, the expression of CD103 and CD44 was significantly increased in the splenic Tregs from RelB$^{\Delta DC}$ mice. The elevated expression of the activation markers tested here reinforced the tissue phenotype of the expanded Treg population in RelB$^{\Delta DC}$ mice. In parallel to the particularly dramatic accumulation of Gata3+Helios+ Tregs within the PEC compared to other organs, the Tregs from the peritoneum exhibited especially pronounced upregulation of tissue Treg markers (compared to the spleen, s. Figure 10). Among those, the frequency of Ox40 was increased by a factor of three and the proportion of ICOS+ Treg cells was more than doubled within PEC of RelB$^{\Delta DC}$ compared to WT mice.

For further validation of the tissue Treg phenotype, the transcriptome of Tregs from the spleen, PEC and thymus of RelB$^{\Delta DC}$ and WT mice was analyzed by RNA-sequencing (RNA-Seq). To this end, Tregs from the indicated organs were FACS-sorted by deploying RelB$^{\Delta DC}$ or WT mice backcrossed onto a FoxP3-mRFP reporter background. Total RNA was extracted from the sorted Tregs and analyzed by RNA-Seq at the Deep Sequencing Core Facility of the Center for Molecular and Cellular Bioengineering, Technical University Dresden.

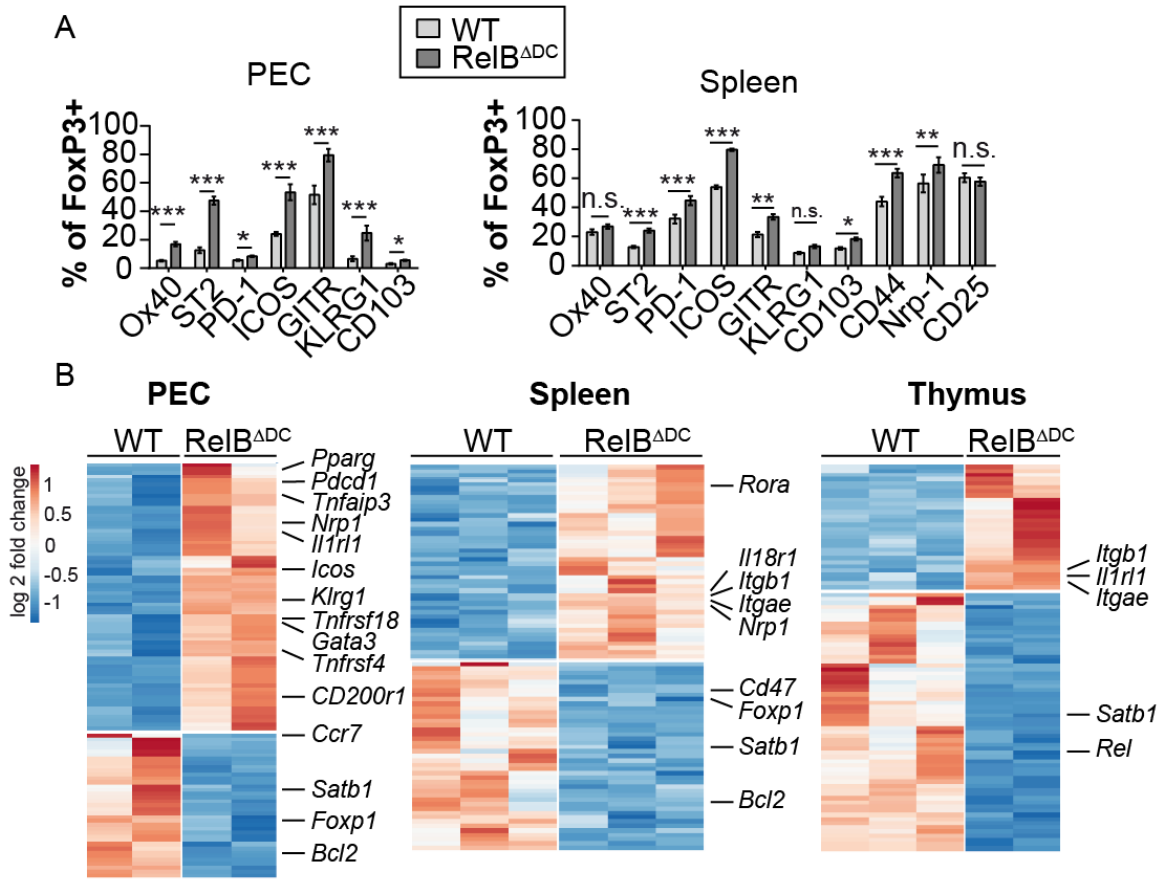

Figure 10. RelB$^{\Delta DC}$ mice show an increased expression of tissue Treg markers. (A) Activation markers within FoxP3+ Tregs from PEC (left) and spleen (right) were analyzed by FACS. Bars represent mean ± SEM percentage of the indicated markers. Data of at least three mice is shown. The data points for CD44 expression in the splenic Tregs were obtained by Nico Andreas. *p ≤ 0.05; **p ≤ 0.01; ***p ≤ 0.001; ****p ≤ 0.0001. Unpaired Student's t-test. (B) FACS-purified FoxP3-mRFP+ Tregs were analyzed by RNA-Seq. The heatmaps depict selected differentially expressed genes in PEC (left), spleen (mid) and thymus (right). Genes were considered as differentially expressed at a significance level of p ≤ 0.1. Heat map diagrams are reused from the related publication, for more details, see Ref. [61].

The transcriptome analysis revealed that FoxP3+ Tregs sorted from PEC exhibited higher expression of several tissue Treg-associated genes such as *Pparg*, *Pdcd1*, *Nrp1*, *Il1rl1*, *Icos*, *Gata3*, *Klrg1*, *Itgae*, and *Tnfrsf4* in absence of RelB in DCs (Figure 10B). In contrast to that, the expression of nTreg markers, such as *Ccr7, Satb1, Foxp1* and *Bcl2* was decreased. The data obtained from the spleen verified the differential gene expression of a part of these genes.

Interestingly, the gene expression profile of FoxP3+ thymocytes also showed a tissue Treg signature. In conclusion, the data pointed out that the absence of RelB in DCs causes a spontaneous systemic accumulation of tissue Tregs.

9.9 The role of the thymus for the expanded Treg population in RelB$^{\Delta DC}$ mice

9.9.1 *Relb*-deletion in DCs has an impact on intrathymic Treg development

Since the frequency of tissue Tregs was not only elevated in the spleen and PEC, but also in the thymus, thymocytes were analyzed into more detail. Specifically, the precursors of thymic Tregs were analyzed. Two alternative routes of Treg generation in the thymus have been previously identified. Thereby, the classical route generates CD25+FoxP3- precursors, whereas the alternative route gives rise to CD25-FoxP3+ precursors [44-47]. Therefore, the two possible progenitor populations as well as mature FoxP3+CD25+ Tregs were analyzed in the thymi of RelB$^{\Delta DC}$ and WT mice by flow cytometry.

In line with the data shown in Figure 5, the frequency of mature CD25+FoxP3+ Tregs was significantly increased by a factor of 1.5 in RelB$^{\Delta DC}$ mice compared to WT mice (Figure 11A). Among thymic Treg precursors, the CD25+FoxP3- population generated via the classical route was expanded almost twofold, whereas the frequency of FoxP3+CD25- Treg precursors arising along the alternative route was not affected by the ablation of *Relb* in DCs. This data points towards an enhanced intrathymic Treg development along the classical route in absence of RelB in DCs.

Furthermore, Helios expression as a marker of highly self-reactive Treg progenitors was assessed within the thymic Treg progenitors in RelB$^{\Delta DC}$ and WT mice [208]. Helios is induced in self-reactive thymocytes experiencing strong TCR signaling during the negative selection upon high-affinity engagement with major histocompatibility complex class II (MHCII)-bound self-antigens [208, 209].

Strikingly, not only mature CD25+FoxP3+ Tregs, but also both CD25+FoxP3- and CD25-FoxP3+ Treg progenitors showed significantly elevated Helios expression in absence of RelB in DCs (Figure 11B). This data suggests that RelB deficiency in DCs permits a stronger stimulation of TCR signaling in Treg progenitors and mature Tregs.

To investigate the implication of apoptosis for the expanded thymic Treg population, Annexin V staining of the thymic Treg precursors and mature Tregs was carried out. Annexin V enables detection of apoptotic cells by high-affinity binding to phosphatidylserine residues, exclusively present on the outer plasma membrane layer of apoptotic cells. Whereas CD25-FoxP3+ Treg progenitors showed a slightly elevated frequency of apoptotic cells, the CD25+FoxP3- and CD25+FoxP3+ subsets were not affected by the absence of RelB in DCs (Figure 11B, middle graph). These findings suggest that RelB-deficient DCs do no mediate an increased survival of Treg precursors or mature Tregs.

The suppression of thymocyte apoptosis by engagement of CD27 with medullary thymic epithelial cell (mTEC) or DC-derived CD70 is one of the possible mechanisms regulating the thymic Treg output [210]. Therefore, it was tested whether RelB deficiency affects CD27 expression on the thymic Treg progenitors and mature Treg populations. Here, no effect of the DC-specific *Relb*-deletion on the expression of CD27 was observed (Figure 11B).

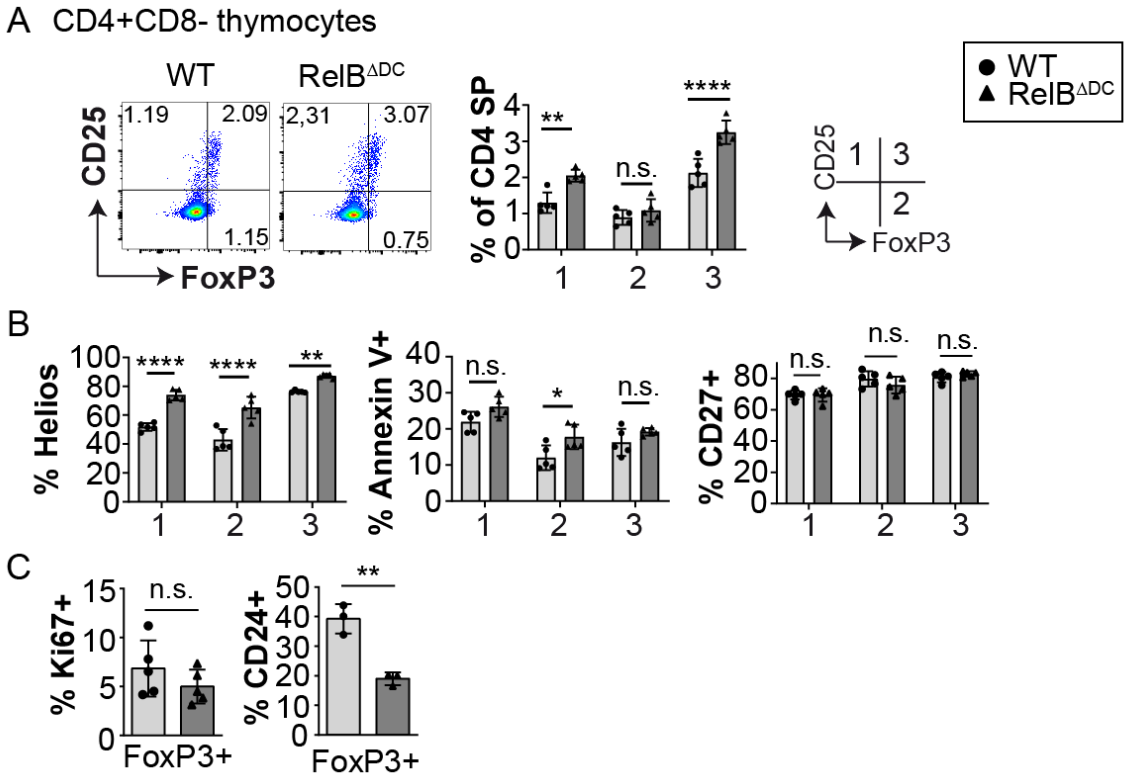

Figure 11. Thymic Treg development is affected by RelB deficiency in DCs. Thymic Treg precursors and mature Tregs from RelB$^{\Delta DC}$ or WT mice were analyzed by flow cytometry. (A) Representative FACS plots showing CD25 vs. FoxP3 expression within CD4+CD8- SP thymocytes of WT and RelB$^{\Delta DC}$ mice (left) and bar diagram showing the frequency of CD25+FoxP3- (1), CD25-FoxP3+ (2) and CD25+FoxP3+ (3) out of CD4 SP thymocytes. (B) Frequencies of Helios+ (left), Annexin V+ (mid) and CD27+ (right) out of the indicated thymocyte populations 1-3. (C) % Ki67+ (left) and % CD24+ (right) out of total FoxP3+ thymocytes. All bars represent mean ± SD. Except from the CD24 data with n = 3 per group, all experiments were performed with n = 5 mice per group. CD24 data was obtained by Nico Andreas. *p ≤ 0.05; **p ≤ 0.01. Unpaired Student's t-test. (A, B) two-way ANOVA with Sidak's correction for multiple testing. (C) Student's t-test.

To test whether RelB-deficient DCs elicit an enhanced proliferation of the FoxP3+ thymocytes, the frequency of Ki67+ cells within total FoxP3+ thymocytes was analyzed. Here, no significant difference in the frequency of Ki67+ cells was detected within FoxP3+ thymocytes from RelB$^{\Delta DC}$ mice in comparison to WT mice (Figure 11C).

CD24 expression is inversely correlated with Treg maturation in the thymus [47, 211]. To address the maturation stage of total FoxP3+ thymocytes, CD24 expression on FoxP3+ thymocytes was examined. Interestingly, RelB$^{\Delta DC}$ mice showed a decreased proportion of CD24+ cells within FoxP3+ thymocytes, suggesting a more mature phenotype of FoxP3+ thymocyte (Figure 11C).

Collectively, these findings suggest that DC-intrinsic RelB deficiency alters Treg development in the thymus resulting in an elevated frequency of classical CD25+FoxP3- Treg precursors and increased total Helios expression. Together, this data indicates that RelB-deficient DCs trigger stronger TCR receptor signaling in the developing Treg intermediates. In contrast to that, the lack of RelB in DCs did not seem to enhance the

proliferation rate or inhibit apoptosis of FoxP3+ thymocytes. Therefore, an increased thymic output as the primary reason for the expanded tissue Treg population in peripheral organs of RelB$^{\Delta DC}$ mice seems unlikely.

9.9.2 Investigation of the thymic Treg populations in young mice

As thymic Treg frequencies in the absence of RelB in DCs were increased, it was assumed that an enlarged peripherally developed Treg population contributes to the elevated thymic Treg frequency. One of the possible mechanisms is migration of iTregs from the periphery back into the thymus. To test this possibility, FoxP3 expression in the thymi of 1-week and 2-week old pre-weaned mice was analyzed. The limited Treg induction in the periphery before weaning allows a reliable assessment of the thymic Treg output [52].

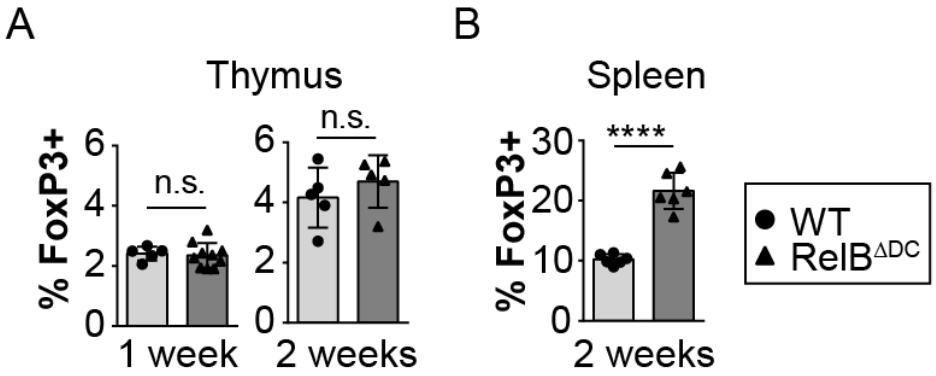

Figure 12. Thymic output of Tregs is not increased in 1 wk and 2 wk old mice in the absence of RelB in DCs. (A) Percentage of FoxP3+ out of CD4+ T cells in 1-week old mice (left) and 2-week old (right) RelB$^{\Delta DC}$ or WT mice. (B) Frequency of splenic Tregs out of CD4+ T cells from RelB$^{\Delta DC}$ or WT mice. All bars represent mean ± SD. Data of at least five mice per group is shown. Data from 2-wk-old mice was obtained by Nico Andreas. *p ≤ 0.05; ****p ≤ 0.0001. Unpaired Student's t-test.

Interestingly, DC-specific *Relb* deletion did not have a significant effect on the FoxP3 expression in thymocytes of 1-week and 2-week old mice (Figure 12A). The spleens of the 2-week old mice, however exhibited a substantial accumulation of Tregs in absence of RelB in DCs (with 10 % in WTs and around 20 % in RelB$^{\Delta DC}$ mice) (Figure 12B). These findings point out that extrathymic accumulation of Tregs in RelB$^{\Delta DC}$ mice begins early in life. Furthermore, this data suggests that thymic output of Tregs is not enhanced in RelB$^{\Delta DC}$ mice. Therefore, the elevated Treg frequency in the thymi of RelB$^{\Delta DC}$ mice most probably originates from recirculating Tregs, which have been generated in the periphery. Furthermore, the recirculation of the Tregs back to the thymus seems to take place either later than at 2 weeks of age or rather slow.

9.9.3 RelB in DCs is dispensable for efficient negative selection in the thymus

DCs are indispensable for negative selection of thymocytes in the thymic medulla [212]. Therefore, it is possible that RelB-deficient thymic DCs are not capable of supporting efficient negative selection. Thus, self-reactive thymocytes evading negative selection

might be converted into Tregs in the periphery, thereby contributing to the Treg accumulation in RelB$^{\Delta DC}$ mice. To rule out this possibility, the fact that BALB/c mice carry the endogenous mammary tumor virus superantigen 6 (Mtv-6) on DCs resulting in full negative deletion of TCR Vβ3+ thymocytes during negative selection was exploited. To this end, BALB/c mice were intercrossed with C57BL/6 RelB$^{\Delta DC}$ mice for one generation (here referred to as 'mix') and the distribution of TCR Vβ chains on Tregs and Teffs was assessed by flow cytometry.

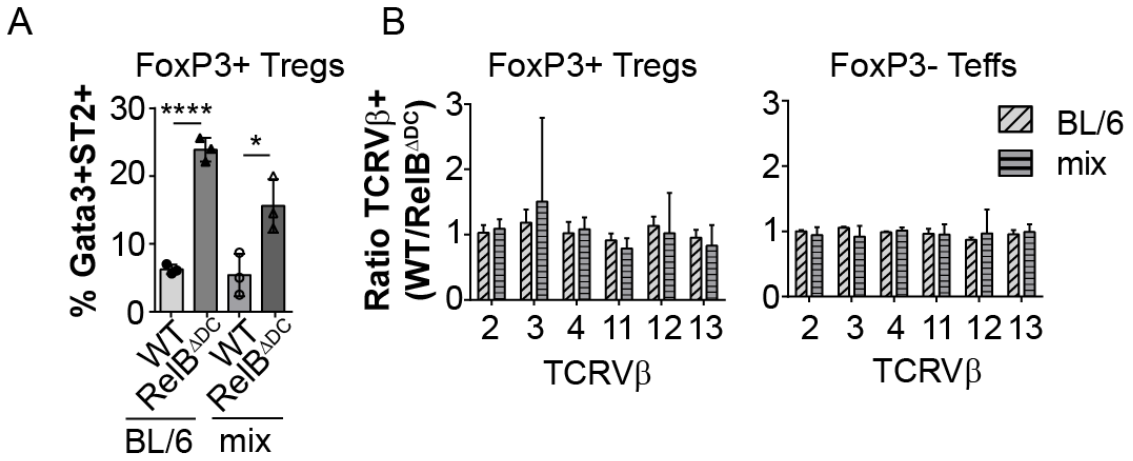

Figure 13. RelB in thymic DCs is dispensable for the negative selection of thymocytes. Treg frequencies and TCR Vβ chain distribution were tested in the thymi from mice with BALB/c x C57BL/6 mixed (mix) background or from C57BL/6 (BL6) mice. (A) Percentages of Gata3+ST2+ out of FoxP3+ Tregs. (B) Ratio (WT/RelB$^{\Delta DC}$) of percentages of each indicated TCRVβ chain out of FoxP3+ (left) and FoxP3- (right) cells. Bars represent mean ± SD. Three mice per group are shown. *p ≤ 0.05; ****p ≤ 0.001. Unpaired Student's t-test.

Notably, the accumulated tissue Treg phenotype in RelB$^{\Delta DC}$ mice remained stable in the mixed background mice (Figure 13A). Here, the frequency of Tregs and the proportion of ST2+Gata3+ tissue Tregs were significantly higher in absence of RelB in DCs.

Comparing the WT and RelB$^{\Delta DC}$ mice on the C57BL/6 background with the respective strains on the mixed background, no differences in the percentages of TCR Vβ3 or any other TCR Vβ chain within Tregs could be detected (Figure 13B). Furthermore, no evidence for clonal expansion of FoxP3- Teff cells in the thymus was detected in this experimental setting. Moreover, the overall frequencies of CD4-CD8- double-negative, CD4+CD8+ double-positive, CD4+ and CD8+ single-positive thymocytes were not affected by DC-specific *Relb* deletion (data not shown).

These findings and the fact that RelB$^{\Delta DC}$ mice do not display any detectable autoimmune infiltrates (unpublished observations and Refs. [190, 192]) indicate that RelB in DCs is dispensable for the negative selection of autoreactive thymocytes.

9.9.4 The role of IL-2 and IL-33 for the accumulation of Tregs in the absence of RelB in DCs

Since the thymus seems to play a minor role in the development of tissue Tregs in absence of RelB in DCs, other possibilities of Treg accumulation were tested. First, the serum levels of IL-2 and IL-33 as major cytokines driving the development of (tissue) Tregs were

measured. To this end, sera from RelB$^{\Delta DC}$ or WT mice were subjected to a highly sensitive multiplex immunoassay. Here, no differences in the IL-2 and IL-33 cytokine levels between RelB$^{\Delta DC}$ and WT mice could be detected (Figure 14A).

To elaborate on the role of IL-33 for the Treg accumulation, IL-33 was blocked by systemic administration of soluble ST2 (sST2) – a decoy receptor for IL-33. In detail, WT or RelB$^{\Delta DC}$ mice were subjected to intraperitoneal (i.p.) injections with sST2 on every other day for three weeks (Figure 14B depicts the experimental scheme). After that, the total and ST2+ Treg frequency was tested by flow cytometry of splenocytes.

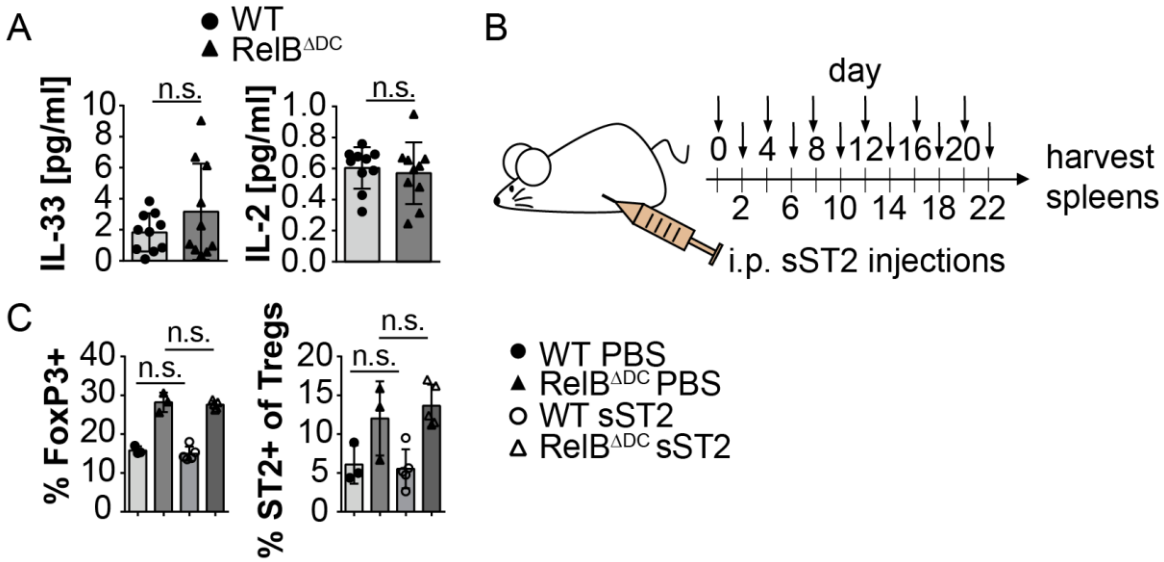

Figure 14. Treatment of RelB$^{\Delta DC}$ mice with sST2 does not reverse the ST2+ Treg accumulation. (A) Sera of untreated RelB$^{\Delta DC}$ or WT mice were subjected to a multiplex immunoassay. Levels of IL-2 (left) or IL-33 (right) in pg/ml. For each group, n = 10 is shown. Bars represent mean ± SD. $p \leq 0.05$. Student's t-test. (B) Experimental scheme for the systemic neutralization of IL-33 by repeated sST2 injection. (C) Splenic Tregs from sST2 treated RelB$^{\Delta DC}$ or WT mice were analyzed by FACS. Percentages of FoxP3+ out of CD4+ T cells (left) and of ST2+ out of FoxP3+ Tregs (right) are shown. Bars represent mean ± SD. At least three mice per group are shown. *$p \leq 0.05$. One-way ANOVA with Sidak test for multiple corrections.

Using this experimental approach, no significant impact of sST2 treatment on neither WT nor RelB$^{\Delta DC}$ mice could be observed: the frequencies of Tregs in the spleens and the abundance of ST2 on Tregs were not changed upon sST2 treatment (Figure 14C). This data indicates that sST2 in this experimental setting was either not able to neutralize IL-33 sufficiently or that IL-33 is not involved in the Treg accumulation in RelB$^{\Delta DC}$ mice.

Since IL-33 is an alarmin mostly produced by epithelial cells upon damage, Treg accumulation in a context of IL-33-deficient non-hematopoietic compartment was tested. To this end, BMCs were generated by reconstitution of lethally irradiated IL-33-deficient (IL-33-KO) or WT recipients with bone marrow (BM) from either RelB$^{\Delta DC}$ or WT mice. After that, the recipient mice were provided with 0.25 mg/ml enrofloxacin in drinking water and examined 10 - 12 weeks (wk) after reconstitution (Figure 15A). Specifically, total and ST2+Helios+ Tregs as well as Gata3+ and ST2+Gata3+ Th2 cells Tregs were analyzed by

flow cytometry. Additionally, the serum levels of IL-33 and IL-2 were measured by a multiplex immunoassay.

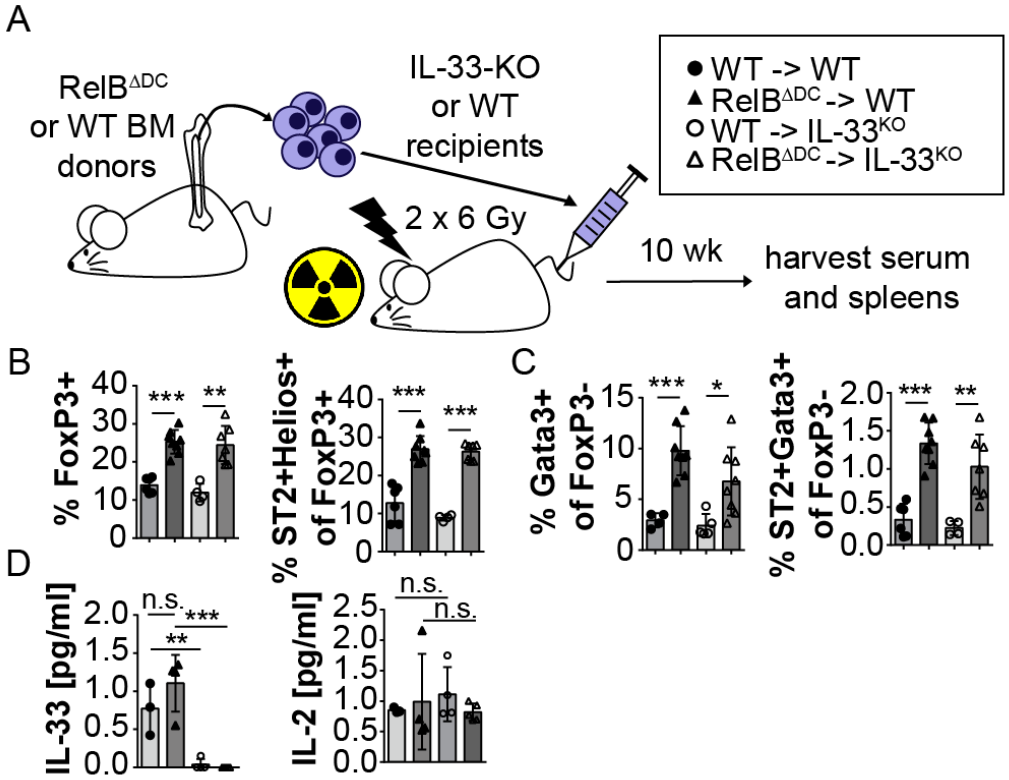

Figure 15. Treg proliferation and Th2 phenotype are established in RelB$^{\Delta DC}$ mice independently of IL-33 from non-hematopoietic cells. Lethally irradiated IL-33 or WT mice were reconstituted with bone marrow from either WT or RelB$^{\Delta DC}$ mice. 10-12 wk after reconstitution, sera and spleens were collected for analysis. (A) Experimental scheme for the generation of bone marrow chimeras. (B, C) The cells recovered from the spleens were analyzed by FACS. (B) Frequency of FoxP3+ Tregs (left) out of CD4+ T cells and percentages of ST2+Helios+ out of FoxP3+ Tregs (right). (C) Percentages Gata3+ out of FoxP3- Teffs (left) and ST2+Gata3+ out of FoxP3- Teffs. (D) The serum concentrations of IL-33 (left) and IL-2 (right), in pg/ml as measured by multiplex immunoassay. Bars show mean ± SD. *p ≤ 0.05; **p ≤ 0.01; ****p ≤ 0.0001. One-way ANOVA with Sidak correction for multiple comparisons.

Interestingly, the accumulation of total and ST2+Helios+ Tregs as well as Th2 cells mediated by the DC-specific *Relb* ablation was not dependent on IL-33 from radioresistant cells (Figures 15B, C). The BM from RelB$^{\Delta DC}$ mice gave rise to significantly higher frequencies of Tregs irrespective on the presence of IL-33, with appr. 10 % Tregs of CD4+ T cells in WT - and more than 20 % Tregs in BMCs reconstituted with RelB$^{\Delta DC}$ BM. The ST2+Helios+ Treg population behaved equivalently with around 10 % in the WT and appr. 30 % ST2+Helios+ Tregs in the chimeras which have received RelB$^{\Delta DC}$ BM. The accumulation of Gata3+ and ST2+Gata3+ Th2 cells in absence of RelB in DCs was also independent of IL-33, albeit the IL-33-deficient BMCs reconstituted with RelB$^{\Delta DC}$ BM showed a slightly, but insignificantly lower frequency of Th2 cells compared to IL-33-sufficient BMCs which were replenished with BM from RelB$^{\Delta DC}$ mice (Figure 15 C).

In terms of the cytokine levels in the sera of the BMCs, IL-33 was not measurable in both IL-33-deficient BM chimeras, supporting the fact that IL-33 commonly originates from the non-hematopoietic compartment (Figure 15D). Similarly to the data shown in Figure 14, the IL-33 level in RelB$^{\Delta DC}$ mice was not higher compared to WT mice. In contrast to that, the serum level of IL-2 was almost equal between all four BMCs examined here.

Taken together, these observations suggest that IL-33 is not involved in the accumulation of ST2+ Tregs in absence of *Relb* expression in DCs. However, these experiments could not rule out the possibility that an increased IL-33 production by hematopoietic cells in absence of RelB in DCs contributes to the expanded Treg and Th2 populations.

9.10 The cell-intrinsic effects of the *Relb* ablation on the DC phenotype

To identify the effect of the DC-specific *Relb* ablation on the DCs compartment, the expression of several DC markers was analyzed. Firstly, the total frequency of DCs in the spleen was assessed. Contrary to the data previously published, suggesting that there is no difference in the total DC frequency, a reduced number of total DCs was observed in absence of RelB in DCs (from 1.2 % in WTs to 0.7 % in RelB$^{\Delta DC}$ mice) (Figure 16A and Ref. [192]).

Classical DCs (cDCs) can be divided into the cDC1 and cDC2 subpopulations based on their ontogeny and phenotypic markers. Therefore, cDC1s and cDC2 were distinguished here by the expression of CD8 and Sirpα, respectively. Corresponding to the previous findings, the frequency of CD8-Sirpα+ cDC2s was significantly reduced in the spleen of RelB$^{\Delta DC}$ mice (Figure 16C and Ref [190]). Whereas around 80 % of all CD11c+MHCII+ DCs in the spleen of WT mice constituted the CD8a-Sirpα+ cDC2s, in absence of RelB in DCs, only around 65 % of DCs exhibited the cDC2 phenotype. In contrast to that, the frequency of CD8+ Sirpα- cDC1s was markedly increased from around 7 % in WTs to over 15 % in RelB$^{\Delta DC}$ mice.

The cDC1 subset co-expressing the endocytotic receptor DEC-205 are efficient mediators of Treg induction, thus the expression of DEC-205 was assessed on splenic DCs from RelB$^{\Delta DC}$ and WT mice [87-91]. In line with the elevated frequency of CD8+Sirpα- DC1s, the abundance of DEC-205+Sirpα- DC1s was significantly elevated from 20 % to 30 % in absence of RelB in DCs (Figure 16D, E). Hence, the expanded cDC1 subpopulation in RelB$^{\Delta DC}$ mice might contribute to the expanded Treg population.

In addition to that, the expression of the co-stimulatory molecules programmed death-ligand 1 (PD-L1), PD-L2 and Ox40L on DCs from the spleen was tested by flow cytometry. Interestingly, the mean fluorescence intensity (MFI) of PD-L1 was reduced (from 1000 to 600) and the PD-L2 MFI was significantly increased (from 75 to 175) in absence of RelB in DCs (Figure 16 F, E). In contrast to that, the Ox40L expression on DCs was not affected by the lack of RelB. In summary, the data suggests that RelB is not only essential for the development of cDC2s and containment of the cDC1 population, but also regulates the expression of co-stimulatory molecules PD-L1 and PD-L2.

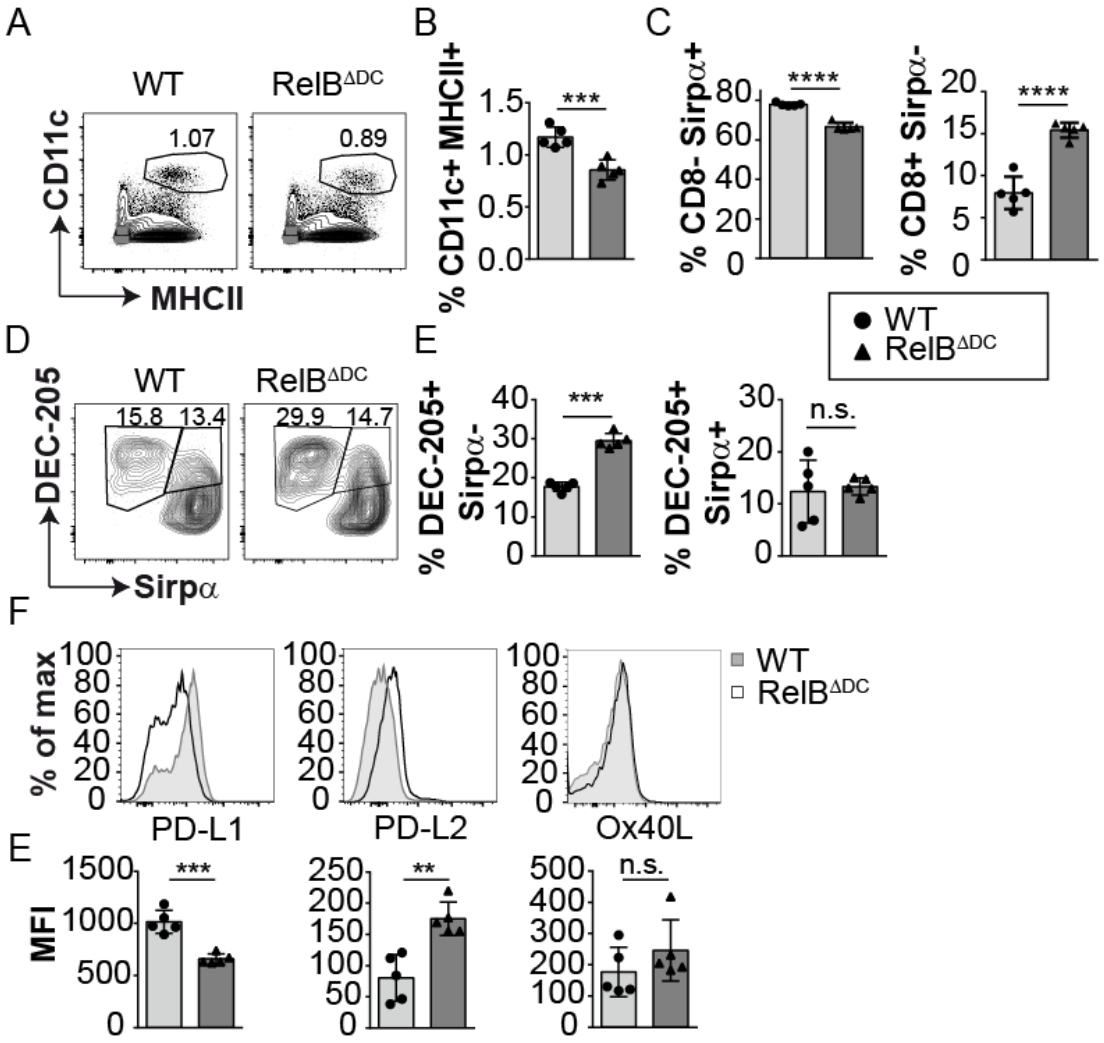

Figure 16. RelB deficiency in splenic DCs causes phenotypic changes of the surface marker expression. DCs from the spleen of either RelB$^{\Delta DC}$ or WT mice were analyzed by FACS. (A) Representative plots showing gating strategy for CD11c+ MHCII+ DCs, pregated on total living splenocytes. (B) Bar diagrams showing total DC frequency out of total living cells. (C) Frequencies of CD8-Sirpα+ (left) and CD8+Sirpα- (right) DCs in percent out of total DCs. (D) Representative FACS plot showing DEC-205 and Sirpα expression on total DCs. (E) Percentages of DEC-205+Sirpα- (left) and DEC-205+Sirpα+ (right) DCs out of total DCs (F) MFIs of PD-L1 (left), PD-L2 (mid) and Ox40L (right) on DCs. (E) MFI quantification of the indicated DC markers. All bars represent mean ± SD. ***p ≤ 0.01; ***p ≤ 0.001; ****p ≤ 0.0001. Unpaired Student's t-test.

RelB$^{\Delta DC}$ mice exhibited an abrogated induction of oral tolerance and mucosal RORγt+ Tregs and CD103+ DCs are critically required for this process in the gut-associated lymphoid tissues (GALT) [95, 104]. Therefore, the implication of RelB in GALT DCs was assessed here. To this end, the total CD11c+MHCII+ DC population was subdivided into four DC subsets based on the expression of CD11b and CD103, and the proportions of each subset in the spleen, mLNs, SI and colon from either RelB$^{\Delta DC}$ or WT mice were assessed by FACS (Figure 17). Notably, the CD103+CD11b+ subset is not present in the spleen (indicated as n.a. in the bar diagram). In line with the data shown in Figure 16, the frequency of

CD11b+CD103- cDC2s was reduced in the spleen with a concomitant expansion of the cDC1 population (Figure 17A, C).

The CD11b+CD103+ DC subpopulation is exclusively present in GALT and especially in the SI, it resembles splenic cDC2 subset and seems to be critically required for the induction of RORγt+ Tregs [213]. Correspondingly to the loss of splenic cDC2s in RelB$^{\Delta DC}$ mice, the frequency of CD11b+CD103+ cDC2s in the SI was significantly reduced from 60 % in WTs to 40 % in RelB$^{\Delta DC}$ mice.

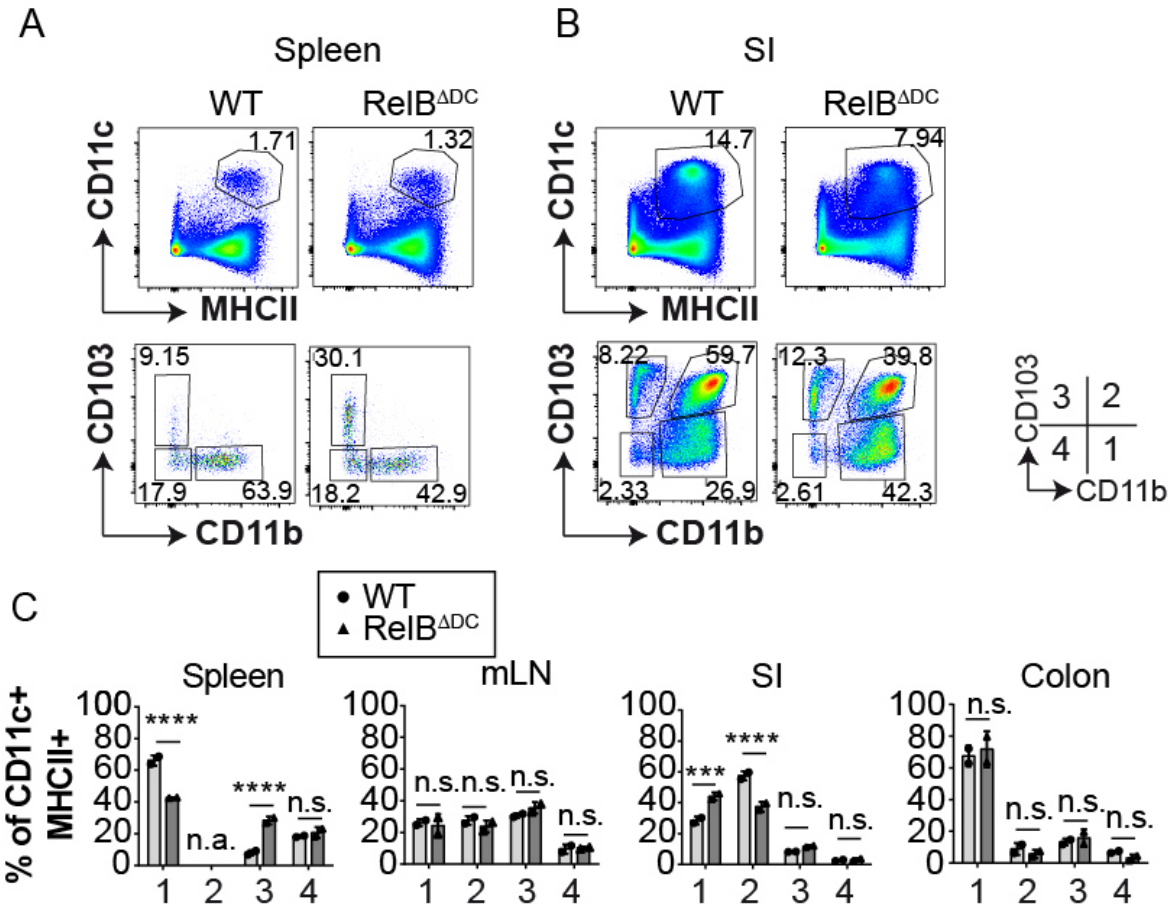

Figure 17. RelB deficiency in DCs significantly affects MNP subset frequencies in the spleen, mLNs and SI. MNPs from the spleen, mLNs and SI of either RelB$^{\Delta DC}$ or WT mice were analyzed by FACS. (A, B) Representative FACS plots showing the gating strategy for MNPs (upper row) and for the indicated subsets (lower row) in the (A) spleen and (B) SI. (C) Frequencies of indicated MNP populations out of total DCs in the spleen, mLNs, SI and colon. Bars represent mean ± SD. One experiment with n = 2 for each genotype is shown. *p ≤ 0.05; ***p ≤ 0.001; ****p ≤ 0.000. Unpaired two-way ANOVA with Sidak's correction for multiple comparisons.

In contrast to that, the abundance of the CD11b-CD103+ DC subpopulation in the SI of RelB$^{\Delta DC}$ mice was increased from 30 % to 40 %. The ontogeny of the CD11b-CD103+ DC subset remains unclear, however they seem to include progenitors of CD103+CD11b+ cells [97, 214]. Therefore, the accumulation of CD11b+CD103- DCs may reflect a developmental defect during the transition to the CD11b+CD103+ stage in absence of RelB. In contrast to that, no differences within the analyzed DC subset could be detected in the mLNs or colon.

Albeit only two mice per group were analyzed, the data shown here is very consistent within each group and goes in line with the aforementioned and previously published data.

However, this data needs to be interpreted with caution as macrophages make up around 70 % of all CD11c+MHCII+ cells in the gut. To distinguish between macrophages and DCs, the CD11c+MHCII+ mononuclear phagocyte (MNP) population showed in Figure 17 was re-analyzed. Thereby, DCs and macrophages were discriminated by a different level of CD11c expression with most *bona fide* DCs exhibiting high levels of CD11c expression ($CD11c^{high}$) and the majority of macrophages showing intermediate CD11c levels ($CD11c^{int}$) (Figure 18).

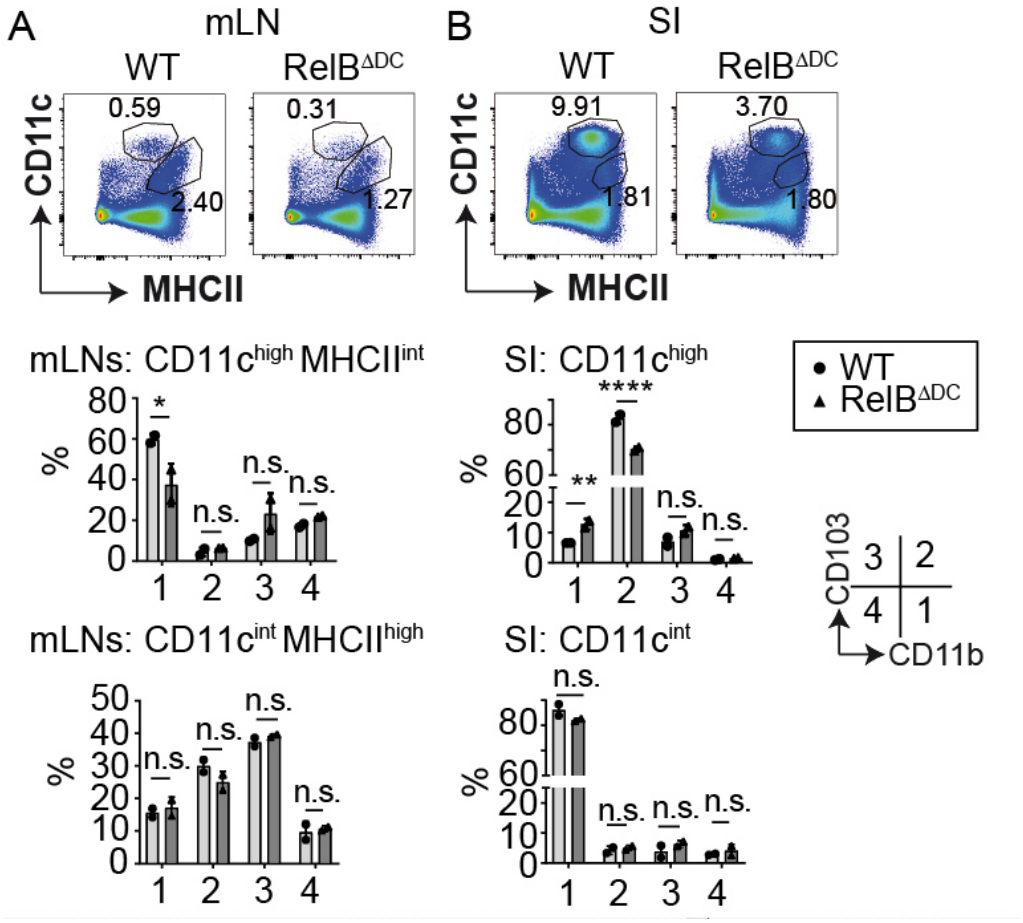

Figure 18. CD11c-specific *Relb* deletion presumably affects $CD11c^{high}$ DCs but not $CD11c^{low}$ macrophages in the SI, as well as migratory, but not resident DCs in the mLNs. Re-analysis of the data from Figure 17. Bars represent mean ± SD. One experiment with n = 2 for each genotype is shown. *p ≤ 0.05; ***p ≤ 0.001; ****p ≤ 0.000. Unpaired two-way ANOVA with Sidak's correction for multiple comparisons.

In the SI-LP, only $CD11c^{high}$, but not $CD11c^{int}$ MNPs were affected by the CD11c-mediated *Relb* deletion. In line with the data shown in Figure 17, the frequency of CD11b+CD103+ $CD11c^{high}$ MNPs presumably comprising cDC2s was significantly reduced in the SI in absence of RelB (from around 90 % in WTs to 70 % in $RelB^{\Delta DC}$ mice). In support of the conclusions drawn from the findings presented in Figure 17, the frequency of CD11b+CD103- $CD11c^{high}$ DCs was significantly increased in the SI-LP of mice with a

CD11c-targeted *Relb* ablation, further underlining a DC-specific impact of CD11c-targeted *Relb* deletion.

Albeit the conclusions are based on a limited number of mice, the data gained here suggests that CD11c-targeted deletion of *Relb* is suitable to analyze the DC-specific role of RelB, since no effects on intestinal macrophages were observed here. Within DCs, RelB is required for the development of normal numbers of intestinal CD11b+CD103+ cDC2s, which are critically required for the generation of RORγt+ Tregs [213]. Hence, the reduced intestinal cDC2 population might contribute to the impaired induction of RORγt+ Tregs as was observed in RelB$^{\Delta DC}$ mice.

As the induction of RORγt+ Tregs is dependent upon proper trafficking of antigen-loaded DCs into the mLNs, the migratory and the resident DC subsets in the mLNs - as shown in Figure 17 - were re-analyzed here. Comparable with the SI-LP, mLNs possess two subsets within the CD11c+MHCII+ MNPs. However, here, the macrophage population is rather small. Instead, CD11^{high} MHCII^{int} and CD11^{int} MHCII^{high} MNP subsets represent resident and migratory DCs, respectively.

Interestingly, only resident CD11^{high} MHCII^{int}, but not migratory CD11^{int} MHCII^{high} DCs from the mLNs were affected by CD11c-mediated *Relb* ablation (Figure 18A). Within the resident DCs, the frequency of the CD11b+CD103- cDC2s was significantly reduced from 60 % in the WT to 40 % in the RelB$^{\Delta DC}$ mice.

In summary, the data showed here suggests a cDC2-specific requirement of RelB in various organs and goes in line with previous publications [93, 185, 190]. Furthermore, the data shown gives a hint towards a subordinate role of RelB for trafficking of CD103+ DCs from the SI to the mLNs.

9.11 RelB is differentially expressed in DCs from various organs

Findings presented here and published before suggested a differential requirement of RelB in DC subtypes [190]. Not only splenic, but also GALT cDC2s were critically dependent on DC-intrinsic RelB. Intriguingly, the loss of the CD11b+CD103+ DC population in the SI was associated with an abrogated induction of oral tolerance and of mucosal RORγt+ Tregs. This prompted the investigation of RelB expression in GALT DCs. In parallel, RelB expression in macrophages was analyzed. Additionally, the expression of RelB in DCs from PEC as the site of the strongest tissue Treg accumulation in RelB$^{\Delta DC}$ mice was addressed.

Due to unavailability of a functional RelB antibody for flow cytometry, a reporter mouse strain which allows the detection of the RelB expression via the far-red fluorescent Katushka fluorophore (Katushka-RelB mouse) was used [190]. To this end, DCs from spleens, PEC, mLNs, PPs, SI and colon of Katushka-RelB reporter mice were subdivided into four subpopulations by the expression of CD11b and CD103 and analyzed by flow cytometry. Whereas DCs from the spleen, mLNs and PPs DCs were identified as CD11c+MHCII+ cells; macrophages were excluded as CD64+ cells for an unambiguous identification of the CD64- DCs in the PEC, SI and colon. In addition to Katushka-RelB mice, WT non-reporter mice were analyzed as a negative control. The data of one representative experiment is shown in Figure 19.

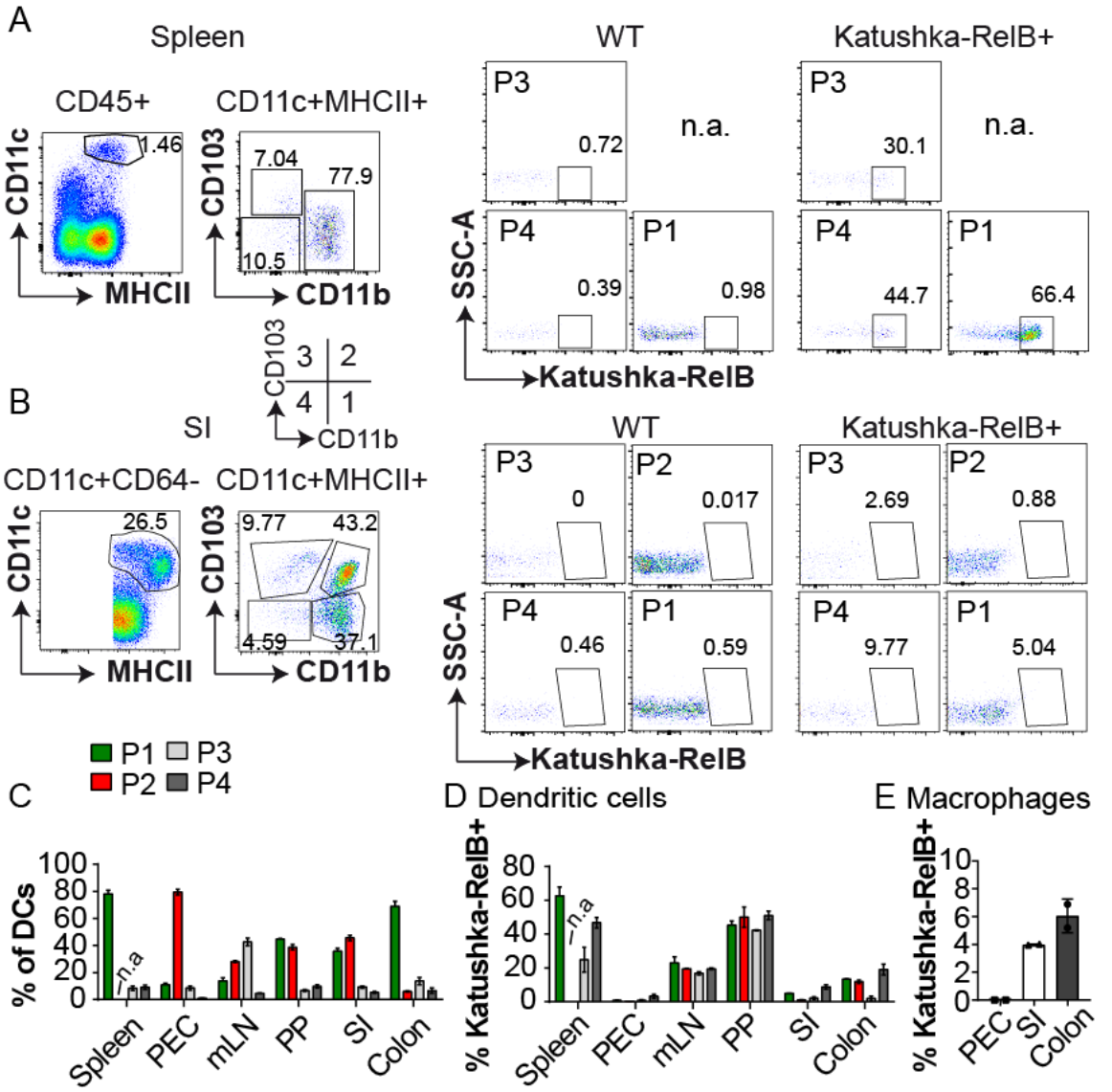

Figure 19. Katushka-RelB is differentially expressed in DCs among different organs. Katushka-RelB expression in DCs from the indicated organs of Katushka-RelB mice was analyzed by flow cytometry. DCs were identified as CD11c+MHCII+ cells. Additionally, for PEC, SI, and colon CD64+ macrophages were excluded. (A, B) Representative FACS plots showing gating strategy for DCs and the Katushka-RelB expression in Katushka-RelB-negative (WT) and Katushka-RelB+ mice (A) in the spleen and (B) in the SI. (C) The distribution of DC subsets as indicated in percentage out of total DCs (upper) and the percentage of Katushka-RelB+ out of the respective DC subset from indicated organs. (D) Frequency of Katushka-RelB+ out of CD64+ macrophages in the indicated organs. Bars show mean ± SD. One representative experiment with two mice per group out of three experiments is shown here.

Flow cytometric analysis of the Katushka-RelB signal revealed that RelB was differentially expressed in DCs from the organs tested (Figure 19 A-E). The total DC population from the spleen and PPs showed the highest proportion of Katushka-RelB+ DCs of appr. 60 % and 50 %, respectively. Compared to the spleen and PPs, mLNs showed an intermediate Katushka-RelB expression of around 20 % Katushka-RelB+ within total CD11c+MHCII+ DCs. In contrast to that, SI and colon showed only a small Katushka-RelB+ population

comprising only up to 10 % of the DC subsets. Interestingly, peritoneal DCs were almost devoid of Katushka-RelB expression.

Regarding the different DC subsets, the most abundant splenic CD11b+CD103- cDC2 subset showed the highest Katushka-RelB expression of around 60 % Katushka-RelB+ of the CD11b+CD103- DC subpopulation. This observation goes in line with previously published data, stressing the fact that the spleen exhibits a large population of RelB+ DCs [190, 192, 215]. Notably, PP-derived DCs had a relatively high level of Katushka-RelB expression, and an almost even distribution of Katushka-RelB+ cells between the four DC subsets (around 50 % Katushka-RelB+ of each of the four DC subsets). Compared to the spleen and PPs, DCs from the mLNs showed throughout lower frequencies of Katushka-RelB expression with around 20 % Katushka-RelB+ cells within each DC subset. In DCs from the SI and colon exhibiting a relatively small Katushka-RelB+ population, the CD11b-CD103- DC subset showed the highest Katushka-RelB expression (of around 20 % in the colon and around 10 % in the SI). This population has been shown to be located in the isolated lymphoid follicles rather than in the lamina propria of the gut [94]. In comparison to DCs, macrophages exhibited undetectable or very low Katushka-RelB expression (Figure 19D). Whereas PEC CD64+ macrophages did not show any detectable Katushka-RelB signal, around 5 % of colonic and small intestinal macrophages were Katushka-RelB+.

Collectively, the data presented here indicates that Katushka-RelB is preferably expressed in the DCs from the spleen and PPs but not in macrophages.

9.12 Microbiota are not involved in the regulation of the RelB expression in DCs

Since Katushka-RelB expression is almost absent in DCs from barrier organs such as the gut and the lung, it has been hypothesized that the microbiota present there downregulate Katushka-RelB expression in DCs [190].

To test this hypothesis, Katushka-RelB mice were depleted of microbiota by a mixture of broad-spectrum antibiotics containing ampicillin, vancomycin, metronidazole, and streptomycin, provided via drinking water *ad libitum*. Specifically, the supplementation with antibiotics started at 2 weeks before birth (by treating the pregnant dams) and was continued until the analysis at 4 weeks of age.

The microbiota-depleted pups were euthanized, the DCs were recovered from spleens, mLNs as well as colon and assessed by flow cytometry. As described above, DCs were identified as CD11c+MHCII+ cells. In the colon, CD64+ macrophages were excluded. The DCs were subdivided into four subsets by the expression of CD11b and CD103.

Flow cytometric analysis showed that the total DC population size was significantly reduced in the spleen from 2 % in untreated to 1 % in antibiotics-treated mice. Further, mLNs and colon exhibited a slight but insignificant loss of DCs upon depletion of bacteria (Figure 20A). Comparing the abundance of CD11b+CD103-, CD11b+CD103+, CD11b-CD103+ and CD11b-CD103- DC subpopulations, only mLNs displayed minor but significant effects upon treatment with antibiotics (Figure 20B). Here, a significant loss of CD11b+CD103+ with a concomitant accumulation of CD11b-CD103+ DCs was observed.

Contrary to the expectations, eradication of bacteria had no significant impact on the Katushka-RelB expression within the analyzed DC subsets (Figure 20 C). Collectively, the data shown here points towards a microbiota-independent mechanism underlying the low expression of Katushka-RelB in the gut.

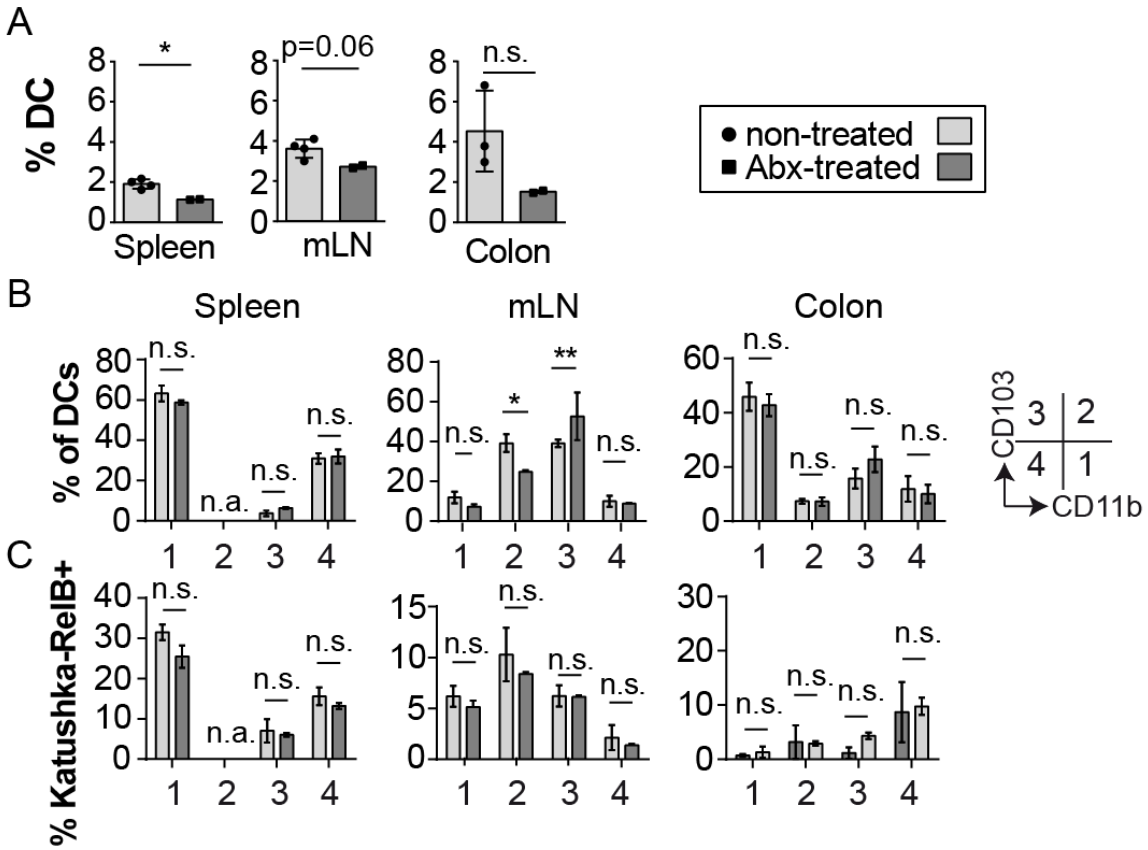

Figure 20: Antibacterial treatment prior and 4 weeks after birth does not have any effect on Katushka-RelB expression the DCs. Pregnant Katushka-RelB mice and subsequently the pups were treated with a cocktail of antibiotics (as described in the materials and methods part). At 4 weeks of age, mice were euthanized and the DCs recovered from the spleen, mLNs and colon were analyzed by FACS. (A) Total DC frequency in the spleen, mLN and colon from antibiotic-treated (referred to as 'Abx-treated') or non-treated mice. DCs are identified as MHCII+ CD11c+ cells, for the colon CD64+ macrophages were excluded. (B) Percentages of the designated DC subpopulations (upper row) and the frequency of Katushka-RelB+ within the indicated populations (lower row). A, B, C: Abx-treated group: n = 2, each of the two data points consist of three pooled mice. Non-treated group: n = 4 in A and B and n= 3 in C, each point represents one mouse. The experiment was performed once. All bar diagrams represent mean ± SD. *p ≤ 0.05. A: Student's t-test. B: unpaired two-way ANOVA with Sidak's correction for multiple comparisons.

9.13 RelB$^{\Delta DC}$ mice are protected from EAE due to the Treg accumulation

The ST2+ tissue Tregs have a self-reactive TCR repertoire and show high suppressive capacity [64, 72]. Therefore, it was hypothesized here, that RelB$^{\Delta DC}$ mice are less prone to develop an autoimmune-type pathology.

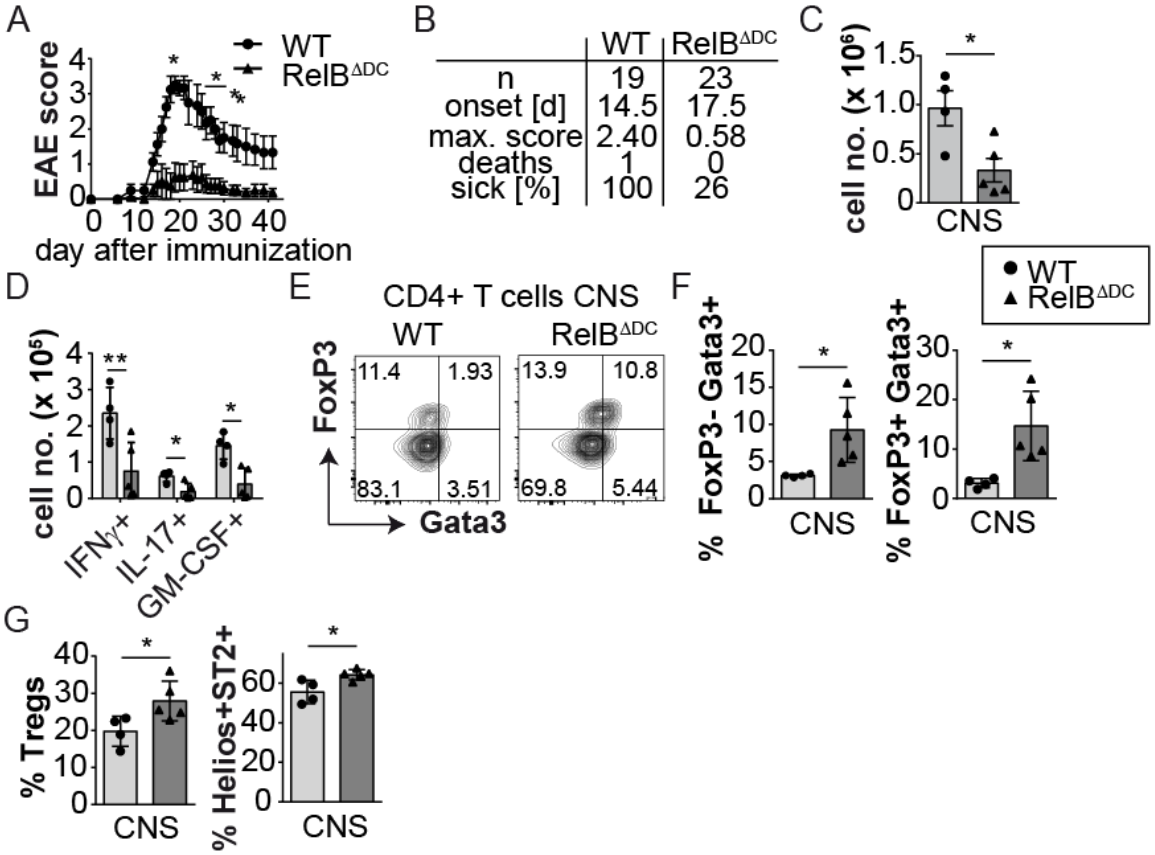

Figure 21. RelB$^{\Delta DC}$ mice are protected from EAE. EAE was induced in RelBΔDC or WT mice by immunization with MOG peptide in CFA. Mononuclear cells were isolated from the CNS at the peak of EAE and analyzed by flow cytometry. (A) EAE scores of RelB$^{\Delta DC}$ or WT mice over 40 days after immunization. Scoring scheme: 1 - tail paralysis; 2 - hind limb impairment; 3 - hind limb paralysis; 4 - front limb paralysis. (B) Summarized EAE data showing total number of mice per group, mean EAE onset day, maximum of mean EAE score per day, deaths due to EAE and percentages of sick mice defined by EAE score ≥ 0.75. Total cell number of (C) mononuclear cells or (D) IFNγ+, IL-17+ and GM-CSF+ Teff cells after restimulation with PMA and ionomycin. (E) A representative FACS plot showing FoxP3 and Gata3 expression among CD4+ T cells recovered from the CNS. (F) Quantification of the data shown in E as % of the indicated populations out of CD4+ T cells. (G) Percentages of FoxP3+ Tregs out of CD4+ T cells (left) and % Helios+ST2+ out of FoxP3+ Tregs (right). (A, C-G) Data from one representative experiment is shown with n ≥ 4 per group. (A, B) Data was obtained by Nico Andreas. (A, C, D) Data shown as mean ± SEM. (F, G) Bars represent mean ± SD. *p ≤ 0.05; ** ≤ 0.01. (A) Mann-Whitney U-test. (D) Multiple Student's t-test with Holm-Sidak correction for multiple comparisons. (C, F, G) Student's t-test.

To test this hypothesis, experimental autoimmune encephalomyelitis (EAE) was actively induced in RelB$^{\Delta DC}$ mice or WT mice by immunization with the immunodominant epitope of myelin oligodendrocyte glycoprotein (MOG fragment 35-55) in complete Freund's adjuvant (CFA) as described in materials and methods. EAE is a demyelinating disease of the central nervous system (CNS) characterized by ascending paralysis and immune infiltrations in the CNS. The EAE disease severity was recorded by a scoring system as follows: 1 – tail paralysis, 2 – hind limbs impairment, 3 – hind limb paralysis, 4 – front limbs paralysis. In addition to that, the total number of mononuclear cells infiltrating the CNS at the peak of disease and the number of cytokine-producing Teffs in the CNS were analyzed at the peak

of disease. For the latter, mononuclear cells recovered from the CNS were restimulated by incubation with phorbol 12-myristate 13-acetate (PMA) in combination with ionomycin and GolgiStop™ for 4 h at 37 °C. Thereafter, the production of interferon γ (IFN-γ), IL-17 and granulocyte-macrophage colony stimulating factor (GM-CSF) was assessed by flow cytometry.

As expected, all WT mice displayed paralysis, here indicated by an EAE score ≥ 0.75 starting from day 14.5 as day of onset (Figure 21A, B). In this group, the EAE score reached its peak at around day 18 after the immunization with a mean score of 2.40. The high level of limb paralysis reflects an aggressive autoimmune inflammation. In contrast to that, the RelB$^{\Delta DC}$ mice displayed only mild EAE pathology with only around a quarter of the RelB$^{\Delta DC}$ mice tested developing paralysis with a score ≥ 0.75 in combination with a delayed day of onset (17.5). The mean EAE score among RelB$^{\Delta DC}$ mice at the peak of disease was 0.58, showing that the mice lacking RelB in DCs were protected from EAE disease development.

Furthermore, only a small population of infiltrating mononuclear cells were recovered from the CNS from RelB$^{\Delta DC}$ mice (appr. 0.25 x 10^6 cells), whereas WT mice displayed a large population of appr. 1 x 10^6 cells (Figure 21C). In line with the total cell number, the abundance of IFN-γ, IL-17 and GM-CSF producing effector T cells was significantly lower in RelB$^{\Delta DC}$ compared to WT mice (Figure 21D).

Since RelB$^{\Delta DC}$ mice showed systemic Treg accumulation and a Th2 bias at steady state, it was assumed that in absence of RelB in DCs, Tregs and Th2 cells accumulate in the CNS and contribute to the suppression of Th1/Th17-dominated inflammation during EAE.

To address this question, the expression of Gata3 in FoxP3+ Tregs and FoxP3- Teffs was investigated in the CNS at the peak of disease. Strikingly, within both populations, Gata3 expression was strongly elevated in RelB$^{\Delta DC}$ mice (Figure 21E, F). In line with that, the total Treg population in the CNS was expanded from 20 % in WTs to 30 % in RelB$^{\Delta DC}$ mice. Further, the proportion of ST2+Helios+ tissue Tregs was mildly, but significantly elevated in the CNS of RelB$^{\Delta DC}$ mice at peak of EAE (Figure 21 G).

These findings show that protection of RelB$^{\Delta DC}$ mice from EAE is associated with elevated Treg frequency and a Th2 bias. However, the possibility that RelB-deficient DCs are not able to mount inflammation upon active immunization with MOG/CFA could not be excluded in this experimental setting. Since RelB deficiency in DCs results in a specific deletion of a subset of splenic Sirpα+ DCs, and this DC subset is especially important in the EAE induction, it is feasible that RelB in DCs is required cell-intrinsically to induce disease [216]. To exclude this possibility and confirm that EAE-resistance in RelB$^{\Delta DC}$ mice originates from expanded Treg population, RelB$^{\Delta DC}$ mice were deleted of Tregs by anti-CD25 antibody treatment prior to MOG-immunization. To this end, PC61 clone of anti-CD25 antibody was injected i.p. twice: 5 days prior to immunization and at the day of immunization (day 0), see Figure 22A.

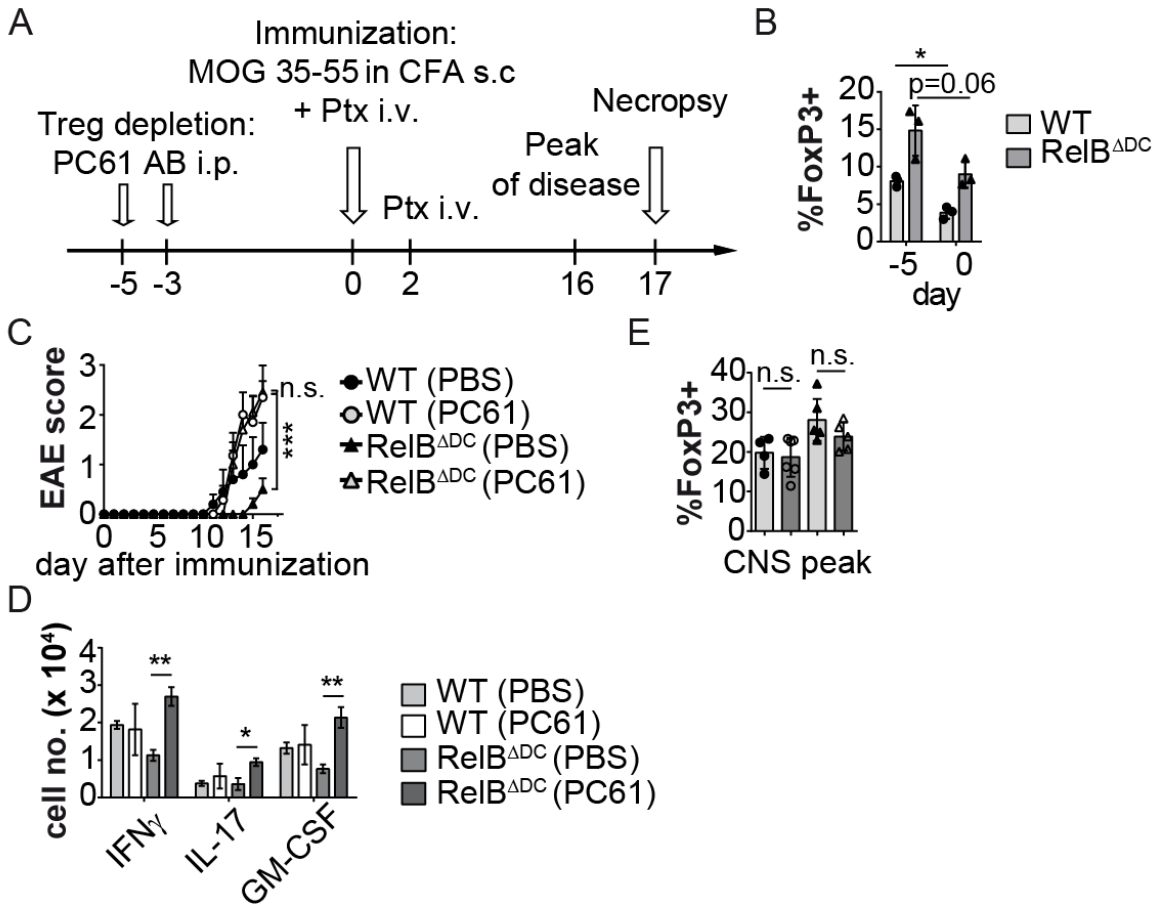

Figure 22. Depletion of Tregs restores EAE pathology in RelB$^{\Delta DC}$ mice. Treg-depletion was done in RelB$^{\Delta DC}$ mice or WT mice by anti-CD25-antibody (PC61 clone) treatment prior to immunization as described before. (A) Timeline of the experimental design. (B) PC61-mediated depletion efficiency of FoxP3+ Tregs as analyzed by FACS from blood. Indicated time points are according to the scheme in (A). (C) EAE scores of Treg-depleted (PC61) and PBS-treated (PBS) WT or RelB$^{\Delta DC}$ mice. The scores were recorded according to the scoring system as described in Figure 21. (D) Total cell number of cytokine producing Teff cells recovered from the CNS after stimulation with PMA/ionomycin. Cell numbers are calculated using the mean of the recorded cell number per group and the total frequency of cytokine-producing FoxP3-CD4+ T cells out of living cells as analyzed by FACS. (E) Percentages of FoxP3+ Tregs in the CNS at peak of EAE. (B, E) Bars represent mean ± SD or (C, D) mean ± SEM. (B-D) One representative experiment of two experiments is shown. (B) n = 3 per group. (C) n ≥ 5 per group (D) WT (PBS): n = 3, WT (PC61): n = 2, RelB$^{\Delta DC}$ (PBS): n = 4, RelB$^{\Delta DC}$ (PC61): n = 4. *p ≤ 0.05; **p ≤ 0.01; ***p ≤ 0.001. (E) at least four mice per group are shown. (C) Two-way ANOVA with Turkey's test for multiple comparisons. Otherwise, Student's t-tests with Holm-Sidak correction for multiple comparisons.

The depletion efficiency was tested before the injection (day -5) and at the day of immunization (day 0) by flow cytometric analysis of FoxP3+ Tregs from blood (Figure 22B). As expected, the Treg frequency was significantly reduced in WT mice by a factor of two from around 8 % to appr. 4 %. Although the Treg frequency in PC61-treated RelB$^{\Delta DC}$ mice also decreased twofold to the level of untreated WT Tregs (from 15 % in untreated mice to appr. 8% in anti-CD25-treated mice), the difference was not statistically significant.

To observe the impact of the Treg ablation on the EAE disease severity, EAE score was recorded until peak of disease at day 16 (Figure 22 C). At the peak of disease, the mice

were sacrificed and the mononuclear cells infiltrating the CNS were isolated, counted, re-stimulated *ex vivo* and analyzed for the cytokine expression by flow cytometry.

As expected, the EAE score of WT mice was higher in Treg-depleted (with a score of 2.5 at the peak of disease) compared to non-depleted WT mice (with a score of 1.5 at the peak of EAE), indicating an aggravated disease severity in absence of CD25+ cells. Strikingly, the EAE score of the Treg-depleted RelB$^{\Delta DC}$ mice was elevated (from a score of 0.5 at the peak of EAE) to the level of the Treg-depleted WT mice (score of appr. 2.5) disregarding the low level of Treg depletion. In line with that, the infiltration of the CNS with cytokine producing Teff cells was restored upon anti-CD25 antibody administration (Figure 22 D). When looking at the CNS-resident Tregs, no differences between the Treg-depleted and untreated mice could be detected suggesting a rapid turnover of Tregs after depletion (Figure 22E).

This data suggests that the RelB$^{\Delta DC}$ mice are protected from EAE due to the expanded Treg population. Furthermore, it could be shown that RelB in DCs is not essential for the initiation of an immune response upon MOG immunization.

9.14 MOG-specific Tregs are *de novo* induced upon EAE induction in RelB$^{\Delta DC}$ mice

In WT mice after MOG-immunization, no self-antigen-specific *de novo* Treg induction takes place [216]. The possibility that RelB deficiency in DCs permits *de novo* induction of MOG-specific Tregs in the inflammatory context of EAE was tested. To this end, naïve MOG-specific 2D2 T cells were FACS sorted from 2D2-FoxP3-GFP reporter mice and injected intravenously into RelB$^{\Delta DC}$ or WT mice prior to MOG immunization. A week later, prior to the onset of disease, GFP-signal indicating FoxP3 expression (indicated as FoxP3(GFP)+ cells) within CD4+ 2D2 T cells from inguinal lymph nodes (iLNs) was assessed by flow cytometry. Thereby, 2D2 cells were characterized as Vα3.2+Vβ11+ CD4 T cells (Figure 23A).

As expected, DCs from WT mice did not support FoxP3 upregulation in MOG-specific 2D2 T cells (Figure 23B). Strikingly, a small but detectable number of FoxP3(GFP)+ cells was detected in the inguinal lymph nodes of RelB$^{\Delta DC}$ mice. This finding indicates that self-antigen specific Tregs can be induced under inflammatory conditions in absence of RelB in DCs.

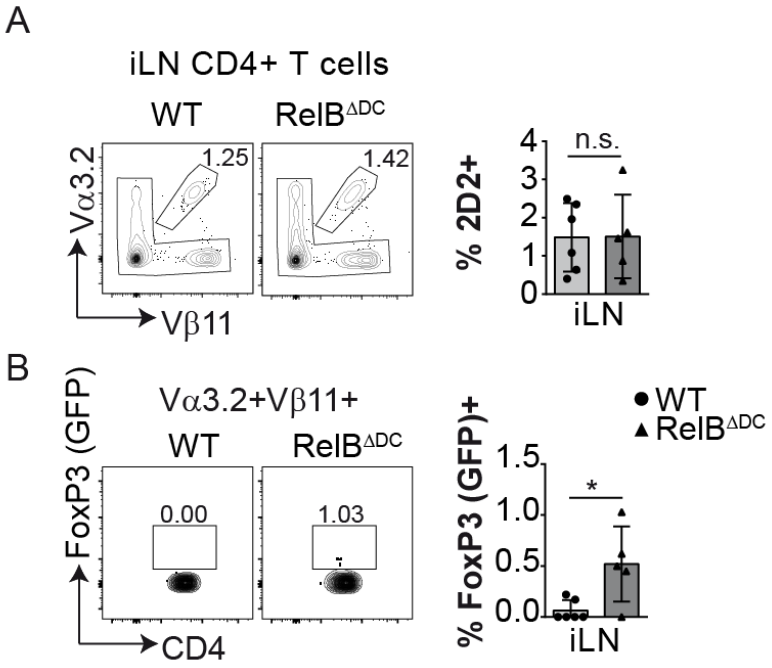

Figure 23. RelB-deficient DCs permit induction of MOG-specific Tregs after MOG-immunization. RelB$^{\Delta DC}$ or WT mice were injected with naïve FoxP3(GFP)-negative MOG-specific 2D2 cells and immunized with MOG in CFA. At day 8, before the onset of disease, FoxP3(GFP) expression in 2D2 cells from iLNs was assessed by FACS. (A) Representative FACS plots showing the gating strategy to identify 2D2 cells by Vα3.2 and Vβ11 and a bar diagram displaying percentage of Vα3.2+ Vβ11+ 2D2 cells out of CD4+ T cells. (B) Representative FACS plots showing FoxP3(GFP) expression within Vα3.2+ Vβ11+ 2D2 cells and quantification of the frequency of FoxP3(GFP)+ out of Vα3.2+ Vβ11+ 2D2 cells. Bars show mean ± SD. *p ≤ 0.05; Student's t-test.

9.15 RORγt+ Tregs are dispensable for the establishment of oral tolerance and suppression of allergic airway inflammation

RORγt+ Tregs have only recently been characterized, thus multiple aspects of their biology remain elusive. Whereas their superior anticolitogenic properties are well established, the role of RORγt in Tregs for the suppression of systemic immunization and challenge via the respiratory tract upon oral tolerance induction has not been addressed yet.

To elucidate this issue, the ability of Tregs lacking RORγt to mediate oral tolerance induction in a context of allergic airway inflammation (AAI) was tested. To this end, oral tolerance was induced in mice lacking RORγt in FoxP3+ Tregs (RORγt$^{\Delta Treg}$ mice) and WT mice by three subsequent intragastric (i.g.) gavages of OVA. Non-tolerized groups were given PBS instead of OVA. After the oral tolerance induction phase, the mice were immunized with three intraperitoneal injections of OVA in aluminium hydroxide adjuvant (alum) to induce a type 2 immune response. Three weeks after the first immunization, the mice were challenged three times with OVA by nebulization (the experimental timeline is depicted in Figure 24A). This experimental setup is established for the induction of type 2-dominated AAI in mice. 24 h after the last challenge, mice were sacrificed, and the disease severity was assessed. To this end, bronchoalveolar lavage (BAL) was performed to determine the

number and identity of lung-infiltrating cells. In addition to that, serum total IgE and OVA-specific IgG1 levels were measured. Furthermore, eosinophils and CD11b+CD11c+ myeloid (myDCs) infiltrating the lung tissue were analyzed by flow cytometry.

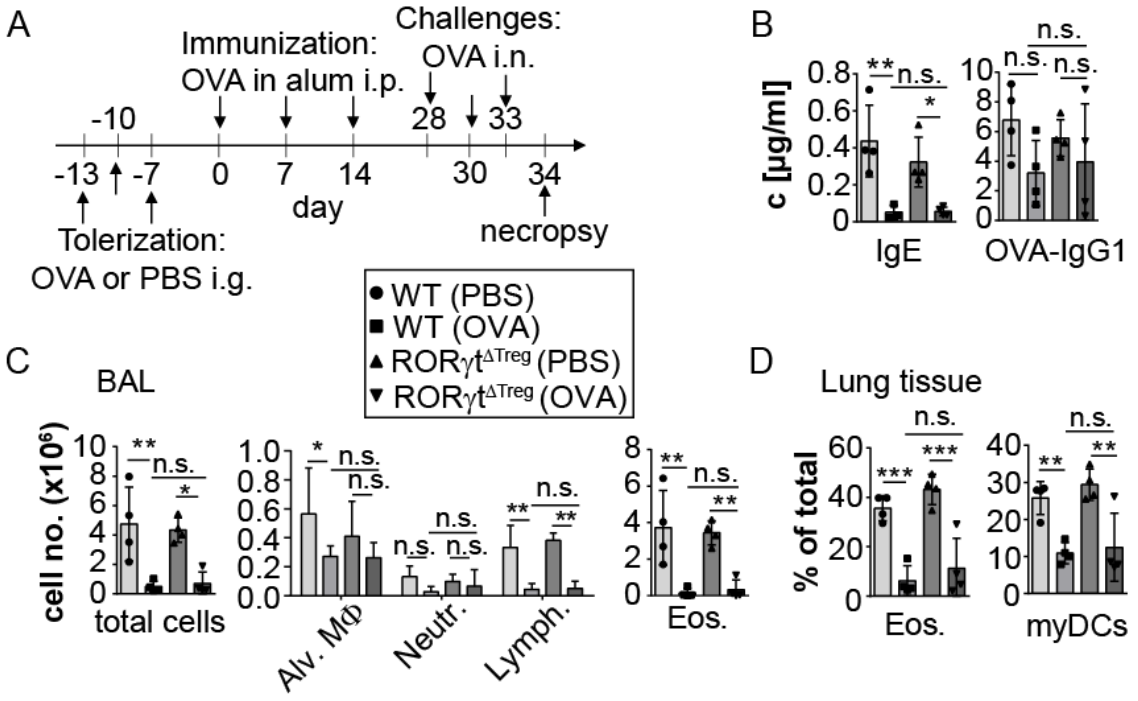

Figure 24. RORγt in Tregs is dispensable for the establishment of oral tolerance in a lung allergy model. Oral tolerance induction (by i.g. gavage of OVA in Rorγt$^{\Delta Treg}$ or WT mice) was tested by subsequent induction of OVA/alum-mediated allergic lung inflammation. PBS-treated groups served as non-tolerized control. (A) Experimental setup for the oral tolerance and allergic airway inflammation induction. (B) Serum total IgE level (left) and serum OVA-specific IgG1 level (right) as measured by ELISA. (C) BAL total and differential cell numbers (no.) including alveolar macrophages (Alv. MΦ), neutrophils (Neutr.), lymphocytes (Lymph) and eosinophils (Eos.) in the BAL. (D) Flow cytometric analysis of lung infiltrating eosinophils defined as Siglec-F+ SSC-A high cells recovered from the lung tissue and myeloid DCs defined as CD11b+CD11c+ cells shown as percent out of living cells. (B-H) Bars represent mean ± SD. *p ≤ 0.05. ANOVA with Turkey's correction for multiple comparisons. One representative experiment out of 3 independent experiments is shown.

Interestingly, oral tolerance induction with OVA prevented OVA sensitization and significantly ameliorated clinical symptoms of AAI in the WT and RORγt$^{\Delta Treg}$ mice to the same extent. Tolerized WT and RORγt$^{\Delta Treg}$ mice exhibited an almost undetectable serum total IgE level in comparison to the respective non-tolerized mice (Figure 24B). In the latter, around 0.4 µg/ml IgE could be detected (irrespective of the genotype).

In line with that, oral tolerance induction prevented infiltration of proinflammatory cells irrespective of the presence of RORγt in Tregs: the total BAL cell number as well as the frequencies of lung-infiltrating eosinophils and myDCs were significantly lower upon oral tolerance induction in WT and RORγt$^{\Delta Treg}$ mice. Whereas both tolerized groups had an almost undetectable number of BAL cells, the non-tolerized mice exhibited a strong BAL infiltration with around 5 x 10^6 cell irrespective of the genotype. In the lung parenchyma, eosinophils constituted the major infiltrating cell population in the non-tolerized mice with

around 40 % eosinophils of total living cells. The tolerized groups harbored only around 10 % eosinophils in the lung parenchyma. Accordingly, the proinflammatory CD11b+ myeloid DCs (CD11c+CD11b+ cells) made up around 30 % of all infiltrating cell in the non-tolerized and only appr. 10 % in the tolerized mice independently of the presence of RORγt in Tregs.

Accordingly, differential counting of BAL cells from tolerized mice showed significantly smaller numbers of lymphocytes and eosinophils compared to non-tolerized mice irrespective of the genotype. Whereas alveolar macrophages (Alv. MΦs) were significantly reduced in tolerized WTs, no difference between the tolerized and the non-tolerized RORγt$^{\Delta Treg}$ mice could be detected.

In contrast to the data suggesting a robust suppression of clinical manifestations of AAI after oral tolerance induction, no significant effects on the OVA-specific IgG1 could be detected after oral OVA administration in WT or RORγt$^{\Delta Treg}$ mice. Of note, in support of previously published data, the severity of the airway inflammation in non-tolerized mice was comparable between RORγt$^{\Delta Treg}$ and WT mice [59]. These findings suggest that the RORγt+ Tregs mainly confined to the GALT are not essential for the suppression of sensitization via the respiratory tract.

In summary, the data shown here suggests that RORγt in Tregs is dispensable for the installation of oral tolerance prior to sensitization with OVA/alum and induction of allergic airway inflammation.

10 Discussion

10.1 RORγt+ Tregs are dispensable for the induction of oral tolerance in a lung allergy model

Immunological tolerance is key for the survival of organisms and proper immunological function. Thereby, two main arms – central and peripheral tolerance can be distinguished. Whereas the central tolerance is a result of negative selection of self-reactive thymocytes and differentiation of thymically-derived Tregs (nTregs), peripheral tolerance induction mainly relies on the generation of induced Tregs (iTreg) in the gut. This not only ensures a systemic state of non-responsiveness towards ingested antigens in a process termed oral tolerance induction, but also suppresses local immune responses towards microbiota, thus mediating mucosal tolerance. Consequently, abrogation of the iTreg development may result in a spontaneous Th2-type inflammation of the gastrointestinal tract and the lung resembling allergic inflammation and asthma and increase the susceptibility to colitis [51, 217].

One of the main mucosal Treg populations co-expresses the nuclear hormone receptor retinoid-related orphan receptor γt (RORγt) and uniquely develop in the gut in the presence of certain microbial species [52, 53]. Hence, perturbations of the gut microbiome or its complete absence result in a reduction or the complete absence of RORγt+ Tregs in mice, respectively [52, 53]. Strikingly, the loss of RORγt+ Tregs is not only associated with an enhanced susceptibility to colitis, but also with an exaggerated activation of type 2 immune responses [52, 53, 57]. In line with that, a reduced capability of microbiota to induce RORγt+ Tregs is associated with the development of food allergy [57]. These findings suggest a critical interrelationship between microbiota-dependent signals, RORγt+ Tregs and establishment of oral tolerance.

Whereas the local role of RORγt+ Tregs in the suppression of intestinal inflammation is established, the role of RORγt+ Tregs in the suppression of allergic airway inflammation (AAI) upon induction of oral tolerance remains elusive. To address this question, the capacity of RORγt-deficient Tregs to inhibit Th2-mediated AAI after oral tolerance induction was investigated. To this end, mice with a FoxP3+ Treg-specific deletion of RORγt (RORγt$^{\Delta Treg}$) or WT mice received three intragastric (i.g.) gavages of ovalbumin (OVA) to establish oral tolerance. The non-tolerized control mice received i.g. phosphate-buffered saline (PBS) instead. Subsequently, AAI was induced in all mice by sensitization with OVA in combination with aluminium hydroxide adjuvant (alum) and subsequent challenges by inhalation of OVA aerosol [218].

Surprisingly, OVA gavage protected WT as well as RORγt$^{\Delta Treg}$ mice from the development of OVA-alum mediated AAI to the same extent. Hence, clinical manifestations of the AAI including total serum immunoglobulin E (IgE) concentration, bronchoalveolar lavage (BAL) cell number and the proportions of eosinophil and myeloid DCs within the lung parenchyma were reduced in tolerized mice irrespectively of the RORγt expression in Tregs. Despite some limitations, the data is consistent and suggests that RORγt expression in FoxP3+

Tregs is dispensable for the establishment of oral tolerance and suppression of type 2 lung inflammation.

Notably, the non-tolerized RORγt$^{\Delta Treg}$ mice showed no signs of exaggerated inflammation in comparison to the non-tolerized WT mice. This notion is supported by own observations and the data obtained by the Chatila group [59]. The latter shows that upon AAI induction, Treg-specific RORγt-ablation did not aggravate the inflammation. Instead, in allergy-susceptible mice (which carry an IL4R alpha chain R576 point mutation), RORγt contributes to the trans-differentiation of iTregs into Th17 cells, thereby promoting lung inflammation upon sensitization [59].

Previous publications propose that the Th2-suppressive action of RORγt+ Tregs is restricted to the gastrointestinal tract [57]. In line with that, RORγt+ Tregs predominantly reside in the gut, whereby the colon harbors the highest frequency of these cells [52, 219]. In contrast to that, the frequency of RORγt+ Tregs in the lungs of non-sensitized wildtype (WT) mice kept under specific pathogen-free (SPF) conditions is very low, albeit inflammation of the respiratory tract triggers the accumulation of RORγt+ Tregs [59]. In addition to that, the microbiota-dependent nature of intestinal Tregs results in a preferential recognition of microbial antigens and may thus contribute to the inefficient suppression of food-antigen-specific effector T cell responses as was investigated in this thesis [50, 220]. Consistently with their microbiota-dependent nature, RORγt+ Tregs show superior anticolitogenic properties, whereas antigen-specific Tregs effectively inhibit sensitization with the cognate antigen and protect from AAI induction [52-54, 221].

In summary, the data presented here suggests that RORγt expression in Tregs is dispensable for suppression of AAI irrespective of the preceding oral tolerance induction.

10.2 NF-κB family member RelB is required in DCs to establish mucosal tolerance and contain excessive tissue Treg accumulation

Dendritic cells (DCs) are indispensable for the induction of central and peripheral tolerance [212]. The T cell receptor (TCR) stimulation via MHCII-bound antigens presented on DCs facilitates negative selection and nTreg development in the thymus conferring central tolerance [212]. In the periphery, DCs are responsible for the transport of antigens from the tissues to the draining lymph nodes (LNs), thereby allowing for efficient iTreg induction [112, 118].

The role of the NF-κB family member RelB in the establishment of central tolerance and for dendritic cell (DC) function has long been recognized [170, 173]. However, the majority of the findings concerning the role of RelB in the development and maturation of DCs derives from studies using systemically RelB-deficient (RelB-KO) mice or corresponding bone marrow chimeras (BMCs). Interpretation of this data is hampered by multiple defects and the severe inflammatory phenotype of the RelB-KO mice. Therefore, the contribution of cell-type-specific RelB remained elusive. The data presented in this thesis added to the understanding of the cell-type-specific requirement of RelB for the initiation of immune

responses, establishment of immunological tolerance and regulation of the regulatory Treg compartment.

This thesis established a critical role of DC-intrinsic RelB expression for the regulation of normal Treg compartment and containment of Th2 polarization. Mice with a DC-specific *Relb* ablation (RelB$^{\Delta DC}$) were generated by crossing mice carrying an *Itgax*-cre allele (here referred to as CD11c-cre) with *Relb*-floxed mice. The DC-specific *Relb* deletion resulted in an expanded total Treg population due to elevated frequency of ST2+ tissue Tregs. In contrast to that, RelB-deficient DCs did not support efficient establishment of mucosal tolerance characterized by defective induction oral antigen-specific as well as microbiota-dependent RORγt+ Tregs. This misbalance within the Treg populations was associated with a spontaneous systemic Th2 bias. Whereas RelB$^{\Delta DC}$ mice mirrored the Th2 and Treg phenotype of systemically RelB-deficient mice, RelB was shown to be dispensable Treg-intrinsically.

Most importantly, the DC-intrinsic requirement of RelB for T cell priming could be ruled out using experimental autoimmune encephalomyelitis (EAE) as a model of autoimmune disease critically dependent on DC [216, 222]. Strikingly, Treg depletion by anti-CD25-antibody allowed for initiation of EAE upon active immunization. Therefore, the data presented here reveals that the expanded Treg population in RelB$^{\Delta DC}$ mice confers protection from EAE.

10.2.1 Systemic RelB is critical for the development of a normal Treg compartment and containment of Th2 polarization

The role of RelB for central tolerance induction is well established. The autoimmune phenotype of RelB-deficient mice has been mainly attributed to the defective development of the medullary thymic epithelial cells (mTECs), which are critical for the synthesis of tissue restricted antigens, thereby facilitating deletion of self-reactive thymocytes and development of nTregs [170, 173, 181, 223]. Albeit autoimmunity is usually mediated by Th1/Th17 cells, systemic ablation of *Relb* in mice results in spontaneously elevated Th2 cell frequency as was shown here and previously [177, 178]. In contrast to the central tolerance critically relying on RelB, its role in the peripheral tolerance establishment has been neglected so far.

To address whether *Relb*-deletion permits the development of a normal mucosal Treg population, the Tregs from the small intestinal lamina propria (SI-LP) were analyzed. In addition to the RORγt+ iTregs, and Helios+ nTregs, Gata3+ tissue Tregs were analyzed in the gut. The latter Treg subset is mainly present in non-lymphoid tissues, accumulating there preferentially upon damage [63, 66, 69, 224]. Thereby, the IL-33 receptor (ST2) highly expressed on tissue Tregs confers responsiveness towards epithelial cell damage associated with release of the alarmin IL-33 [73]. In line with superior tissue-protective features, tissue Tregs exhibit a Th2-prone phenotype, which is thought to be supportive during tissue repair and homeostasis [63, 65, 225, 226].

Whereas the total Treg frequency was dramatically elevated due to the accumulation of Helios+ Tregs in the SI-LP of RelB-KO mice, the RORγt+ iTregs were almost completely absent. In the gut, Helios is a reliable marker of thymus-derived nTregs and allows for a

clear distinction between RORγt+ and Helios+ Tregs [52]. However, Helios is co-expressed by a substantial fraction of tissue Tregs, the etiology of which is not completely understood [60, 63, 77]. In line with that, Tregs from RelB-deficient mice expressed significantly higher levels of Gata3. Whereas the vast majority of the Gata3+ SI-LP Tregs co-express Helios in WT mice, RelB-deficient mice accumulated high proportions of Gata3+ Tregs irrespective of Helios expression (Ref. [63] and Figure 1). In support of the notion that RelB-deficient mice show an impaired intrathymic nTreg development, the expanded Gata3+ Treg subset presumably constitutes of tissue, rather than of thymus-derived Tregs (Refs. [170, 173] and Figure 1).

Furthermore, the expansion of Gata3+ Tregs might be a consequence of the defective negative selection in RelB-deficient mice [170, 181, 223]. Consequently, self-reactive T cell clones escaping the negative selection can be converted into Tregs in the periphery. The elevated levels of Treg-inducing cytokines in RelB-deficient mice may contribute to the accumulation of Gata3+ Tregs. Among those, the levels of IL-2, TSLP, IL-25 and IL-33 are significantly elevated in absence of RelB [174, 178, 183, 205].

As a consequence of the expanded Gata3+ Treg population and a diminished RORγt+ Treg subset, the equilibrium of the Treg subsets was dramatically shifted in the RelB-deficient mice and this bias towards Th2-linked Gata3+ away from Th2-suppressive RORγt+ Tregs was associated with a profound Th2-type inflammation in the SI-LP of RelB-KO mice. Therefore, the previously recognized implications of RelB in controlling normal Treg compartment and suppressing Th2 immunity in the gut extend previous knowledge. Whereas the Th2 phenotype in the skin and lungs of RelB-KO mice has been previously well characterized, the implication of the RelB deficiency for the gut remained elusive [177, 178, 227].

In terms of cell-specific requirement of RelB for the containment of aberrant Th2 cell activation, a DC-intrinsic requirement of RelB for the suppression of Th2 polarization was established in this thesis and is discussed later. This implication is supported by the spontaneous Th2 bias observed in $RelB^{\Delta DC}$ mice in combination with previous findings suggesting that Th2-dominated inflammation and autoimmunity are reversible upon transfer of WT DC [178, 184].

In contrast to that, DC-specific *Relb* deletion was not associated with spontaneous autoimmune inflammation, suggesting a subordinate role of DC-intrinsic RelB for the establishment of central tolerance. Furthermore, a Treg-intrinsic requirement of RelB for the establishment of immunological tolerance could be ruled out here. This data supports the notion that the abrogated mTEC development is the key event triggering autoimmune inflammation in RelB-deficient mice [170, 181, 223].

Since the extent of autoimmune inflammation upon TEC-specific *Relb* ablation is less severe than in systemically RelB-deficient mice, further defects may contribute to the fatal autoimmunity in absence of RelB [170, 181, 184, 223]. In addition to mTECs, negative selection is critically dependent on thymic DCs, which receive self-antigens from mTECs and are responsible for their efficient presentation to eliminate self-reactive T cell clones and support Treg induction [212, 228]. mTECs, in turn support localization and maturation of DCs in the thymus [229]. Indeed, the supplementation of RelB-KO mice with WT DCs

suppresses the autoimmune inflammation [178, 184]. Interestingly the amelioration of disease is in part mediated by suppression of autoimmune thymic inflammation [184]. This illustrates that although RelB is not required DC-intrinsically for the establishment of central tolerance, DC-extrinsic RelB establishes and maintains a niche which support proper DC development and function, thereby contributing to the establishment of central tolerance.

In line with abrogated induction of RORγt+ Tregs, RelB-deficient mice showed a severely diminished frequency of RORγt+ Th17 cells. These two RORγt+ T cell types are major players of the mucosal immune system, thus defective mucosal immunity might contribute to the multiorgan inflammation of RelB-deficient mice [52-54, 56, 230-232]. Previous observations showing that barrier organs like the lung and skin are particularly affected by the inflammation further corroborates this theory [177, 178, 227].

Whereas DC-intrinsic requirement of RelB for the induction of RORγt+ Tregs is shown here and will be discussed later, the development of Th17 cells was independent of RelB expression in DCs. Furthermore, the data presented here and previous findings show that RelB in T cells and Tregs is dispensable for the induction of Th17 cells [233, 234]. Therefore, the cell-type-specific requirement of RelB for the induction of Th17 cells remains elusive. Instead, the lack of mesenteric lymph nodes (mLNs) as the main inductive site of Th17 (and RORγt+ Tregs) might be causative for the defective induction of these two microbiota dependent cell types [104, 118, 170-172, 231].

Since the loss of RORγt+ Treg induction is even more pronounced in systemically RelB-deficient mice compared to $RelB^{\Delta DC}$ mice, the lack of mLNs and the proinflammatory microenvironment dominating the SI-LP RelB-deficient mice might contribute to the abrogated RORγt+ Treg induction [230, 235]. RORγt+ Treg and Th17 development requires stimulation by mature DC [52, 213, 219]. However systemic RelB deficiency does not permit DC maturation [185]. Whereas the DC-intrinsic requirement of RelB for DC maturation and antigen presentation could be ruled here and is discussed later, non-hematopoietic cells seem to require RelB to support normal DC development [93]. Therefore, the immature phenotype of DCs from RelB-KO mice might not be permissive for an efficient generation of RORγt+ cells [52].

In summary, despite the severe inflammatory phenotype of RelB-deficient mice has been ascribed to a defective central tolerance induction, resulting in autoimmunity, the data presented here suggests that a compromised mucosal immune function may contribute to the autoimmune phenotype.

10.2.2 NF-κB signaling is critical for the Treg development

To gain an insight into the Treg-intrinsic requirement of RelB for the development of a normal Treg compartment, mice with a Treg-specific *Relb* ablation ($RelB^{\Delta Treg}$ mice) were analyzed. Surprisingly, Treg-intrinsic deletion of RelB did not have any detectable effect on the total, RORγt+ or Gata3+ Treg frequencies (Figure 4). These finding go in line with the recently published data suggesting that RelB is dispensable in Tregs [204, 205]. In contrast to RelB, its binding partner NF-κB2 (p100) is critically required Treg-intrinsically for the development of normal frequencies of functional Tregs [204, 205]. Despite the elevated total Treg frequency, Tregs deficient for NF-κB2 fail to suppress autoimmune inflammation [204,

205]. Interestingly, the expansion of *Nfkb2*-deficient Tregs and autoimmune inflammation are associated with elevated RelB activation and nuclear translocation [204]. Consequently, the phenotype is reversed in mice with double deficiency of RelB and NF-κB2 in Tregs [204]. Therefore, NF-κB2 plays an essential role as a RelB inhibitor in Tregs [204]. In line with that, Treg-intrinsic constitutive activation of the alternative NF-κB signaling via transgenic expression of NF-κB inducing kinase (NIK) from the ROSA-26 locus causes loss of regulatory function and ultimately results in autoimmune inflammation [236]. These findings suggest that whereas a Treg-specific overactivation of RelB abrogates Treg function, a loss of RelB in Tregs is most probably compensated for by other NF-κB proteins. Among those, p50-NF-kB complexes may compensate for the absence of RelB, as a double deficiency of RelB and p50 aggravates the severity of multiorgan inflammation compared to RelB-deficient mice [237].

The transcriptional activity of RelB is regulated by other NF-κB and IκB family members. The effects of the ablation of p50 and BCL3 as examples of a potential RelB binding partner and an atypical IκB, respectively, have been studied here [163]. In contrast to RelB-KO mice, neither p50-KO nor BCL3-KO lacked mLNs, suggesting no cooperation of RelB with either of the factors in the regulation of the LN development. These observations go in line with the notion that RelB-p52 but not RelA-p50 heterodimers are critical for the LTβR-mediated lymphoid organogenesis [171, 238].

Notably, genetic ablation of p50 biased the mLN Treg compartment slightly, but significantly towards Helios+ nTreg. In contrast to that, BCL3-deficiency dramatically skewed the Tregs towards RORγt+ iTreg phenotype (Figure 3). The strong accumulation of RORγt+ Tregs in the BCL3-deficient mice resulted in an elevated total Treg frequency. In reverse, the T-cell-specific overexpression of BCL3 ($BCL3^{TOE}$) almost completely abrogated the development of RORγt+ Tregs, but had no significant effects on the total or Helios+ Treg frequencies [199]. Whereas previous data showed that the total Treg frequency from mLNs was reduced in $BCL3^{TOE}$ mice, no such difference was observed here, probably due to large variation between the samples or reflecting different microbial colonization of the mice [199]. Strikingly, $BCL3^{TOE}$ mice develop spontaneous colitis, possibly in part mediated by decreased suppressive Treg function, underpinning the critical role of RORγt+ Tregs in mucosal homeostasis [199]. Mechanistically, BCL3 directly interacts with p50, thereby preventing p50-c-Rel and p50-RelA heterodimers from binding to the target genes relevant for Treg development and function such as *Foxp3*, *Rorc*, *Il2ra* and *Il10* [199, 239].

Together, the data presented here point towards a reciprocal role of systemically expressed RelB and BCL3 in the development of RORγt+ Tregs. In contrast to RelB which is dispensable T-cell-intrinsically for the development of Th17 and Treg cells, BCL3 seems to act T-cell-intrinsically and in a dose-dependent manner to suppress RORγt+ Treg development [204, 205, 233, 234]. However, T-cell-extrinsic effects in mice with constitutive BCL3-deletion or off-target effects of CD4-cre mediated gene excision could not be excluded [240].

In summary, the results presented here highlight the differential requirement of NF-κB family members for the development of Helios+ and RORγt+ Treg subpopulations and establishment of normal Treg numbers. Furthermore, the data acquired here stresses the

T-cell-intrinsic role of the atypical IκB subfamily member BCL3 in the establishment of normal frequencies of RORγt+ Tregs.

10.2.3 RelB is differentially required between DC subsets

Conventional DCs (cDCs) is a heterogenous population, which can be divided into two major subsets upon their ontogeny and phenotype: the CD8α+CD11b- cDC1s and the CD8α-CD11b+ cDC2s. Former studies deploying systemically RelB-deficient mice, or the respective BMCs suggested a rather broad requirement of RelB for the development and function of cDCs. RelB-deficient mice completely lack the CD8- cDC2 population with the remaining DCs exhibiting developmental and functional deficits [185]. However, due to the multifocal defects in the used mouse models, the DC-intrinsic requirement of RelB remained elusive. With the generation of the DC-specific *Relb* ablation model, the DC-intrinsic RelB requirement could be confined to the splenic Sirpα+CD11b+ cDC2 subset co-expressing CD117 [190]. However, the implication of RelB in GALT DCs still remained elusive.

The data shown here suggests that the requirement of RelB is confined to a subset of cDC2s across different organs: the partially reduced cDC2 population was observed in the SI, spleen and within the resident CD11c^{high} MHCII^{int} population of mLNs from RelB$^{\Delta DC}$ mice (Figures 16 - 18). At the same time, the splenic cDC1 (CD103+CD11b-/CD8+Sirpα-) population was expanded [190].

The finding that the cDC2s but not cDC1s were reduced upon ablation of RelB in DCs goes in line with the currently accepted concept of separate lineage requirements of these two DC subsets. In contrast to the BATF3-dependent cDC1s, the cDC2 subpopulation is a heterogenous subset of DCs. The latter encompasses Klf4-dependent Sirpα- DCs and the Sirpα+ DC population, which requires RelB, IRF4, Notch and Runx for its development [92-94, 100, 101, 103, 190, 213, 241-245]. Interestingly, the latter Notch2-dependent DC subpopulation requires LTβR for homeostatic population expansion [101]. Since LTβR signaling recruits RelB, the abrogated signal transmission upon LTβR activation might result in the reduced cDC2 population. In summary, the data presented here have shown that RelB is required for the development of a subset of cDC2s in the spleen as well as in the gut.

To gain a deeper insight into the requirement of RelB in DCs, the expression of RelB in DCs from various organs was compared here by deploying RelB-Katushka reporter mouse line (Figure 19). To this end, four DC subsets were distinguished by the expression of CD11b and CD103. Interestingly, the spleen showed the highest frequency of RelB-Katushka-positive DCs in comparison to other organs tested. Within splenic DC subsets, RelB-Katushka was predominantly expressed in CD11b+CD103- cDC2s. In contrast to that, CD11b-CD103+ cDC1s showed very few RelB-Katushka+ cells. The expression pattern of RelB observed in the spleen is in agreement with the da previously published and shown here and reflects the cDC2-specific RelB requirement [190, 246]. Of note, Seki et al deployed an alternative reporter mouse strain termed RelB-Venus and detected mature DCs exclusively within the RelB-Venus+ DC population suggesting that in the spleen, RelB may represent a DC maturation marker [246]. Previous findings showing that mature DCs exhibit a higher RelB expression further corroborate this notion [94, 215, 230, 247, 248].

Strikingly, in contrast to the spleen, PEC, SI and colon displayed very low RelB-Katushka expression. In line with previous data, the highest frequency of RelB-Katushka+ cells was detected within the CD11b-CD103- DCs [246]. Low RelB-Katushka expression might correlate with high presence of DC-activating signals such as TLR ligands in the SI and colonic LP. These bacteria-derived signals may induce fast egress of mature DCs from the LP into the draining LNs upon TLR activation [94, 215, 230, 247, 248]. Indeed, the SI-draining mLNs exhibited higher RelB-Katushka expression (of around 20 %, with almost equal distribution of the signal within the four DC subsets) in comparison to the SI-LP.

The gut microbiome exhibits strong immunomodulatory effects, thereby supporting the establishment of a tolerogenic microenvironment in the lamina propria and permitting an efficient Treg induction. For example, short-chain fatty acids, a metabolite from the starch fermentation produced by certain bacterial species, have been previously demonstrated to downregulate *Relb* expression in gut DCs [153, 155]. To gain an insight whether bacterial eradication consequently results in an upregulation of RelB in DCs, mice were treated with broad-spectrum antibiotics prior and four weeks after birth. Unexpectedly, no significant effect of the bacterial extinction on the RelB expression in DCs was observed (Figure 20). In line with that, there is data suggesting that RelB expression in DCs of germ-free mice is not significantly altered in comparison to SPF-reared mice [248]. Taken together, RelB is expressed at different levels in distinct organs, however the mechanisms behind the regulation of RelB in DCs need to be elucidated in further experiments.

10.2.4 RelB is required in DCs to contain exaggerated tissue Treg accumulation

It was shown here that the DC-specific ablation of *Relb* mirrored the accumulation of total and tissue Tregs, loss of RORγt+ Tregs and the Th2 bias found in systemically RelB-deficient mice, albeit to a lesser extent. These finding suggest that RelB is critically required in DCs for the establishment of a normal Treg composition and suppression of spontaneous Th2 polarization.

A comprehensive assessment of the Treg phenotype by flow cytometry and gene expression analysis has revealed that the accumulated Tregs in the RelB$^{\Delta DC}$ mice exhibited an activated tissue Treg phenotype (Figures 5, 9 and 10). This phenotype was characterized by an increased expression of tissue-Treg-associated markers like ST2, Helios and Gata3. Further, Tregs from RelB$^{\Delta DC}$ mice showed a panel of upregulated genes which are associated with a tissue Treg phenotype including *Pparg*, *Nrp1* and *Tnfrsf14*. The expansion of tissue Tregs in absence of RelB in DCs was observed in the non-lymphoid tissues as well as in primary and secondary lymphoid organs, suggesting a systemic effect.

To gain a mechanistic insight orchestrating the expansion of tissue Tregs, negative selection and Treg generation in the thymus were investigated, as these processes are critically dependent upon DCs [212, 228]. First, the endogenous expression of the mammary tumor virus (Mtv)-6 superantigen in BALB/c mice was exploited. In conjunction with MHCII molecules present on DCs, Mtv6 mediates the deletion of TCRVβ3+ thymocytes during the negative selection in the thymus [249, 250]. Hence, a defective negative selection and potentially diverted differentiation into Treg would become apparent upon elevated frequency of TCRVβ3+ among FoxP3+ thymocytes. Consequently, *Relb*-floxed BALB/c

mice were interbred with RelB$^{\Delta DC}$ mice on C57/BL6 background for one generation to obtain RelB$^{\Delta DC}$ mice on a mixed BALB/c x C57/BL6 background. However, no defect in the negative selection was observed when comparing the frequencies of FoxP3+ thymocytes expressing TCRVβ3 in RelB$^{\Delta DC}$ and WT mice on the mixed background (Figure 13).

The thymic Treg development takes place in a two-step process via two independent routes, whereby the classical route involves generation of CD25+FoxP3- intermediates and the alternative route is characterized by the development of CD25-FoxP3+ Treg precursors [44-47]. Interestingly, the frequency of CD25+FoxP3- but not CD25-FoxP3+ Treg precursors was elevated in RelB$^{\Delta DC}$ mice. This data points towards an enhanced intrathymic Treg development along the classical route in absence of RelB in DCs. Thereby, the TCR activation in line with co-stimulatory molecules elevates the responsiveness to IL-2 first, after which IL-2 completes the Treg development by facilitating FoxP3 expression without further TCR stimulation in a second step [44-46, 251]. Therefore, it may be speculated that RelB-deficient DCs permit an enhanced TCR stimulation in the initial step of the Treg generation. In line with that, an elevated Helios expression indicative of an increased TCR stimulation was observed in thymic Treg progenitors and mature FoxP3+CD25+ thymocytes of RelB$^{\Delta DC}$ mice [208, 209].

The abundance of thymic Treg precursors is tightly regulated by apoptosis, however, no significant reduction of apoptotic Annexin V+ cells within intermediate and mature Treg populations was observed here. Instead, the frequency of apoptotic cells within the CD25-FoxP3+ Treg intermediate developing along the alternative route of thymic Treg generation was significantly elevated in RelB$^{\Delta DC}$ mice. Thereby, FoxP3 upregulated prior to CD25 is a strong proapoptotic signal, unless rescued by IL-2, thereby making CD25-FoxP3+ thymocytes particularly apoptosis-prone [47]. Since IL-2 availability is rather limited in the thymus, most CD25-FoxP3+ intermediates undergo apoptosis [47]. Thus, the enlarged CD25+FoxP3- precursor and CD25+FoxP3+ mature Treg population may contribute to the elevated apoptosis of the CD25- intermediates by competing for the available IL-2 in the thymus of RelB$^{\Delta DC}$ mice. In contrast to that, no significant difference of the CD27 expression on Treg progenitors and Tregs was found: CD27 activation constitutes one of the possible mechanisms of DC-mediated suppression of Treg apoptosis in the thymus [210].

On the opposite, the observation that the thymic Treg accumulation was not present in 2-week old mice yet, whereas the spleens of RelB$^{\Delta DC}$ mice already showed an elevated Treg frequency, challenges the theory of an enhanced thymic Treg output. At 2 weeks of age, when the weaning has not took place yet, the generation of iTregs is limited, thereby allowing for a faithful investigation of thymic-derived Tregs [52]. Furthermore, the data on apoptosis and proliferation shown here do not point towards an increased survival of thymic Treg progenitors or mature Tregs.

A further explanation for the elevated Treg frequency is the recirculation of the Tregs from the periphery back to the thymus [252, 253]. Since the Treg compartment is systemically expanded, the pool of recirculating Tregs homing to the thymus is possibly enlarged, thereby elevating the intrathymic Treg frequency. The activated phenotype observed in the thymic Tregs of RelB$^{\Delta DC}$ mice are in support of this theory. The decreased expression of CD24 -a marker of immature Tregs and recent thymic emigrants - by FoxP3+ thymocytes

further supports this hypothesis [211, 254]. However, additional experiments are required to corroborate on this theory.

Taken together, the data shown here suggests that RelB deficiency in DCs may permit an enhanced generation of nTreg via the classical route, possibly by an increased TCR stimulation of Treg precursors. However, homing of peripherally developed Tregs back to the thymus could not be excluded. Furthermore, RelB in DCs seems to play a subordinate role for the negative selection and establishment of central tolerance.

As tissue Tregs express the IL-33 receptor ST2, and systemic IL-33 administration expands tissue Tregs, the role of IL-33 for the Treg accumulation in RelB$^{\Delta DC}$ mice was investigated [71, 75]. Surprisingly, a panel of experiments pointed out that tissue Tregs in RelB$^{\Delta DC}$ mice accumulate independently of IL-33 (Figures 14 and 15):

First, systemic level of IL-33 was not elevated in the RelB$^{\Delta DC}$ mice. Second, systemic neutralization of IL-33 with soluble ST2 (sST2) - a decoy receptor for released IL-33 - did not have any effect on the total FoxP3+ or ST2+ Treg frequencies [255]. Third, IL-33 derived from the non-hematopoietic cells was dispensable for the accumulation of total and tissue Tregs, as well as for the generation of excessive Th2 cells, as was shown by BMC experiments. To this end, BMCs lacking IL-33 in the radioresistant cells were generated by replenishing lethally irradiated IL-33-deficient recipients with WT or RelB$^{\Delta DC}$ bone marrow (BM). In line with previous data suggesting a primarily non-hematopoietic origin of IL-33, the latter was undetectable in the sera of IL-33-deficient-recipients reconstituted with either WT or RelB$^{\Delta DC}$ BM [65, 71, 72]. However, the hematopoietic origin and a locally restricted action of IL-33 could not be excluded by the BMC experiments. One of the possible candidates within the hematopoietic compartment are mast cells: they mainly reside in barrier tissues and release IL-33 after IgE-mediated activation [256, 257]. Most prominently, high-affinity IgE receptor (FcεRI) and its crosslinking by binding to antigen-IgE complexes has been shown to mediate mast cell activation and IL-33 release [257, 258]. Strikingly, RelB$^{\Delta DC}$ mice showed elevated IgE levels in the serum as well as FcεRI-bound on mast cells [61]. Therefore, mast cells may constitute a possible source for IL-33 in RelB$^{\Delta DC}$ mice.

Since the data shown here suggested an IL-33-independent mechanism of tissue Treg accumulation, the implication of IL-2 as the most critical cytokine for the development, homeostasis and expansion of Tregs was addressed [259, 260]. Considering the general expansion of tissue Treg compartment in RelB$^{\Delta DC}$ and the fact that systemic supplementation of IL-2 elevates Treg numbers, the serum IL-2 concentration in RelB$^{\Delta DC}$ mice was measured [260]. Surprisingly, the IL-2 concentration in the serum was not affected by the genetic deletion of *Relb* in DCs. In contrast to that, an elevated production of IL-2 by effector T cells has been previously shown to be responsible for the Treg accumulation in RelB$^{\Delta DC}$ mice [68, 192]. The disparity between the elevated T-cell-derived but not systemic abundance of IL-2 may reflect the locally restricted availability of IL-2 to the T cell zones of lymphoid organs *in vivo* [42, 68].

To address the mechanisms by which RelB-deficient DCs may trigger the accumulation of the Treg population, the phenotype of DCs from RelB$^{\Delta DC}$ mice was analyzed (Figures 16 - 18). In line with previous publications, the splenic CD11b+/CD8-Sirpα+ cDC2 population was significantly reduced, whereas the CD103+CD11b-/CD8+Sirpα- cDC1

population was expanded [190]. Strikingly, the expansion of the cDC1 population was associated with an elevated expression of DEC-205, a DC marker associated with highly tolerogenic properties [91]. Additionally, the RelB-deficient DCs showed an elevated expression of PD-L2, a molecule attenuating proinflammatory T cell responses [261]. In summary, the enhanced tolerogenic properties of splenic DCs in RelB$^{\Delta DC}$ mice may contribute to the expanded Treg population.

In line with an increased tolerogenic potential of RelB-deficient DCs, previous publication showed that RelB$^{\Delta DC}$ mice harbor more steady-state migratory DCs with a CCR7+CD40+ phenotype in the pLNs and that these DCs preferentially mediate Treg conversion [192, 215]. In addition to that, *Relb*-deletion is associated with an increased CCR7 expression in splenic DCs [190]. Taken together, the elevated CCR7 expression in RelB-deficient DCs may promote their localization to the T-cell zones of secondary lymphoid follicles and, in combination with the elevated IL-2 levels, contribute to the Treg expansion. Of note, although DCs do not produce IL-2 in secondary lymphoid organs, they can trans-present IL-2 bound to CD25 on their surface to T cells [262].

Since Treg induction predominantly takes place in the gut and may contribute to the Treg expansion in absence of RelB in DCs, the DCs from the gut-associated lymphoid tissues (GALT) were investigated. In contrast to the spleen, the identification of GALT DCs as CD11c+MHCII+ cells is not univocal as some macrophages share this phenotype [263]. Therefore, the CD11c+MHCII+ mononuclear phagocytes (MNPs) from the SI were divided into cells expressing high levels of CD11c (CD11c^{high}), mainly consisting of *bona fide* DCs, and into MNPs with intermediate CD11c (CD11c^{int}) levels, mostly including macrophages [99]. This subdivision suggested a genuine DC-intrinsic effect, since the CD11c-specific genetic ablation of *Relb* exclusively affected the CD11c^{high}, but not CD11c^{int} MNPs.

Among the CD11c^{high} MNPs, the CD11b+CD103+ subset including the cDC2 subpopulation was significantly reduced in the SI-LP of RelB$^{\Delta DC}$ mice. The cDC2s, upon activation, constitute a critical source of IL-23, which opposes the action of IL-33, thereby inhibiting Treg induction [63, 101]. Furthermore, RelB is required for the TLR-induced IL-23 production, as was revealed by experiments involving BM-derived DCs from RelB-deficient mice [168, 264]. However, it remains unclear, whether DC-specific *Relb* ablation has a similar effect on the IL-23 production *in vivo*. Of note, a DC-intrinsic Notch2-ablation partially mirrors the DC phenotype in the SI-LP of RelB$^{\Delta DC}$ mice, resulting in the loss of the entire cDC2 population accompanied by an elevated frequency of CD11b+CD103- DCs [93, 101, 241]. Interestingly, the remaining Notch2-deficient DCs express higher levels of IL-33 [101]. Taken together, it may be speculated that instead of an elevated IL-33 level, merely its tissue Treg-inducing action is boosted due to a defective IL-23 production from RelB-deficient DCs.

10.2.5 RelB in DCs is essential for the induction of mucosal tolerance and for the containment of Th2 polarization

In sharp contrast to the tissue Treg accumulation, RelB-deficient DCs failed to support efficient generation of RORγt+ microbiota-dependent Tregs. In line with that, RelB$^{\Delta DC}$ mice supplemented with naïve TCR-transgenic T cells specifically recognizing OVA peptide in

context of MHCII (OT-II cells) and fed with OVA, failed to support efficient induction of OVA-specific Tregs and to upregulate RORγt within the Treg compartment. Instead, in this setting, OT-II cells preferentially developed into Gata3+ Th2 cells in mice lacking RelB in DCs. These findings go in line with data showing that OVA-specific iTreg conversion upon continuous subcutaneous OVA delivery is reduced in RelB$^{\Delta DC}$ mice [192]. Together, these results have uncovered a defective mucosal tolerance induction in absence of RelB in DCs.

The induction of RORγt+ Tregs is dependent on the presence of CD103+ DCs in the SI-LP [213, 214, 230, 242]. Especially the CD11b+CD103+ cDC2s have been shown to be crucial for the induction of RORγt+ Tregs [213, 214, 242]. Strikingly, the loss of RORγt+ Tregs in RelB$^{\Delta DC}$ mice was associated with a partial reduction of the CD11b+CD103+ CD11c^{high} MNPs in the SI, largely consisting of the corresponding DCs. Although the phenotypic changes in the SI of RelB$^{\Delta DC}$ mice were restricted to the CD11c^{high} MNP subset mainly containing *bona-fide* DC, macrophage-specific effects could not be excluded.

The defective mucosal tolerance induction in combination with the expanded tissue Treg population in absence of RelB in DCs were associated with a spontaneous type 2 activation (Figure 6-8). This was characterized by a significantly elevated serum IgE level, increased percentage of blood eosinophils and increased frequency of Th2 cells in the SI, spleen and PEC [61]. Due to the spontaneous nature of the Th2 activation in absence of pathogenic stimuli, the involvement of an allergic reaction upon the disrupted mucosal tolerance is likely.

In support with the idea of a defective mucosal tolerance induction, the frequency of T follicular helper (Tfh) cells in the mLN and Peyer's patches (PPs), but not in the spleen was elevated in absence of RelB in DCs. As Tfh cells critically support production of immunoglobulins by B cells, and among immunoglobulins tested in the serum of RelB$^{\Delta DC}$ mice, only IgE was elevated, it may be speculated that the expanded Tfh cell population exclusively supports the enhanced IgE production. In line with that, recent studies have revealed that IL-4 and IL-13 secreted by Tfh cells, rather than by Th2 cells, drive the induction of IgE [265, 266]. Hence, the elevated Tfh frequency in RelB$^{\Delta DC}$ mice might not only support elevated IgE production, but also contribute to the Th2 polarization. However, it remains unclear whether RelB-deficient DCs directly perpetuate Tfh cell formation or whether their accumulation is a consequence of the break of mucosal tolerance.

Whereas RORγt+ Tregs are highly protective against immune reactions towards microbiota and food-derived peptides, tissue Treg-mediated repair and preservation of a tolerogenic environment in the non-lymphoid organs have been shown to depend on a Th2-related transcriptional program [66]. In allergy-prone mice, Gata3+ Tregs may even contribute to the perpetuation of food allergy [52, 53, 57, 66, 225]. Therefore, an uncontrolled tissue Treg accumulation might contribute to the systemic Th2 polarization observed in RelB$^{\Delta DC}$ mice. However, the transcriptional analysis of Tregs from RelB$^{\Delta DC}$ mice does not suggest an elevated expression of genes encoding Th2 cytokines. Albeit it cannot be excluded that expression analysis would not reveal enhanced cytokine production as this process is regulated by post-transcriptional processes [267]. Furthermore, no increase in the serum levels of IL-4 and IL-13 was detected by multiplex assay (data not shown) corroborating the RNA-Seq data. Although the definitive mechanism of the Th2 polarization remains elusive,

the data presented here points towards a defective mucosal tolerance due to impaired RORγt+ Treg and antigen-specific oral tolerance induction in absence of RelB in DCs.

10.2.6 Expanded Treg population protects RelB$^{\Delta DC}$ mice from experimental autoimmune encephalomyelitis

RelB is critically involved in the development and function of DCs. DCs, in turn are pivotal for the initiation of experimental autoimmune encephalomyelitis (EAE), a demyelinating autoimmune disease of the central nervous system (CNS) [268]. To test the functional consequences of the DC-specific *Relb*-deletion, EAE was induced in RelB$^{\Delta DC}$ mice via active immunization with the immunodominant epitope of myelin oligodendrocyte glycoprotein (MOG fragment 35-55) in complete Freund's adjuvant (CFA). Strikingly, RelB$^{\Delta DC}$ mice were protected from EAE (Figure 21). In contrast to WT mice, RelB$^{\Delta DC}$ mice developed only mild disease symptoms associated with a low degree of mononuclear infiltration in the CNS as well as a small number of Teffs producing proinflammatory cytokines.

Like in other organs at steady state, RelB$^{\Delta DC}$ mice showed higher frequencies of total and tissue Tregs in the CNS at the peak of EAE. The role of Tregs in the suppression of inflammatory reactions and during EAE recovery are well established [260, 269-271]. Upon CNS inflammation, activated Tregs accumulate in the CNS [269]. An expanded Treg compartment has been associated with EAE resistance, whereas Treg-depletion renders the mice highly EAE susceptible [260, 269, 270]. Furthermore, the activated phenotype of the Tregs accumulating in the inflammatory conditions of the CNS during EAE confers superior suppressive function and maintains Treg stability in this challenging environment [269, 270]. Therefore, not only the elevated frequency but also the activated Treg phenotype in the RelB$^{\Delta DC}$ mice might contribute to the EAE resistance in RelB$^{\Delta DC}$ mice.

To corroborate on the role of the accumulated Tregs in the RelB$^{\Delta DC}$ mice in the suppression of EAE, Tregs were depleted transiently by anti-CD25 (PC61) treatment prior to the EAE induction (Figure 22). Strikingly, Treg depletion rendered the RelB$^{\Delta DC}$ mice highly EAE susceptible with dramatic aggravation of the EAE disease symptoms. The EAE severity score and the number of IFNγ-, IL-17 and GM-CSF-producing T cells in the CNS of Treg-depleted RelB$^{\Delta DC}$ mice were significantly elevated above the level of the non-Treg-depleted WT mice. In accordance with previous findings, the Treg-depleted WT mice showed an increased EAE score [270]. Interestingly, the disease severity in Treg-depleted WT and RelB$^{\Delta DC}$ mice was equal, suggesting a similar extend of inflammation.

Intriguingly, the low Treg-depletion efficiency (of around 40 %) still sufficient to aggravate the EAE disease in RelB$^{\Delta DC}$ mice, most likely resulted from the initially high Treg numbers, thus diluting the available antibody molecules. Interestingly, only a part of circulating ST2+ Tregs in the blood co-expressed CD25 with around 30 % in WT and only 20 % in RelB$^{\Delta DC}$ mice. Given that PC61 antibody cannot pass the blood-brain-barrier, the phenotype of Tregs accumulating in the CNS during EAE before and after Treg depletion needs further clarification. Whereas for CD25, the data clearly points out that the vast majority of the CNS-accumulating Tregs co-express CD25, the data on the ST2 expression in Tregs from CNS is scarce [270]. For the mouse models of EAE and stroke, the elevated ST2 expression was

merely shown at the gene expression, but not on the protein level [226]. In support of that, Tregs from the CNS of MS patients exhibit a high ST2 protein level [272]. Therefore, given the high availability of IL-33 in the damaged brain and a general tissue Treg character of Tregs infiltrating the CNS during inflammation, a high degree of co-expression of CD25 and ST2 can be assumed [226].

Strikingly, after anti-CD25-treatement, Tregs seem to recover relatively rapidly, so that the frequency of FoxP3+ Tregs in the CNS at the peak of EAE is comparable to that found in the CNS of non-Treg-depleted mice. This suggests that Tregs are critical during the immunization or onset phase of EAE rather than at the peak of disease. Treg-mediated suppression of DCs during priming might contribute to the protection from EAE. In conclusion, since Treg-depleted RelB$^{\Delta DC}$ mice exhibited severe EAE symptoms upon immunization with MOG/CFA, it may be reasoned that RelB in DCs is dispensable for efficient priming.

In addition to the systemically expanded tissue Treg population, it was shown here that RelB in DCs is required to control overt Th2 polarization. Like other organs at steady state, the CNS of RelB$^{\Delta DC}$ mice harbored a significantly increased Th2 cell population at the peak of EAE. Hence, Th2 cell expansion might contribute to the EAE resistance in RelB$^{\Delta DC}$ mice [273-275]. IL-33 is an alarmin facilitating Th2 polarization as well as expansion of tissue Tregs, thereby suppressing EAE [13, 276]. Although immune-cell-derived IL-33 seemed to have a negligible role in the expansion of both of these cell types in RelB$^{\Delta DC}$ mice as was shown here, previous studies suggest that IL-33 from mast cells suppresses EAE by expanding Th2 cell population [275]. In addition to that, neurons within the CNS produce large amounts of IL-33 [153]. Therefore, an elevated level of IL-33 in the CNS upon EAE induction may contribute to the observed Th2 and Treg accumulation, thus contributing to the EAE protection.

Furthermore, *de novo* induction of MOG-specific Tregs in proinflammatory conditions after EAE-induction was assessed. In contrast to WT mice, which show no *de novo* induction of MOG-specific Tregs, RelB-deficient DCs supported a low, but detectable MOG-specific Treg population [269]. This finding suggests that RelB-deficient DCs are highly tolerogenic, even in proinflammatory settings. Mechanistically, it may be speculated that the reduced frequency of Sirpα+ DCs (cDC2s), which normally inhibit Treg induction via IL-6 trans-presentation, contribute to the facilitated MOG-specific Treg-induction under inflammatory conditions [216]. Additionally, the elevated frequency of tolerogenic DEC-205+ DCs in the spleen of RelB$^{\Delta DC}$ mice might contribute to the Treg induction. In line with that, DEC-205-targeted MOG 35-55 peptide delivery to DEC-205+ DCs prior and even after sensitization ameliorated EAE symptoms via induction of CD25+FoxP3+ Tregs [90, 277].

In line with the data presented here, the ablation of *Relb* in DCs has been shown to ameliorate proinflammatory and autoimmune conditions such as myasthenia gravis, rheumatoid arthritis as well as graft-versus-host disease; and this protective effect has been partially linked to elevated Treg numbers and elicited Th2 immune responses [183, 278-284]. Altogether, the data presented in this thesis has revealed that the expanded Treg population confers resistance towards EAE in mice lacking RelB in DCs.

11 Conclusion

Tregs constitute the key cell type conveying immunological tolerance. The data presented here has shown that the transcription factor RelB in DCs is a critical regulator of the Treg compartment and therefore may be regarded as the central switch regulating the balance between the central (tissue Treg-mediated) and peripheral (RORγt+ Treg-dependent) tolerance. Herein, RelB in DCs was necessary to contain exaggerated accumulation of tissue Tregs and, on the other hand, was required for the induction of oral tolerance as well as microbiota-dependent RORγt+ Tregs. Consequently, DC-specific ablation of RelB resulted in a spontaneous and systemic activation of type 2 immunity.

Although Treg generation in the thymus was affected in absence of RelB in DCs, the tissue Treg accumulation seemed to take place outside of the thymus and in an IL-33 independent manner. Therefore, further studies are required to elucidate the exact mechanism deployed by RelB in DCs to suppress exaggerated tissue Treg development. Strikingly, the outgrowth of tissue Tregs conferred protection against experimental autoimmune encephalomyelitis (EAE), an autoimmune demyelinating condition resembling multiple sclerosis in human patients.

The data shown here provides evidence that the inhibition of RelB-mediated gene transcription represents a promising approach in the therapy of autoimmune diseases. For this purpose, blocking of the nuclear import of RelB by SN5 peptide or prevention of DNA-binding using decoy oligonucleotides, as well as inhibition of signaling proteins upstream of RelB in DCs are a few possibilities [285]. However, side effects associated with an expanded Treg population including suppressed defense against pathogens and an elevated tumor tolerance should be kept in mind. In addition to that, an increased allergy predisposition due to the impaired mucosal tolerance might appear to be a major drawback of the therapeutic approach involving RelB inhibition in DCs.

Importantly, the data presented here has shown for the first time that RelB is not required in DCs *per se* for the initiation of an immune response. By a transient depletion of Tregs with anti-CD25 antibodies prior to the induction of EAE, it could be shown that the expanded Treg population in mice lacking RelB in DCs is causative for the EAE resistance. However, whether RelB is equally dispensable for the induction of other immune responses remains to be analyzed in future studies.

Furthermore, it remains unclear whether the allergy-suppressing and tolerance-conveying action of RORγt+ Tregs is restricted to the gastrointestinal tract or plays a role in the systemic suppression of allergies. The data shown here suggests that RORγt in Tregs is dispensable for oral tolerance induction and suppression of inflammation in a model of allergic airway inflammation. However, it is possible that in the FoxP3$^{\Delta Treg}$ mouse used here, the slow recombination kinetics of the *Foxp3*-cre mediated excision of *Rorc* (gene encoding RORγt) permits for a transient induction of RORγt+ Tregs, which may be sufficient to trigger the RORγt-dependent program necessary for the suppressive function of RORγt+ Tregs.

12 List of figures and schemes

13 List of tables

14 Bibliography

1. Mokhtar, N.M., et al., *A four-decade analysis of the incidence trends, sociodemographic and clinical characteristics of inflammatory bowel disease patients at single tertiary centre, Kuala Lumpur, Malaysia.* BMC Public Health, 2019. **19**(4): p. 550.
2. Safiri, S., et al., *Global, regional and national burden of rheumatoid arthritis 1990–2017: a systematic analysis of the Global Burden of Disease study 2017.* Annals of the Rheumatic Diseases, 2019. **78**(11): p. 1463-1471.
3. Ross Anderson, H., et al., *50 years of asthma: UK trends from 1955 to 2004.* Thorax, 2007. **62**(1): p. 85-90.
4. Murphy, K., Paul Travers, Mark Walport, and Charles Janeway, *Janeway's immunobiology*, ed. t. edition. Vol. 9th ed. 2017, New York: Garland Science/Taylor & Francis.
5. Xing, Y., S.C. Jameson, and K.A. Hogquist, *Thymoproteasome subunit-β5T generates peptide-MHC complexes specialized for positive selection.* Proc Natl Acad Sci U S A, 2013. **110**(17): p. 6979-84.
6. Aichinger, M., et al., *Macroautophagy substrates are loaded onto MHC class II of medullary thymic epithelial cells for central tolerance.* J Exp Med, 2013. **210**(2): p. 287-300.
7. Aschenbrenner, K., et al., *Selection of Foxp3+ regulatory T cells specific for self antigen expressed and presented by Aire+ medullary thymic epithelial cells.* Nature Immunology, 2007. **8**(4): p. 351-358.
8. Stritesky, G.L., et al., *Murine thymic selection quantified using a unique method to capture deleted T cells.* Proc Natl Acad Sci U S A, 2013. **110**(12): p. 4679-84.
9. Legoux, F.P., et al., *CD4(+) T Cell Tolerance to Tissue-Restricted Self Antigens Is Mediated by Antigen-Specific Regulatory T Cells Rather Than Deletion.* Immunity, 2015. **43**(5): p. 896-908.
10. Macatonia, S.E., et al., *Dendritic cells produce IL-12 and direct the development of Th1 cells from naive CD4+ T cells.* The Journal of Immunology, 1995. **154**(10): p. 5071.
11. Liblau, R.S., S.M. Singer, and H.O. McDevitt, *Th1 and Th2 CD4+ T cells in the pathogenesis of organ-specific autoimmune diseases.* Immunol Today, 1995. **16**(1): p. 34-8.
12. Ohnmacht, C., et al., *Basophils orchestrate chronic allergic dermatitis and protective immunity against helminths.* Immunity, 2010. **33**(3): p. 364-74.
13. Schmitz, J., et al., *IL-33, an interleukin-1-like cytokine that signals via the IL-1 receptor-related protein ST2 and induces T helper type 2-associated cytokines.* Immunity, 2005. **23**(5): p. 479-90.
14. Zhu, J., et al., *Conditional deletion of Gata3 shows its essential function in T(H)1-T(H)2 responses.* Nat Immunol, 2004. **5**(11): p. 1157-65.
15. Zheng, W. and R.A. Flavell, *The transcription factor GATA-3 is necessary and sufficient for Th2 cytokine gene expression in CD4 T cells.* Cell, 1997. **89**(4): p. 587-96.
16. Chu, C.C. and W.E. Paul, *Expressed genes in interleukin-4 treated B cells identified by cDNA representational difference analysis.* Molecular Immunology, 1998. **35**(8): p. 487-502.
17. Williams, C.M. and S.J. Galli, *Mast cells can amplify airway reactivity and features of chronic inflammation in an asthma model in mice.* The Journal of experimental medicine, 2000. **192**(3): p. 455-462.

18. Kobayashi, T., et al., *An essential role of mast cells in the development of airway hyperresponsiveness in a murine asthma model.* Journal of immunology (Baltimore, Md. : 1950), 2000. **164**(7): p. 3855-3861.
19. Chen, F., et al., *An essential role for TH2-type responses in limiting acute tissue damage during experimental helminth infection.* Nat Med, 2012. **18**(2): p. 260-6.
20. Harrington, L.E., et al., *Interleukin 17-producing CD4+ effector T cells develop via a lineage distinct from the T helper type 1 and 2 lineages.* Nat Immunol, 2005. **6**(11): p. 1123-32.
21. Park, H., et al., *A distinct lineage of CD4 T cells regulates tissue inflammation by producing interleukin 17.* Nat Immunol, 2005. **6**(11): p. 1133-41.
22. Ivanov, I.I., et al., *The orphan nuclear receptor RORgammat directs the differentiation program of proinflammatory IL-17+ T helper cells.* Cell, 2006. **126**(6): p. 1121-33.
23. Atarashi, K., et al., *Induction of colonic regulatory T cells by indigenous Clostridium species.* Science, 2011. **331**(6015): p. 337-41.
24. Ivanov, II, et al., *Induction of intestinal Th17 cells by segmented filamentous bacteria.* Cell, 2009. **139**(3): p. 485-98.
25. Happel , K.I., et al., *Divergent roles of IL-23 and IL-12 in host defense against Klebsiella pneumoniae.* Journal of Experimental Medicine, 2005. **202**(6): p. 761-769.
26. Conti, H.R., et al., *Th17 cells and IL-17 receptor signaling are essential for mucosal host defense against oral candidiasis.* J Exp Med, 2009. **206**(2): p. 299-311.
27. Yue, F.Y., et al., *Virus-specific interleukin-17-producing CD4+ T cells are detectable in early human immunodeficiency virus type 1 infection.* J Virol, 2008. **82**(13): p. 6767-71.
28. Crotty, S., *Follicular helper CD4 T cells (TFH).* Annu Rev Immunol, 2011. **29**: p. 621-63.
29. Vogelzang, A., et al., *A fundamental role for interleukin-21 in the generation of T follicular helper cells.* Immunity, 2008. **29**(1): p. 127-37.
30. Shi, J., et al., *PD-1 Controls Follicular T Helper Cell Positioning and Function.* Immunity, 2018. **49**(2): p. 264-274.e4.
31. Johnston, R.J., et al., *Bcl6 and Blimp-1 Are Reciprocal and Antagonistic Regulators of T Follicular Helper Cell Differentiation.* Science, 2009. **325**(5943): p. 1006-1010.
32. Choi, J., et al., *Bcl-6 is the nexus transcription factor of T follicular helper cells via repressor-of-repressor circuits.* Nature Immunology, 2020. **21**(7): p. 777-789.
33. Goenka, R., et al., *Cutting edge: dendritic cell-restricted antigen presentation initiates the follicular helper T cell program but cannot complete ultimate effector differentiation.* J Immunol, 2011. **187**(3): p. 1091-5.
34. Hirota, K., et al., *Plasticity of Th17 cells in Peyer's patches is responsible for the induction of T cell-dependent IgA responses.* Nat Immunol, 2013. **14**(4): p. 372-9.
35. Tsuji, M., et al., *Preferential Generation of Follicular B Helper T Cells from Foxp3+ T Cells in Gut Peyer's Patches.* Science, 2009. **323**(5920): p. 1488-1492.
36. Schmidt, A., N. Oberle, and P. Krammer, *Molecular Mechanisms of Treg-Mediated T Cell Suppression.* Frontiers in Immunology, 2012. **3**(51).
37. Fontenot, J.D., M.A. Gavin, and A.Y. Rudensky, *Foxp3 programs the development and function of CD4+CD25+ regulatory T cells.* Nature Immunology, 2003. **4**(4): p. 330-336.
38. Hori, S., T. Nomura, and S. Sakaguchi, *Control of Regulatory T Cell Development by the Transcription Factor Foxp3.* Science, 2003. **299**(5609): p. 1057-1061.
39. Brunkow, M.E., et al., *Disruption of a new forkhead/winged-helix protein, scurfin, results in the fatal lymphoproliferative disorder of the scurfy mouse.* Nature Genetics, 2001. **27**(1): p. 68-73.

40. Bennett, C.L., et al., *The immune dysregulation, polyendocrinopathy, enteropathy, X-linked syndrome (IPEX) is caused by mutations of FOXP3.* Nat Genet, 2001. **27**(1): p. 20-1.
41. Toomer, K.H., et al., *Essential and non-overlapping IL-2Ralpha-dependent processes for thymic development and peripheral homeostasis of regulatory T cells.* Nat Commun, 2019. **10**(1): p. 1037.
42. Owen, D.L., et al., *Identification of Cellular Sources of IL-2 Needed for Regulatory T Cell Development and Homeostasis.* J Immunol, 2018. **200**(12): p. 3926-3933.
43. Chinen, T., et al., *An essential role for the IL-2 receptor in T(reg) cell function.* Nat Immunol, 2016. **17**(11): p. 1322-1333.
44. Burchill, M.A., et al., *Linked T cell receptor and cytokine signaling govern the development of the regulatory T cell repertoire.* Immunity, 2008. **28**(1): p. 112-21.
45. Lio, C.W. and C.S. Hsieh, *A two-step process for thymic regulatory T cell development.* Immunity, 2008. **28**(1): p. 100-11.
46. Vang, K.B., et al., *IL-2, -7, and -15, but not thymic stromal lymphopoeitin, redundantly govern CD4+Foxp3+ regulatory T cell development.* J Immunol, 2008. **181**(5): p. 3285-90.
47. Tai, X., et al., *Foxp3 transcription factor is proapoptotic and lethal to developing regulatory T cells unless counterbalanced by cytokine survival signals.* Immunity, 2013. **38**(6): p. 1116-28.
48. Thornton, A.M., et al., *Expression of Helios, an Ikaros transcription factor family member, differentiates thymic-derived from peripherally induced Foxp3+ T regulatory cells.* J Immunol, 2010. **184**(7): p. 3433-41.
49. Kim, H.J., et al., *Stable inhibitory activity of regulatory T cells requires the transcription factor Helios.* Science, 2015. **350**(6258): p. 334-9.
50. Kim, K.S., et al., *Dietary antigens limit mucosal immunity by inducing regulatory T cells in the small intestine.* Science, 2016.
51. Josefowicz, S.Z., et al., *Extrathymically generated regulatory T cells control mucosal TH2 inflammation.* Nature, 2012. **482**(7385): p. 395-9.
52. Ohnmacht, C., et al., *MUCOSAL IMMUNOLOGY. The microbiota regulates type 2 immunity through RORgammat(+) T cells.* Science, 2015. **349**(6251): p. 989-93.
53. Sefik, E., et al., *MUCOSAL IMMUNOLOGY. Individual intestinal symbionts induce a distinct population of RORgamma(+) regulatory T cells.* Science, 2015. **349**(6251): p. 993-7.
54. Yang, B.H., et al., *Foxp3(+) T cells expressing RORgammat represent a stable regulatory T-cell effector lineage with enhanced suppressive capacity during intestinal inflammation.* Mucosal Immunol, 2016. **9**(2): p. 444-57.
55. Kim, M., et al., *Critical Role for the Microbiota in CX3CR1(+) Intestinal Mononuclear Phagocyte Regulation of Intestinal T Cell Responses.* Immunity, 2018. **49**(1): p. 151-163 e5.
56. Britton, G.J., et al., *Microbiotas from Humans with Inflammatory Bowel Disease Alter the Balance of Gut Th17 and RORgammat(+) Regulatory T Cells and Exacerbate Colitis in Mice.* Immunity, 2019. **50**(1): p. 212-224 e4.
57. Abdel-Gadir, A., et al., *Microbiota therapy acts via a regulatory T cell MyD88/RORgammat pathway to suppress food allergy.* Nat Med, 2019. **25**(7): p. 1164-1174.
58. Hill, D.A., et al., *Commensal bacteria-derived signals regulate basophil hematopoiesis and allergic inflammation.* Nat Med, 2012. **18**(4): p. 538-46.
59. Massoud, A.H., et al., *An asthma-associated IL4R variant exacerbates airway inflammation by promoting conversion of regulatory T cells to TH17-like cells.* Nat Med, 2016. **22**(9): p. 1013-22.

60. Pratama, A., et al., *Developmental and cellular age direct conversion of CD4+ T cells into RORgamma+ or Helios+ colon Treg cells.* J Exp Med, 2020. **217**(1).
61. Andreas, N., et al., *RelB Deficiency in Dendritic Cells Protects from Autoimmune Inflammation Due to Spontaneous Accumulation of Tissue T Regulatory Cells.* J Immunol, 2019. **203**(10): p. 2602-2613.
62. Burzyn, D., et al., *A special population of regulatory T cells potentiates muscle repair.* Cell, 2013. **155**(6): p. 1282-95.
63. Schiering, C., et al., *The alarmin IL-33 promotes regulatory T-cell function in the intestine.* Nature, 2014.
64. Li, C., et al., *TCR Transgenic Mice Reveal Stepwise, Multi-site Acquisition of the Distinctive Fat-Treg Phenotype.* Cell, 2018. **174**(2): p. 285-299 e12.
65. Kolodin, D., et al., *Antigen- and cytokine-driven accumulation of regulatory T cells in visceral adipose tissue of lean mice.* Cell Metab, 2015. **21**(4): p. 543-57.
66. Siede, J., et al., *IL-33 Receptor-Expressing Regulatory T Cells Are Highly Activated, Th2 Biased and Suppress CD4 T Cell Proliferation through IL-10 and TGFbeta Release.* PLoS One, 2016. **11**(8): p. e0161507.
67. Miragaia, R.J., et al., *Single-Cell Transcriptomics of Regulatory T Cells Reveals Trajectories of Tissue Adaptation.* Immunity, 2019. **50**(2): p. 493-504 e7.
68. Smigiel, K.S., et al., *CCR7 provides localized access to IL-2 and defines homeostatically distinct regulatory T cell subsets.* J Exp Med, 2014. **211**(1): p. 121-36.
69. Wohlfert, E.A., et al., *GATA3 controls Foxp3(+) regulatory T cell fate during inflammation in mice.* J Clin Invest, 2011. **121**(11): p. 4503-15.
70. He, Z., et al., *Epithelial-derived IL-33 promotes intestinal tumorigenesis in Apc (Min/+) mice.* Sci Rep, 2017. **7**(1): p. 5520.
71. Delacher, M., et al., *Genome-wide DNA-methylation landscape defines specialization of regulatory T cells in tissues.* Nat Immunol, 2017. **18**(10): p. 1160-1172.
72. Kuswanto, W., et al., *Poor Repair of Skeletal Muscle in Aging Mice Reflects a Defect in Local, Interleukin-33-Dependent Accumulation of Regulatory T Cells.* Immunity, 2016. **44**(2): p. 355-67.
73. Pichery, M., et al., *Endogenous IL-33 is highly expressed in mouse epithelial barrier tissues, lymphoid organs, brain, embryos, and inflamed tissues: in situ analysis using a novel Il-33-LacZ gene trap reporter strain.* J Immunol, 2012. **188**(7): p. 3488-95.
74. Molofsky, A.B., et al., *Interleukin-33 and Interferon-gamma Counter-Regulate Group 2 Innate Lymphoid Cell Activation during Immune Perturbation.* Immunity, 2015. **43**(1): p. 161-74.
75. Matta, B.M., et al., *IL-33 Is an Unconventional Alarmin That Stimulates IL-2 Secretion by Dendritic Cells To Selectively Expand IL-33R/ST2+ Regulatory T Cells.* J Immunol, 2014.
76. Vasanthakumar, A., et al., *The transcriptional regulators IRF4, BATF and IL-33 orchestrate development and maintenance of adipose tissue-resident regulatory T cells.* Nat Immunol, 2015. **16**(3): p. 276-85.
77. Delacher, M., et al., *Precursors for Nonlymphoid-Tissue Treg Cells Reside in Secondary Lymphoid Organs and Are Programmed by the Transcription Factor BATF.* Immunity, 2020.
78. Steinman, R.M. and Z.A. Cohn, *Identification of a novel cell type in peripheral lymphoid organs of mice. I. Morphology, quantitation, tissue distribution.* J Exp Med, 1973. **137**(5): p. 1142-62.
79. Sallusto, F., et al., *Dendritic cells use macropinocytosis and the mannose receptor to concentrate macromolecules in the major histocompatibility complex class II compartment: downregulation by cytokines and bacterial products.* J Exp Med, 1995. **182**(2): p. 389-400.

80. Winzler, C., et al., *Maturation stages of mouse dendritic cells in growth factor-dependent long-term cultures.* The Journal of experimental medicine, 1997. **185**(2): p. 317-328.
81. Pentcheva-Hoang, T., et al., *B7-1 and B7-2 Selectively Recruit CTLA-4 and CD28 to the Immunological Synapse.* Immunity, 2004. **21**(3): p. 401-413.
82. van de Laar, L., P.J. Coffer, and A.M. Woltman, *Regulation of dendritic cell development by GM-CSF: molecular control and implications for immune homeostasis and therapy.* Blood, 2012. **119**(15): p. 3383-3393.
83. Fogg, D.K., et al., *A Clonogenic Bone Marrow Progenitor Specific for Macrophages and Dendritic Cells.* Science, 2006. **311**(5757): p. 83-87.
84. Liu, K., et al., *In Vivo Analysis of Dendritic Cell Development and Homeostasis.* Science, 2009. **324**(5925): p. 392-397.
85. Naik, S.H., et al., *Development of plasmacytoid and conventional dendritic cell subtypes from single precursor cells derived in vitro and in vivo.* Nature Immunology, 2007. **8**(11): p. 1217-1226.
86. Guilliams, M., et al., *Dendritic cells, monocytes and macrophages: a unified nomenclature based on ontogeny.* Nat Rev Immunol, 2014. **14**(8): p. 571-8.
87. Dudziak, D., et al., *Differential Antigen Processing by Dendritic Cell Subsets in Vivo.* Science, 2007. **315**(5808): p. 107-111.
88. Wadwa, M., et al., *Targeting Antigens to Dec-205 on Dendritic Cells Induces Immune Protection in Experimental Colitis in Mice.* European journal of microbiology & immunology, 2016. **6**(1): p. 1-8.
89. Petzold, C., et al., *Targeted antigen delivery to DEC-205⁺ dendritic cells for tolerogenic vaccination.* The review of diabetic studies : RDS, 2012. **9**(4): p. 305-318.
90. Jones, A., et al., *Immunomodulatory Functions of BTLA and HVEM Govern Induction of Extrathymic Regulatory T Cells and Tolerance by Dendritic Cells.* Immunity, 2016. **45**(5): p. 1066-1077.
91. Yamazaki, S., et al., *CD8+ CD205+ splenic dendritic cells are specialized to induce Foxp3+ regulatory T cells.* J Immunol, 2008. **181**(10): p. 6923-33.
92. Tussiwand, R., et al., *Klf4 expression in conventional dendritic cells is required for T helper 2 cell responses.* Immunity, 2015. **42**(5): p. 916-28.
93. Briseno, C.G., et al., *Deficiency of transcription factor RelB perturbs myeloid and DC development by hematopoietic-extrinsic mechanisms.* Proc Natl Acad Sci U S A, 2017. **114**(15): p. 3957-3962.
94. Cerovic, V., et al., *Intestinal CD103(-) dendritic cells migrate in lymph and prime effector T cells.* Mucosal Immunol, 2013. **6**(1): p. 104-13.
95. Sun, C.M., et al., *Small intestine lamina propria dendritic cells promote de novo generation of Foxp3 T reg cells via retinoic acid.* J Exp Med, 2007. **204**(8): p. 1775-85.
96. Scott, C.L., et al., *CCR2(+)CD103(-) intestinal dendritic cells develop from DC-committed precursors and induce interleukin-17 production by T cells.* Mucosal Immunol, 2015. **8**(2): p. 327-39.
97. Persson, E.K., et al., *Dendritic cell subsets in the intestinal lamina propria: Ontogeny and function.* Eur J Immunol, 2013. **43**(12): p. 3098-107.
98. Rivollier, A., et al., *Inflammation switches the differentiation program of Ly6Chi monocytes from antiinflammatory macrophages to inflammatory dendritic cells in the colon.* J Exp Med, 2012. **209**(1): p. 139-55.
99. Harusato, A., et al., *Phenotypic and functional profiling of mouse intestinal antigen presenting cells.* J Immunol Methods, 2015. **421**: p. 20-26.
100. Schlitzer, A., et al., *IRF4 transcription factor-dependent CD11b+ dendritic cells in human and mouse control mucosal IL-17 cytokine responses.* Immunity, 2013. **38**(5): p. 970-83.

101. Satpathy, A.T., et al., *Notch2-dependent classical dendritic cells orchestrate intestinal immunity to attaching-and-effacing bacterial pathogens.* Nat Immunol, 2013. **14**(9): p. 937-48.
102. Mayer, J.U., et al., *Different populations of CD11b(+) dendritic cells drive Th2 responses in the small intestine and colon.* Nat Commun, 2017. **8**: p. 15820.
103. Bogunovic, M., et al., *Origin of the lamina propria dendritic cell network.* Immunity, 2009. **31**(3): p. 513-25.
104. Coombes, J.L., et al., *A functionally specialized population of mucosal CD103+ DCs induces Foxp3+ regulatory T cells via a TGF-beta and retinoic acid-dependent mechanism.* J Exp Med, 2007. **204**(8): p. 1757-64.
105. Klebanoff, C.A., et al., *Retinoic acid controls the homeostasis of pre-cDC-derived splenic and intestinal dendritic cells.* J Exp Med, 2013. **210**(10): p. 1961-76.
106. Zeng, R., et al., *Retinoic acid regulates the development of a gut-homing precursor for intestinal dendritic cells.* Mucosal Immunol, 2013. **6**(4): p. 847-56.
107. Schraml, B.U., et al., *Genetic tracing via DNGR-1 expression history defines dendritic cells as a hematopoietic lineage.* Cell, 2013. **154**(4): p. 843-58.
108. McDonald, K.G., et al., *Dendritic cells produce CXCL13 and participate in the development of murine small intestine lymphoid tissues.* Am J Pathol, 2010. **176**(5): p. 2367-77.
109. Chase, M.W., *Inhibition of experimental drug allergy by prior feeding of the sensitizing agent.* Proc Soc Exp Biol Med, 1946. **61**: p. 257-9.
110. Jaensson, E., et al., *Small intestinal CD103+ dendritic cells display unique functional properties that are conserved between mice and humans.* J Exp Med, 2008. **205**(9): p. 2139-49.
111. Abdel-Gadir, A., et al., *Oral immunotherapy with omalizumab reverses the Th2 cell-like programme of regulatory T cells and restores their function.* Clin Exp Allergy, 2018. **48**(7): p. 825-836.
112. Pabst, O. and A.M. Mowat, *Oral tolerance to food protein.* Mucosal Immunol, 2012. **5**(3): p. 232-9.
113. Rios, D., et al., *Antigen sampling by intestinal M cells is the principal pathway initiating mucosal IgA production to commensal enteric bacteria.* Mucosal Immunol, 2016. **9**(4): p. 907-16.
114. Mazzini, E., et al., *Oral Tolerance Can Be Established via Gap Junction Transfer of Fed Antigens from CX3CR1 Macrophages to CD103 Dendritic Cells.* Immunity, 2014.
115. Niess, J.H., et al., *CX3CR1-mediated dendritic cell access to the intestinal lumen and bacterial clearance.* Science, 2005. **307**(5707): p. 254-8.
116. Scott, C.L., A.M. Aumeunier, and A.M. Mowat, *Intestinal CD103+ dendritic cells: master regulators of tolerance?* Trends Immunol, 2011. **32**(9): p. 412-9.
117. Hadis, U., et al., *Intestinal tolerance requires gut homing and expansion of FoxP3+ regulatory T cells in the lamina propria.* Immunity, 2011. **34**(2): p. 237-46.
118. Worbs, T., et al., *Oral tolerance originates in the intestinal immune system and relies on antigen carriage by dendritic cells.* J Exp Med, 2006. **203**(3): p. 519-27.
119. Pezoldt, J., et al., *Neonatally imprinted stromal cell subsets induce tolerogenic dendritic cells in mesenteric lymph nodes.* Nat Commun, 2018. **9**(1): p. 3903.
120. Pasztoi, M., et al., *Mesenteric lymph node stromal cell-derived extracellular vesicles contribute to peripheral de novo induction of Foxp3(+) regulatory T cells.* Eur J Immunol, 2017. **47**(12): p. 2142-2152.
121. Iwasaki, A. and B.L. Kelsall, *Freshly isolated Peyer's patch, but not spleen, dendritic cells produce interleukin 10 and induce the differentiation of T helper type 2 cells.* J Exp Med, 1999. **190**(2): p. 229-39.
122. Kang, S.G., et al., *Vitamin A metabolites induce gut-homing FoxP3+ regulatory T cells.* J Immunol, 2007. **179**(6): p. 3724-33.

123. Mucida, D., et al., *Reciprocal TH17 and regulatory T cell differentiation mediated by retinoic acid.* Science, 2007. **317**(5835): p. 256-60.
124. Stagg, A.J., M.A. Kamm, and S.C. Knight, *Intestinal dendritic cells increase T cell expression of alpha4beta7 integrin.* Eur J Immunol, 2002. **32**(5): p. 1445-54.
125. Mora, J.R., et al., *Selective imprinting of gut-homing T cells by Peyer's patch dendritic cells.* Nature, 2003. **424**(6944): p. 88-93.
126. Iwata, M., et al., *Retinoic acid imprints gut-homing specificity on T cells.* Immunity, 2004. **21**(4): p. 527-38.
127. Denning, T.L., et al., *Lamina propria macrophages and dendritic cells differentially induce regulatory and interleukin 17-producing T cell responses.* Nat Immunol, 2007. **8**(10): p. 1086-94.
128. Ochoa-Reparaz, J., et al., *Role of gut commensal microflora in the development of experimental autoimmune encephalomyelitis.* J Immunol, 2009. **183**(10): p. 6041-50.
129. Bunker, J.J., et al., *Innate and Adaptive Humoral Responses Coat Distinct Commensal Bacteria with Immunoglobulin A.* Immunity, 2015. **43**(3): p. 541-53.
130. Komban, R.J., et al., *Activated Peyer's patch B cells sample antigen directly from M cells in the subepithelial dome.* Nat Commun, 2019. **10**(1): p. 2423.
131. Nagatani, K., et al., *Antigen-specific regulatory T cells are detected in Peyer's patches after the interaction between T cells and dendritic cells loaded with orally administered antigen.* Immunobiology, 2011. **216**(3): p. 416-22.
132. Macpherson, A.J. and T. Uhr, *Induction of protective IgA by intestinal dendritic cells carrying commensal bacteria.* Science, 2004. **303**(5664): p. 1662-5.
133. Tsuji, M., et al., *Requirement for lymphoid tissue-inducer cells in isolated follicle formation and T cell-independent immunoglobulin A generation in the gut.* Immunity, 2008. **29**(2): p. 261-71.
134. Macpherson, A.J., et al., *A Primitive T Cell-Independent Mechanism of Intestinal Mucosal IgA Responses to Commensal Bacteria.* Science, 2000. **288**(5474): p. 2222-2226.
135. Mora, J.R., et al., *Generation of gut-homing IgA-secreting B cells by intestinal dendritic cells.* Science, 2006. **314**(5802): p. 1157-60.
136. Rakoff-Nahoum, S., et al., *Recognition of commensal microflora by toll-like receptors is required for intestinal homeostasis.* Cell, 2004. **118**(2): p. 229-41.
137. Mortha, A., et al., *Microbiota-Dependent Crosstalk Between Macrophages and ILC3 Promotes Intestinal Homeostasis.* Science, 2014. **343**(6178).
138. Diehl, G.E., et al., *Microbiota restricts trafficking of bacteria to mesenteric lymph nodes by CX(3)CR1(hi) cells.* Nature, 2013. **494**(7435): p. 116-20.
139. Nakahashi-Oda, C., et al., *Apoptotic epithelial cells control the abundance of Treg cells at barrier surfaces.* Nat Immunol, 2016. **17**(4): p. 441-50.
140. Shaw, M.H., et al., *Microbiota-induced IL-1beta, but not IL-6, is critical for the development of steady-state TH17 cells in the intestine.* J Exp Med, 2012. **209**(2): p. 251-8.
141. Villablanca, E.J., et al., *MyD88 and retinoic acid signaling pathways interact to modulate gastrointestinal activities of dendritic cells.* Gastroenterology, 2011. **141**(1): p. 176-185.
142. Ivanov, I.I. and D.R. Littman, *Modulation of immune homeostasis by commensal bacteria.* Curr Opin Microbiol, 2011. **14**(1): p. 106-14.
143. Liang, S.C., et al., *Interleukin (IL)-22 and IL-17 are coexpressed by Th17 cells and cooperatively enhance expression of antimicrobial peptides.* J Exp Med, 2006. **203**(10): p. 2271-9.
144. Round, J.L., et al., *The Toll-Like Receptor 2 Pathway Establishes Colonization by a Commensal of the Human Microbiota.* Science, 2011. **332**(6032): p. 974-977.

145. Wang, S., et al., *MyD88 Adaptor-Dependent Microbial Sensing by Regulatory T Cells Promotes Mucosal Tolerance and Enforces Commensalism.* Immunity, 2015.
146. Cerutti, A. and M. Rescigno, *The biology of intestinal immunoglobulin A responses.* Immunity, 2008. **28**(6): p. 740-50.
147. Katsenelson, N., et al., *Synthetic CpG oligodeoxynucleotides augment BAFF- and APRIL-mediated immunoglobulin secretion.* European Journal of Immunology, 2007. **37**(7): p. 1785-1795.
148. Bombardieri, M., et al., *A BAFF/APRIL-dependent TLR3-stimulated pathway enhances the capacity of rheumatoid synovial fibroblasts to induce AID expression and Ig class-switching in B cells.* Ann Rheum Dis, 2011. **70**(10): p. 1857-65.
149. Hardenberg, G., et al., *Specific TLR ligands regulate APRIL secretion by dendritic cells in a PKR-dependent manner.* European Journal of Immunology, 2007. **37**(10): p. 2900-2911.
150. Smith, P.M., et al., *The microbial metabolites, short-chain fatty acids, regulate colonic Treg cell homeostasis.* Science, 2013. **341**(6145): p. 569-73.
151. Macia, L., et al., *Metabolite-sensing receptors GPR43 and GPR109A facilitate dietary fibre-induced gut homeostasis through regulation of the inflammasome.* Nature Communications, 2015. **6**(1).
152. Tan, J., et al., *Dietary Fiber and Bacterial SCFA Enhance Oral Tolerance and Protect against Food Allergy through Diverse Cellular Pathways.* Cell Rep, 2016. **15**(12): p. 2809-24.
153. Singh, N., et al., *Blockade of dendritic cell development by bacterial fermentation products butyrate and propionate through a transporter (Slc5a8)-dependent inhibition of histone deacetylases.* J Biol Chem, 2010. **285**(36): p. 27601-8.
154. Singh, N., et al., *Activation of gpr109a, receptor for niacin and the commensal metabolite butyrate, suppresses colonic inflammation and carcinogenesis.* Immunity, 2014. **40**(1): p. 128-39.
155. Arpaia, N., et al., *Metabolites produced by commensal bacteria promote peripheral regulatory T-cell generation.* Nature, 2013. **504**(7480): p. 451-5.
156. Chang, P.V., et al., *The microbial metabolite butyrate regulates intestinal macrophage function via histone deacetylase inhibition.* Proc Natl Acad Sci U S A, 2014. **111**(6): p. 2247-52.
157. Scott, N.A., et al., *Antibiotics induce sustained dysregulation of intestinal T cell immunity by perturbing macrophage homeostasis.* Science Translational Medicine, 2018. **10**(464): p. eaao4755.
158. Hayden, M.S. and S. Ghosh, *Shared principles in NF-kappaB signaling.* Cell, 2008. **132**(3): p. 344-62.
159. Rice, N.R., M.L. MacKichan, and A. Israël, *The precursor of NF-kappa B p50 has I kappa B-like functions.* Cell, 1992. **71**(2): p. 243-53.
160. Solan, N.J., et al., *RelB cellular regulation and transcriptional activity are regulated by p100.* J Biol Chem, 2002. **277**(2): p. 1405-18.
161. Schuster, M., et al., *Atypical IκB proteins - nuclear modulators of NF-κB signaling.* Cell communication and signaling : CCS, 2013. **11**(1): p. 23-23.
162. Mordmüller, B., et al., *Lymphotoxin and lipopolysaccharide induce NF-kappaB-p52 generation by a co-translational mechanism.* EMBO reports, 2003. **4**(1): p. 82-87.
163. Vallabhapurapu, S. and M. Karin, *Regulation and function of NF-kappaB transcription factors in the immune system.* Annu Rev Immunol, 2009. **27**: p. 693-733.
164. Oeckinghaus, A. and S. Ghosh, *The NF-kappaB family of transcription factors and its regulation.* Cold Spring Harb Perspect Biol, 2009. **1**(4): p. a000034.
165. Vallabhapurapu, S., et al., *Nonredundant and complementary functions of TRAF2 and TRAF3 in a ubiquitination cascade that activates NIK-dependent alternative NF-kappaB signaling.* Nat Immunol, 2008. **9**(12): p. 1364-70.

166. Xiao, G., E.W. Harhaj, and S.C. Sun, *NF-kappaB-inducing kinase regulates the processing of NF-kappaB2 p100.* Mol Cell, 2001. **7**(2): p. 401-9.
167. Hayden, M.S., *A less-canonical, canonical NF-κB pathway in DCs.* Nature Immunology, 2012. **13**(12): p. 1139-1141.
168. Shih, V.F., et al., *Control of RelB during dendritic cell activation integrates canonical and noncanonical NF-kappaB pathways.* Nat Immunol, 2012. **13**(12): p. 1162-70.
169. Fusco, A.J., et al., *NF-kappaB p52:RelB heterodimer recognizes two classes of kappaB sites with two distinct modes.* EMBO Rep, 2009. **10**(2): p. 152-9.
170. Weih, F., et al., *Multiorgan inflammation and hematopoietic abnormalities in mice with a targeted disruption of RelB, a member of the NF-kappa B/Rel family.* Cell, 1995. **80**(2): p. 331-40.
171. Yilmaz, Z.B., et al., *RelB is required for Peyer's patch development: differential regulation of p52-RelB by lymphotoxin and TNF.* EMBO J, 2003. **22**(1): p. 121-30.
172. dos Santos, N.R., et al., *RelB-Dependent Stromal Cells Promote T-Cell Leukemogenesis.* PLOS ONE, 2008. **3**(7): p. e2555.
173. Burkly, L., et al., *Expression of relB is required for the development of thymic medulla and dendritic cells.* Nature, 1995. **373**(6514): p. 531-536.
174. Weih, F., et al., *Multifocal defects in immune responses in RelB-deficient mice.* The Journal of Immunology, 1997. **158**(11): p. 5211-5218.
175. DeKoning, J., et al., *Thymic cortical epithelium is sufficient for the development of mature T cells in relB-deficient mice.* J Immunol, 1997. **158**(6): p. 2558-66.
176. O'Sullivan, B.J., et al., *Autoimmune-Mediated Thymic Atrophy Is Accelerated but Reversible in RelB-Deficient Mice.* Front Immunol, 2018. **9**: p. 1092.
177. Barton, D., H. HogenEsch, and F. Weih, *Mice lacking the transcription factor RelB develop T cell-dependent skin lesions similar to human atopic dermatitis.* European Journal of Immunology, 2000. **30**(8): p. 2323-2332.
178. Nair, P.M., et al., *RelB-Deficient Dendritic Cells Promote the Development of Spontaneous Allergic Airway Inflammation.* Am J Respir Cell Mol Biol, 2018. **58**(3): p. 352-365.
179. Xia, Y., et al., *RelB regulation of chemokine expression modulates local inflammation.* Am J Pathol, 1997. **151**(2): p. 375-87.
180. Weih, D.S., Z.B. Yilmaz, and F. Weih, *Essential Role of RelB in Germinal Center and Marginal Zone Formation and Proper Expression of Homing Chemokines.* The Journal of Immunology, 2001. **167**(4): p. 1909-1919.
181. Riemann, M., et al., *Central immune tolerance depends on crosstalk between the classical and alternative NF-kappaB pathways in medullary thymic epithelial cells.* J Autoimmun, 2017. **81**: p. 56-67.
182. Carrasco, D., R.P. Ryseck, and R. Bravo, *Expression of relB transcripts during lymphoid organ development: specific expression in dendritic antigen-presenting cells.* Development, 1993. **118**(4): p. 1221-1231.
183. MacDonald, K.P., et al., *Effector and regulatory T-cell function is differentially regulated by RelB within antigen-presenting cells during GVHD.* Blood, 2007. **109**(11): p. 5049-57.
184. O'Sullivan, B.J., et al., *Immunotherapy with costimulatory dendritic cells to control autoimmune inflammation.* J Immunol, 2011. **187**(8): p. 4018-30.
185. Wu, L., et al., *RelB Is Essential for the Development of Myeloid-Related CD8- Dendritic Cells but Not of Lymphoid-Related CD8+ Dendritic Cells.* Immunity, 1998. **9**(6): p. 839-847.
186. Castiglioni, P., et al., *Cross-priming is under control of the relB gene.* Scand J Immunol, 2002. **56**(3): p. 219-23.
187. Zanetti, M., et al., *The Role of relB in Regulating the Adaptive Immune Response.* Annals of the New York Academy of Sciences, 2003. **987**(1): p. 249-257.

188. Castiglioni, P., et al., *CD4 T cell priming in dendritic cell-deficient mice.* Int Immunol, 2003. **15**(1): p. 127-36.
189. Castiglioni, P., et al., *Protection against Influenza A Virus by Memory CD8 T Cells Requires Reactivation by Bone Marrow-Derived Dendritic Cells.* The Journal of Immunology, 2008. **180**(7): p. 4956-4964.
190. Andreas, N., et al., *A new RelB-dependent CD117+CD172a+ murine DC subset preferentially induces Th2 differentiation and supports airway hyperresponses in vivo.* European Journal of Immunology, 2018. **48**(6): p. 923-936.
191. Oriss, T.B., et al., *Dendritic cell c-kit signaling and adaptive immunity: implications for the upper airways.* Current opinion in allergy and clinical immunology, 2014. **14**(1): p. 7-12.
192. Döhler, A., et al., *RelB(+) Steady-State Migratory Dendritic Cells Control the Peripheral Pool of the Natural Foxp3(+) Regulatory T Cells.* Front Immunol, 2017. **8**: p. 726.
193. Franzoso, G., et al., *Critical roles for the Bcl-3 oncoprotein in T cell-mediated immunity, splenic microarchitecture, and germinal center reactions.* Immunity, 1997. **6**(4): p. 479-90.
194. Sha, W.C., et al., *Targeted disruption of the p50 subunit of NF-kappa B leads to multifocal defects in immune responses.* Cell, 1995. **80**(2): p. 321-30.
195. Zhou, X., et al., *Selective miRNA disruption in T reg cells leads to uncontrolled autoimmunity.* J Exp Med, 2008. **205**(9): p. 1983-91.
196. Caton, M.L., M.R. Smith-Raska, and B. Reizis, *Notch-RBP-J signaling controls the homeostasis of CD8- dendritic cells in the spleen.* J Exp Med, 2007. **204**(7): p. 1653-64.
197. Choi, G.B., et al., *The maternal interleukin-17a pathway in mice promotes autism-like phenotypes in offspring.* Science, 2016. **351**(6276): p. 933-9.
198. Hövelmeyer, N., et al., *Overexpression of Bcl-3 inhibits the development of marginal zone B cells.* Eur J Immunol, 2014. **44**(2): p. 545-52.
199. Reissig, S., et al., *Elevated levels of Bcl-3 inhibits Treg development and function resulting in spontaneous colitis.* Nat Commun, 2017. **8**: p. 15069.
200. Bettelli, E., et al., *Reciprocal developmental pathways for the generation of pathogenic effector TH17 and regulatory T cells.* Nature, 2006. **441**(7090): p. 235-8.
201. Bettelli, E., et al., *Myelin oligodendrocyte glycoprotein-specific T cell receptor transgenic mice develop spontaneous autoimmune optic neuritis.* J Exp Med, 2003. **197**(9): p. 1073-81.
202. Wan, Y.Y. and R.A. Flavell, *Identifying Foxp3-expressing suppressor T cells with a bicistronic reporter.* Proceedings of the National Academy of Sciences of the United States of America, 2005. **102**(14): p. 5126-5131.
203. Barnden, M.J., et al., *Defective TCR expression in transgenic mice constructed using cDNA-based alpha- and beta-chain genes under the control of heterologous regulatory elements.* Immunol Cell Biol, 1998. **76**(1): p. 34-40.
204. Grinberg-Bleyer, Y., et al., *The Alternative NF-kappaB Pathway in Regulatory T Cell Homeostasis and Suppressive Function.* J Immunol, 2018. **200**(7): p. 2362-2371.
205. Li, J., et al., *Role of the NF-kappaB Family Member RelB in Regulation of Foxp3(+) Regulatory T Cells In Vivo.* J Immunol, 2018. **200**(4): p. 1325-1334.
206. Messina, N., et al., *The NF-kappaB transcription factor RelA is required for the tolerogenic function of Foxp3(+) regulatory T cells.* J Autoimmun, 2016. **70**: p. 52-62.
207. Oh, H., et al., *An NF-κB Transcription-Factor-Dependent Lineage-Specific Transcriptional Program Promotes Regulatory T Cell Identity and Function.* Immunity, 2017. **47**(3): p. 450-465.e5.

208. Daley, S.R., D.Y. Hu, and C.C. Goodnow, *Helios marks strongly autoreactive CD4+ T cells in two major waves of thymic deletion distinguished by induction of PD-1 or NF-kappaB.* J Exp Med, 2013. **210**(2): p. 269-85.
209. Ross, E.M., et al., *Helios defines T cells being driven to tolerance in the periphery and thymus.* Eur J Immunol, 2014.
210. Coquet, J.M., et al., *Epithelial and dendritic cells in the thymic medulla promote CD4+Foxp3+ regulatory T cell development via the CD27–CD70 pathway.* Journal of Experimental Medicine, 2013. **210**(4): p. 715-728.
211. Boursalian, T.E., et al., *Continued maturation of thymic emigrants in the periphery.* Nature Immunology, 2004. **5**(4): p. 418-425.
212. Ohnmacht, C., et al., *Constitutive ablation of dendritic cells breaks self-tolerance of CD4 T cells and results in spontaneous fatal autoimmunity.* The Journal of Experimental Medicine, 2009. **206**(3): p. 549-559.
213. Tenno, M., et al., *Essential functions of Runx/Cbfbeta in gut conventional dendritic cells for priming Rorgammat(+) T cells.* Life Sci Alliance, 2020. **3**(1).
214. Bain, C.C., et al., *TGFbetaR signalling controls CD103(+)CD11b(+) dendritic cell development in the intestine.* Nat Commun, 2017. **8**(1): p. 620.
215. Azukizawa, H., et al., *Steady state migratory RelB+ langerin+ dermal dendritic cells mediate peripheral induction of antigen-specific CD4+ CD25+ Foxp3+ regulatory T cells.* Eur J Immunol, 2011. **41**(5): p. 1420-34.
216. Heink, S., et al., *Trans-presentation of IL-6 by dendritic cells is required for the priming of pathogenic TH17 cells.* Nat Immunol, 2017. **18**(1): p. 74-85.
217. Ghosh, S., et al., *The transcription factor Foxp1 preserves integrity of an active Foxp3 locus in extrathymic Treg cells.* Nature Communications, 2018. **9**(1): p. 4473.
218. Schramm, C.M., et al., *Chronic inhaled ovalbumin exposure induces antigen-dependent but not antigen-specific inhalational tolerance in a murine model of allergic airway disease.* The American journal of pathology, 2004. **164**(1): p. 295-304.
219. Solomon, B.D. and C.S. Hsieh, *Antigen-Specific Development of Mucosal Foxp3+RORgammat+ T Cells from Regulatory T Cell Precursors.* J Immunol, 2016. **197**(9): p. 3512-3519.
220. Lathrop, S.K., et al., *Peripheral education of the immune system by colonic commensal microbiota.* Nature, 2011. **478**(7368): p. 250-4.
221. Noval Rivas, M., et al., *A microbiota signature associated with experimental food allergy promotes allergic sensitization and anaphylaxis.* J Allergy Clin Immunol, 2013. **131**(1): p. 201-12.
222. Keller, C.W., et al., *ATG-dependent phagocytosis in dendritic cells drives myelin-specific CD4(+) T cell pathogenicity during CNS inflammation.* Proceedings of the National Academy of Sciences of the United States of America, 2017. **114**(52): p. E11228-E11237.
223. Jin, C. and M. Zhu, *RelB intrinsically regulates the development and function of medullary thymic epithelial cells.* Sci China Life Sci, 2018. **61**(9): p. 1039-1048.
224. Cipolletta, D., et al., *PPAR-gamma is a major driver of the accumulation and phenotype of adipose tissue Treg cells.* Nature, 2012. **486**(7404): p. 549-53.
225. Noval Rivas, M., et al., *Regulatory T Cell Reprogramming toward a Th2-Cell-like Lineage Impairs Oral Tolerance and Promotes Food Allergy.* Immunity, 2015. **42**(3): p. 512-23.
226. Ito, M., et al., *Brain regulatory T cells suppress astrogliosis and potentiate neurological recovery.* Nature, 2019. **565**(7738): p. 246-250.
227. Freyschmidt, E.J., et al., *Skin inflammation in RelB(-/-) mice leads to defective immunity and impaired clearance of vaccinia virus.* J Allergy Clin Immunol, 2007. **119**(3): p. 671-9.

228. Anderson, G. and Y. Takahama, *Thymic epithelial cells: working class heroes for T cell development and repertoire selection.* Trends Immunol, 2012. **33**(6): p. 256-63.
229. Lei, Y., et al., *Aire-dependent production of XCL1 mediates medullary accumulation of thymic dendritic cells and contributes to regulatory T cell development.* The Journal of experimental medicine, 2011. **208**(2): p. 383-394.
230. Barthels, C., et al., *CD40-signalling abrogates induction of RORgammat(+) Treg cells by intestinal CD103(+) DCs and causes fatal colitis.* Nat Commun, 2017. **8**: p. 14715.
231. Fonseca, D.M., et al., *Microbiota-Dependent Sequelae of Acute Infection Compromise Tissue-Specific Immunity.* Cell, 2015. **163**(2): p. 354-66.
232. Andreas, N., *RelB-dependent CD117+ CD172a+ cDCs induce Th2 cell responses and maintain RORγt+ Treg homeostasis in mucosal tissues.* 2016.
233. Powolny-Budnicka, I., et al., *RelA and RelB transcription factors in distinct thymocyte populations control lymphotoxin-dependent interleukin-17 production in gammadelta T cells.* Immunity, 2011. **34**(3): p. 364-74.
234. Ruan, Q., et al., *The Th17 immune response is controlled by the Rel–RORγ–RORγT transcriptional axis.* Journal of Experimental Medicine, 2011. **208**(11): p. 2321-2333.
235. Laffont, S., K.R. Siddiqui, and F. Powrie, *Intestinal inflammation abrogates the tolerogenic properties of MLN CD103+ dendritic cells.* Eur J Immunol, 2010. **40**(7): p. 1877-83.
236. Polesso, F., et al., *Constitutive expression of NF-kappaB inducing kinase in regulatory T cells impairs suppressive function and promotes instability and pro-inflammatory cytokine production.* Sci Rep, 2017. **7**(1): p. 14779.
237. Weih, F., et al., *p50–NF-κB Complexes Partially Compensate for the Absence of RelB: Severely Increased Pathology in p50−/−relB−/−Double-knockout Mice.* Journal of Experimental Medicine, 1997. **185**(7): p. 1359-1370.
238. Bénézech, C., et al., *Lymphotoxin-β receptor signaling through NF-κB2-RelB pathway reprograms adipocyte precursors as lymph node stromal cells.* Immunity, 2012. **37**(4): p. 721-734.
239. Tang, W., et al., *The Oncoprotein and Transcriptional Regulator Bcl-3 Governs Plasticity and Pathogenicity of Autoimmune T Cells.* Immunity, 2014. **41**(4): p. 555-566.
240. Becher, B., A. Waisman, and L.F. Lu, *Conditional Gene-Targeting in Mice: Problems and Solutions.* Immunity, 2018. **48**(5): p. 835-836.
241. Lewis, K.L., et al., *Notch2 receptor signaling controls functional differentiation of dendritic cells in the spleen and intestine.* Immunity, 2011. **35**(5): p. 780-91.
242. Nutsch, K., et al., *Rapid and Efficient Generation of Regulatory T Cells to Commensal Antigens in the Periphery.* Cell Rep, 2016. **17**(1): p. 206-220.
243. Hildner, K., et al., *Batf3 Deficiency Reveals a Critical Role for CD8α+ Dendritic Cells in Cytotoxic T Cell Immunity.* Science, 2008. **322**(5904): p. 1097-1100.
244. Edelson, B.T., et al., *Peripheral CD103+ dendritic cells form a unified subset developmentally related to CD8alpha+ conventional dendritic cells.* J Exp Med, 2010. **207**(4): p. 823-36.
245. Jackson, J.T., et al., *Id2 expression delineates differential checkpoints in the genetic program of CD8alpha+ and CD103+ dendritic cell lineages.* Embo j, 2011. **30**(13): p. 2690-704.
246. Seki, T., et al., *Visualization of RelB expression and activation at the single-cell level during dendritic cell maturation in Relb-Venus knock-in mice.* J Biochem, 2015. **158**(6): p. 485-95.
247. Kobayashi, T., et al., *TRAF6 is a critical factor for dendritic cell maturation and development.* Immunity, 2003. **19**(3): p. 353-63.

248. Ardouin, L., et al., *Broad and Largely Concordant Molecular Changes Characterize Tolerogenic and Immunogenic Dendritic Cell Maturation in Thymus and Periphery.* Immunity, 2016. **45**(2): p. 305-18.
249. Scherer, M.T., et al., *The use of mammary tumor virus (Mtv)-negative and single-Mtv mice to evaluate the effects of endogenous viral superantigens on the T cell repertoire.* The Journal of experimental medicine, 1995. **182**(5): p. 1493-1504.
250. Barnett, A., et al., *Expression of mouse mammary tumor virus superantigen mRNA in the thymus correlates with kinetics of self-reactive T-cell loss.* Journal of virology, 1999. **73**(8): p. 6634-6645.
251. Mahmud, S.A., et al., *Costimulation via the tumor-necrosis factor receptor superfamily couples TCR signal strength to the thymic differentiation of regulatory T cells.* Nat Immunol, 2014. **15**(5): p. 473-81.
252. Thiault, N., et al., *Peripheral regulatory T lymphocytes recirculating to the thymus suppress the development of their precursors.* Nature Immunology, 2015. **16**(6): p. 628-634.
253. Nikolouli, E., et al., *Recirculating IL-1R2(+) Tregs fine-tune intrathymic Treg development under inflammatory conditions.* Cell Mol Immunol, 2020.
254. Houston, E.G. and P.J. Fink, *MHC Drives TCR Repertoire Shaping, but not Maturation, in Recent Thymic Emigrants.* The Journal of Immunology, 2009. **183**(11): p. 7244.
255. Hayakawa, H., et al., *Soluble ST2 blocks interleukin-33 signaling in allergic airway inflammation.* J Biol Chem, 2007. **282**(36): p. 26369-80.
256. Krystel-Whittemore, M., K.N. Dileepan, and J.G. Wood, *Mast Cell: A Multi-Functional Master Cell.* Frontiers in immunology, 2016. **6**: p. 620-620.
257. Hsu, C.-L., C.V. Neilsen, and P.J. Bryce, *IL-33 Is Produced by Mast Cells and Regulates IgE-Dependent Inflammation.* PLOS ONE, 2010. **5**(8): p. e11944.
258. Gilfillan, A.M. and C. Tkaczyk, *Integrated signalling pathways for mast-cell activation.* Nature Reviews Immunology, 2006. **6**(3): p. 218-230.
259. Tang, Q., et al., *Central role of defective interleukin-2 production in the triggering of islet autoimmune destruction.* Immunity, 2008. **28**(5): p. 687-97.
260. Webster, K.E., et al., *In vivo expansion of T reg cells with IL-2-mAb complexes: induction of resistance to EAE and long-term acceptance of islet allografts without immunosuppression.* J Exp Med, 2009. **206**(4): p. 751-60.
261. Zhang, Y., et al., *Regulation of T cell activation and tolerance by PDL2.* Proceedings of the National Academy of Sciences, 2006. **103**(31): p. 11695-11700.
262. Wuest, S.C., et al., *A role for interleukin-2 trans-presentation in dendritic cell-mediated T cell activation in humans, as revealed by daclizumab therapy.* Nat Med, 2011. **17**(5): p. 604-9.
263. Kang, B., et al., *Commensal microbiota drive the functional diversification of colon macrophages.* Mucosal Immunol, 2020. **13**(2): p. 216-229.
264. Moriwaki, K., et al., *The necroptosis adaptor RIPK3 promotes injury-induced cytokine expression and tissue repair.* Immunity, 2014. **41**(4): p. 567-78.
265. Kobayashi, T., et al., *Follicular helper T cells mediate IgE antibody response to airborne allergens.* J Allergy Clin Immunol, 2017. **139**(1): p. 300-313 e7.
266. Gowthaman, U., J.S. Chen, and S.C. Eisenbarth, *Regulation of IgE by T follicular helper cells.* Journal of Leukocyte Biology, 2020. **107**(3): p. 409-418.
267. Anderson, P., *Post-transcriptional control of cytokine production.* Nature Immunology, 2008. **9**(4): p. 353-359.
268. Giles, D.A., et al., *CNS-resident classical DCs play a critical role in CNS autoimmune disease.* The Journal of Clinical Investigation, 2018. **128**(12): p. 5322-5334.
269. Korn, T., et al., *Myelin-specific regulatory T cells accumulate in the CNS but fail to control autoimmune inflammation.* Nat Med, 2007. **13**(4): p. 423-31.

270. McGeachy, M.J., L.A. Stephens, and S.M. Anderton, *Natural recovery and protection from autoimmune encephalomyelitis: contribution of CD4+CD25+ regulatory cells within the central nervous system.* J Immunol, 2005. **175**(5): p. 3025-32.
271. Dombrowski, Y., et al., *Regulatory T cells promote myelin regeneration in the central nervous system.* Nat Neurosci, 2017. **20**(5): p. 674-680.
272. Zandee, S.E.J., et al., *IL-10-producing, ST2-expressing Foxp3(+) T cells in multiple sclerosis brain lesions.* Immunol Cell Biol, 2017. **95**(5): p. 484-490.
273. Butti, E., et al., *IL4 gene delivery to the CNS recruits regulatory T cells and induces clinical recovery in mouse models of multiple sclerosis.* Gene Ther, 2008. **15**(7): p. 504-15.
274. Cua, D.J., D.R. Hinton, and S.A. Stohlman, *Self-antigen-induced Th2 responses in experimental allergic encephalomyelitis (EAE)-resistant mice. Th2-mediated suppression of autoimmune disease.* J Immunol, 1995. **155**(8): p. 4052-9.
275. Russi, A.E., et al., *Male-specific IL-33 expression regulates sex-dimorphic EAE susceptibility.* Proc Natl Acad Sci U S A, 2018. **115**(7): p. E1520-e1529.
276. Jiang, H.R., et al., *IL-33 attenuates EAE by suppressing IL-17 and IFN-γ production and inducing alternatively activated macrophages.* Eur J Immunol, 2012. **42**(7): p. 1804-14.
277. Ring, S., et al., *Targeting of autoantigens to DEC205(+) dendritic cells in vivo suppresses experimental allergic encephalomyelitis in mice.* J Immunol, 2013. **191**(6): p. 2938-47.
278. Dong, Z., et al., *Concurrent CCR7 Overexpression and RelB Knockdown in Immature Dendritic Cells Induces Immune Tolerance and Improves Skin-Graft Survival in a Murine Model.* Cell Physiol Biochem, 2017. **42**(2): p. 455-468.
279. Wu, H., et al., *RelB-modified dendritic cells possess tolerogenic phenotype and functions on lupus splenic lymphocytes in vitro.* Immunology, 2016. **149**(1): p. 48-61.
280. Yang, H., et al., *Suppression of ongoing experimental autoimmune myasthenia gravis by transfer of RelB-silenced bone marrow dentritic cells is associated with a change from a T helper Th17/Th1 to a Th2 and FoxP3+ regulatory T-cell profile.* Inflamm Res, 2010. **59**(3): p. 197-205.
281. Feng, B., et al., *Small interfering RNA targeting RelB protects against renal ischemia-reperfusion injury.* Transplantation, 2009. **87**(9): p. 1283-9.
282. Li, M., et al., *Immune modulation and tolerance induction by RelB-silenced dendritic cells through RNA interference.* J Immunol, 2007. **178**(9): p. 5480-7.
283. Xie, J., et al., *Immune tolerance induced by RelB short-hairpin RNA interference dendritic cells in liver transplantation.* Journal of Surgical Research, 2013. **180**(1): p. 169-175.
284. Popov, I., et al., *Preventing autoimmune arthritis using antigen-specific immature dendritic cells: a novel tolerogenic vaccine.* Arthritis Res Ther, 2006. **8**(5): p. R141.
285. Xu, Y., et al., *SN52, a novel nuclear factor-kappaB inhibitor, blocks nuclear import of RelB:p52 dimer and sensitizes prostate cancer cells to ionizing radiation.* Mol Cancer Ther, 2008. **7**(8): p. 2367-76.

15 Acknowledgement

I would like to thank my beloved family and in particular:

my husband Jörg for bringing me back on my feet, for supporting me in every situation, for the lively scientific and non-scientific discussions and for giving me the strength and energy to complete my dissertation;

my son Tim for being such a sunshine and brightening up my mood;

my parents-in-law Jochen and Muchel for the great support, taking over the day care of Tim and believing in me;

my grandma for being there for me, always, no matter how far apart we are;

my dad who has always impressed me with his broad knowledge, his ingenuity, his curiosity and his eagerness to understand the world around us - leaving a deep imprint on me and triggering my own scientific curiosity;

my mum for waking up my interest in science and paving the way for me to pursue the dissertation.

I want to take this opportunity to thank my dearest friend Annalisa Schaub. Thank you for being there. Thank you for being a true scientist and a true friend.

Further, I express my gratitude to my colleagues from the Institute for Allergy Research, and especially Johanna Grosch and Benjamin Schnautz for organizing the lab and providing great support inside and outside the lab, Dr. Francesca Alessandrini for giving me so much of her precious time to help me with the lung allergy experiments; Dr. Maximilian Schiener for proofreading the thesis and always being a great support, as well as Anna-Lena Geiselhöringer, Dennis Rußkamp and Renske de Jong for their great help and support during the tough phase of my PhD.

Furthermore, I would like to express my appreciation to my mentor Dr. Caspar Ohnmacht, who provided the framework and took care of the whole project. Thank you for supporting me, for the lively discussions and the invaluable input. Thank you for believing in me and my ideas. Thank you for being patient and giving me the free space to develop my own scientific approach.

I want to thank my cooperation partner and friend Dr. Nico Andreas for the great teamwork and terrific scientific discussions. On this occasion, I would like to thank Prof. Falk Weih as the initiator of this project, who unfortunately passed away too soon, for having been a great scientist and a good friend.

My special gratitude goes to Prof. Carsten Schmidt-Weber for giving me the fantastic opportunity to accomplish my PhD thesis in the Institute for Allergy Research.